

# Protein fragment complementation assay for studying viral protein-protein interactions



Dissertation der Fakultät für Biologie  
der Ludwig-Maximilians-Universität München  
zur Erlangung des Dr. rer. nat.

vorgelegt von  
**Margit Schnee**  
München, August 2006

Erstgutachterin: PD Dr. Bettina Kempkes

Zweitgutachterin: Prof. Dr. Elisabeth Weiß

Sondergutachter: Prof. Dr. Ulrich Koszinowski

Tag der mündlichen Prüfung: 16. Februar 2007

## **Ehrenwörtliche Versicherung**

Hiermit versichere ich, dass ich die vorliegende Arbeit selbstständig angefertigt habe. Es wurden keine anderen als die angegebenen Hilfsmittel und Quellen verwendet. Ich habe weder anderweitig versucht, eine Dissertation einzureichen oder eine Doktorprüfung durchzuführen, noch habe ich diese Dissertation oder Teile derselben einer anderen Prüfungskommission vorgelegt.

München, 23. August 2006

---

Margit Schnee

**1. Table of contents**

<b>1. Table of contents .....</b>	<b>I</b>
<b>2. Summary.....</b>	<b>1</b>
2.1. Zusammenfassung .....	2
<b>3. Introduction.....</b>	<b>3</b>
3.1. Herpesviruses.....	3
3.1.1. Evolution of herpesviruses.....	4
3.1.2. Herpesvirus subfamilies.....	6
3.1.3. Structure of herpesviruses.....	7
3.1.4. Replication of herpesviruses.....	7
3.1.4.1. The nuclear egress .....	9
3.1.4.2. The nuclear egress complex (NEC) in MCMV .....	11
3.1.5. Studying herpesviruses .....	12
3.1.5.1. MCMV and MHV68 infection of mice as an animal model .....	12
3.1.5.2. Mutagenesis of herpesviruses .....	13
3.2. Clinical relevance of herpesviruses in humans.....	15
3.2.1. Chemotherapy of herpesvirus infection.....	15
3.2.1.1. Targeting virus entry.....	16
3.2.1.2. Targeting the herpesvirus DNA replication and gene expression .....	16
3.2.1.3. Targeting virus morphogenesis.....	18
3.2.1.4. Targeting cellular proteins .....	18
3.2.2. Approaches in drug development .....	19
3.3. Protein-protein interactions.....	21
3.3.1. Tools for monitoring protein-protein interactions .....	21
3.3.2. Protein complementation assay .....	22
3.3.3. The TEM-1 $\beta$ -lactamase in the PCA .....	23
3.4. Aims of this work .....	25
3.4.1. Establishment of the PCA.....	25
3.4.2. Study of the UL34/UL31 interaction in herpesviruses .....	26
3.4.3. Establishment of a potential high-throughput screen using the PCA .....	26
<b>4. Material.....</b>	<b>27</b>
4.1. Devices.....	27
4.2. Reagents and Consumables .....	27
4.2.1. Kits.....	28
4.3. Plasmids.....	29
4.3.1. Commercially available and published plasmids.....	29
4.3.2. Plasmids constructed over the project. ....	29
4.3.2.1. Basic Bla-fusion vectors .....	29
4.3.2.2. Expression plasmids .....	31
4.3.2.3. Shuttle plasmids for BAC mutagenesis .....	36
4.3.2.4. Plasmids for bacterial expression .....	36
4.3.2.5. MCMV BACs .....	38
4.4. Cells .....	39
4.5. Bacteria .....	39

## Table of contents

---

4.6.	Viruses .....	39
4.7.	Oligonucleotides .....	39
4.8.	Antibodies .....	39
4.9.	Viral template DNA .....	39
<b>5.</b>	<b>Methods.....</b>	<b>40</b>
5.1.	Isolation and purification of DNA .....	40
5.1.1.	Small scale isolation of plasmid DNA .....	40
5.1.2.	Large scale isolation of plasmid DNA .....	40
5.1.3.	Small scale isolation of BAC-DNA .....	41
5.1.4.	Large scale isolation of BAC-DNA .....	41
5.1.5.	Determination of DNA concentration and purity .....	41
5.2.	Analysis and cloning of DNA .....	42
5.2.1.	Restriction enzyme digest .....	42
5.2.2.	Agarose gel electrophoresis .....	42
5.2.3.	Isolation of DNA fragments from agarose gels .....	42
5.2.4.	Dephosphorylation of DNA ends .....	43
5.2.5.	Phenol/chloroform extraction and ethanol precipitation .....	43
5.2.6.	Annealing of synthetic oligonucleotides .....	43
5.2.7.	Amplification of DNA by Polymerase Chain Reaction (PCR) .....	43
5.2.8.	Ligation of DNA fragments .....	44
5.2.9.	Preparation of electrocompetent bacteria .....	45
5.2.10.	Transformation of electrocompetent bacteria .....	45
5.2.11.	Preparation of chemocompetent bacteria .....	45
5.2.12.	Transformation of chemocompetent bacteria .....	46
5.2.13.	Glycerol cultures of bacteria .....	46
5.2.14.	Sequencing of DNA fragments .....	46
5.3.	Analysis of proteins .....	46
5.3.1.	SDS page gel electrophoresis .....	46
5.3.2.	Commassie Blue Stain .....	47
5.3.3.	Western Blot .....	47
5.3.4.	Determination of protein concentration .....	48
5.4.	Tissue culture .....	48
5.4.1.	Cultivation of cells .....	48
5.4.2.	Freezing of cells .....	49
5.4.3.	Determination of cell number .....	49
5.4.4.	Thawing of cells .....	50
5.4.5.	Transfection of eukaryotic cells using Superfect (Quiagen) .....	50
5.4.6.	Transfection of eukaryotic cells using Ca <sub>2</sub> PO <sub>4</sub> precipitation .....	50
5.5.	Working with MCMV .....	51
5.5.1.	Generation of recombinant viral BACs .....	51
5.5.2.	MCMV virus reconstitution .....	51
5.5.3.	MCMV virus stock preparation .....	51
5.5.4.	Growth curves .....	52
5.5.5.	MCMV virus titration .....	52
5.6.	Bacterial expression .....	53
5.6.1.	Expression of heterologous proteins .....	53
5.6.2.	Lysis of bacteria .....	53
5.6.3.	Purification of His-tagged proteins .....	54
5.6.4.	Purification by anion-exchange chromatography (MonoQ) .....	54

## Table of contents

---

5.6.5.	Purification by gel filtration (Superose 6) .....	55
5.6.6.	Purification by an HA-matrix .....	55
5.6.7.	Concentration of proteins.....	56
5.6.8.	Edman sequencing .....	56
5.6.9.	Crystallization .....	56
5.7.	Biochemical assays .....	57
5.7.1.	Nitrocefin assay in cell lysates.....	57
5.7.2.	Rapamycin induced FRB/FKBP12 interaction.....	57
5.7.3.	Nitrocefin assay with purified proteins.....	58
5.8.	Statistical analysis.....	58
5.9.	Bioinformatics .....	58
<b>6.</b>	<b>Results .....</b>	<b>59</b>
6.1.	Establishment of the protein complementation assay (PCA) .....	59
6.1.1.	TEM-1 $\beta$ -lactamase in the PCA.....	59
6.1.2.	Insertion of a flexible spacer into the Bla ORF .....	59
6.1.3.	Determination of Bla activity .....	59
6.1.4.	Bla complementation induced by the interaction of FKBP12 and FRB. 61	
6.2.	The NEC-PCA .....	63
6.2.1.	M50 and M53 in the PCA.....	63
6.2.2.	Validation of the NEC-PCA .....	64
6.2.2.1.	Background of the NEC-PCA.....	65
6.2.2.2.	Specificity of the NEC-PCA.....	66
6.2.2.3.	Functionality of the fusion proteins used in the NEC-PCA.....	67
6.2.2.3.1.	Fitness of the $\Delta$ M50/N-M50 and $\Delta$ M53/C-M53 virus.....	72
6.3.	The UL34/UL31 interaction of different herpesviruses .....	73
6.3.1.	UL34 and UL31 family members in the NEC-PCA.....	74
6.3.2.	Cross-complementation within the UL34 and UL31 families.....	75
6.3.2.1.	Cross-complementation by UL31 family members.....	75
6.3.2.2.	Cross-complementation by UL34 family members.....	76
6.3.3.	Study of the binding sites in the UL34 and UL31 protein family .....	78
6.3.3.1.	The binding site in the UL31 family.....	78
6.3.3.1.1.	The binding site in UL31 homologues in $\beta$ -herpesviruses.....	80
6.3.3.1.2.	The binding site in UL31 homologues in $\alpha$ - and $\gamma$ -herpesviruses..	81
6.3.3.2.	The binding site in the UL34 family.....	82
6.4.	Complementation within the MCMV virus context .....	87
6.4.1.	UL34 and UL31 family members in MCMV deletion genomes.....	87
6.4.2.	UL34 and UL31 family members in the wt MCMV genome.....	89
6.4.3.	Chimeric UL31 family members inserted into the MCMV genome .....	91
6.4.3.1.	An essential function is located in the CR2 to CR4 of M53.....	92
6.5.	The UL34/UL31 interaction as a potential drug target.....	95
6.5.1.	Bacterial expression of the NEC proteins.....	95
6.5.1.1.	Expression and purification of UL50_His.....	96
6.5.1.1.1.	Anion exchange chromatography of UL50_His.....	98
6.5.1.1.2.	Gel filtration of UL50_His .....	99
6.5.1.1.3.	Solubility of the purified UL50_His.....	100
6.5.1.1.4.	Limited proteolysis of UL50_His .....	102
6.5.1.2.	Bicistronic expression of UL50_His and UL53 fragments .....	103
6.5.1.2.1.	Anion exchange purification and gel filtration of the complex ....	104
6.5.1.3.	Crystallization attempts of UL50_His or UL50_His/UL53_1 .....	106

## Table of contents

---

6.5.2.	The <i>in vitro</i> NEC-PCA .....	107
6.5.2.1.	Purification of Bla-tagged NEC proteins from bacteria .....	108
6.5.2.1.1.	Further purification steps .....	109
6.5.2.2.	Bla complementation by purified NEC proteins.....	110
6.5.2.3.	Specificity of the Bla signal in the <i>in vitro</i> PCA .....	110
<b>7.</b>	<b>Discussion.....</b>	<b>112</b>
7.1.	Search for new targets of antiherpesviral drugs.....	112
7.2.	Exploring protein–protein interactions .....	113
7.3.	The nuclear egress complex: a potential drug target .....	114
7.4.	The NEC-PCA .....	115
7.4.1.	UL34 and UL31 homologues in the NEC-PCA .....	116
7.4.2.	Evaluation of binding sites in the NEC proteins.....	117
7.4.3.	Study of dominant negative NEC proteins .....	120
7.4.4.	Study of core proteins by functional replacement .....	121
7.5.	Towards an NEC inhibitor .....	123
7.5.1.	NEC proteins expressed in bacteria .....	123
7.5.2.	The <i>in vitro</i> NEC-PCA .....	125
7.6.	The potential of the NEC-PCA.....	127
<b>8.</b>	<b>References .....</b>	<b>128</b>
<b>9.</b>	<b>Abbreviations .....</b>	<b>142</b>
<b>10.</b>	<b>Acknowledgements .....</b>	<b>145</b>
<b>11.</b>	<b>Supplementary information.....</b>	<b>146</b>
11.1.	List of figures.....	146
11.2.	List of tables.....	147
11.3.	Oligonucleotides .....	148
11.3.1.	Oligonucleotides for the establishment of the NEC-PCA .....	148
11.3.2.	Oligonucleotides for the UL34 and UL31 family in the NEC-PCA.....	149
11.3.3.	Oligonucleotides for the chimeric UL31 proteins .....	150
11.3.4.	Oligonucleotides for the UL34 and UL31 family in MCMV .....	151
11.3.5.	Oligonucleotides for the bacterial expression of NEC proteins .....	152
<b>12.</b>	<b>Publications.....</b>	<b>153</b>
<b>13.</b>	<b>Curriculum vitae .....</b>	<b>154</b>

## 2. Summary

Herpesviruses cause highly prevalent infections associated with usually mild symptoms resulting in life long latency. However, they can provoke fatal disease in susceptible individuals such as immunocompromised patients either in the context of primary infection or after reactivation from latency. Despite of their emerging medical importance, herpesvirus infections can so far only be controlled by antiviral therapy targeting viral DNA replication, accompanied with side effects and occurrence of resistant strains.

In this work, a novel platform for drug discovery was established that is based on a protein complementation assay (PCA), which can be used to study viral protein-protein interactions in a simple cell based assay. In a PCA two inactive fragments of a reporter enzyme are fused to two interacting proteins. Interaction of the proteins leads to proximity of the enzyme fragments, followed by reconstitution of the reporter enzyme activity.

Members of the UL34 and UL31 families are conserved herpesvirus proteins. They interact with one another forming the nuclear egress complex (NEC), which is essential for the export of viral capsids from the cell nucleus. This crucial protein-protein interaction might serve as a potential drug target for anti-herpesvirus chemotherapy. In this work the mutual binding sites of the two proteins were localized and studied for their conservation.

A PCA was established for M50 and M53 – the NEC proteins of the murine cytomegalovirus (MCMV) - by fusion of the N- and C-terminal part of the TEM-1  $\beta$ -lactamase of *E. coli*. The assay was validated and applied to representative members of the three herpesvirus subfamilies. Cross-complementation assays showed that partners derived from the same subfamily can replace each other in the PCA, however, homologues from different subfamilies can not. This cross-complementation reflects the *in vivo* situation: the human cytomegalovirus (HCMV), but not the HSV-1 or PrV homologues are able to rescue the M50 or M53 null phenotype in the viral context of MCMV. The lack of complementation between the subfamilies is due to their diverged binding sites, which are located in all cases within the first conserved region of the UL31 family proteins. The study of the binding site in UL34 family members revealed a bipartite binding motif.

With the aim of a future high-throughput inhibitor screen an *in vitro* NEC-PCA was established using purified fusion proteins of HCMV.



## **2.1. Zusammenfassung**

Herpesviren verursachen weit verbreitete und in immun-kompetenten Menschen meist mit milden Symptomen einhergehende Infektionen, welche zu lebenslanger Latenz der Viren im Körper führen. In immun-supprimierten Patienten verursachen die Viren während einer Erstinfektion oder der Reaktivierung aus der Latenz jedoch drastische Symptome. Trotz wachsender Bedeutung von Herpesvirusinfektionen ist derzeit eine Behandlung nur durch Medikamente, welche die virale DNS Polymerase angreifen, möglich. Diese rufen schwerwiegende Nebenwirkungen hervor und führen zudem zum Entstehen resistenter Virusstämme.

Im Rahmen dieser Arbeit wurde eine neue Plattform für das Prüfen von Inhibitoren etabliert. Sie basiert auf einem Protein Complementations Assay (PCA), welcher eine einfache Untersuchung von Proteininteraktionen auf zellulärer Ebene erlaubt. In einem PCA werden zwei inaktive Proteinteile eines Reporterenzym mit Proteinen verschmolzen, deren Interaktion zur räumlichen Nähe der beiden Enzymteile und zur aktiven Form des Reporterenzym führt.

Proteine der konservierten UL34 und UL31 Proteinfamilien interagieren miteinander und bilden den sogenannten Kern-Austritt-Komplex. Dieser ist wichtig für das Ausschleusen von Viruskapsiden aus dem Kern, und stellt somit einen möglichen Angriffspunkt neuer Therapeutika gegen Herpesviren dar. Der PCA wurde durch die Fusion des N- und C-terminalen Teil der TEM-1  $\beta$ -lactamase an die beiden NEC Proteine des murinen Cytomegalovirus (MCMV), M50 und M53, etabliert und später auf UL34 und UL31 Proteine repräsentativer Viren der drei Herpesvirusunterfamilien ausgeweitet. Experimente zur Kreuzreaktion zeigten, dass Proteine von Herpesviren der gleichen Unterfamilie im PCA interagieren können, homologe Proteine anderer Unterfamilien jedoch nicht. Die Fähigkeit der Kreuzreaktion im PCA spiegelt die Situation im Virus wieder: die homologen Proteine des humanen Cytomegalovirus (HCMV), jedoch nicht Proteine von HSV-1 oder PrV, ermöglichen das Wachstum eines M50 oder M53 defizienten MCMV. Das Scheitern einer Kreuzreaktion zwischen den Unterfamilien ist auf divergente Entwicklung der Bindedomänen zurückzuführen. In dieser Arbeit konnte die Bindedomäne in UL31 Proteinen in der ersten konservierten Region lokalisiert werden, in UL34 Proteinen wird ein zweigeteiltes Bindemotiv vermutet.

Im Hinblick auf ein späteres Hochdurchsatzverfahren zur Entdeckung neuer Inhibitoren des HCMV, wurde ein *in vitro* NEC-PCA entwickelt.

### **3. Introduction**

#### **3.1. Herpesviruses**

Herpesviruses are large DNA viruses widely spread in vertebrates including humans. To date, more than 120 virus species have been identified sharing the features that define the family of the *herpesviridae*, which is further subdivided into three subfamilies based on genetic and biological relations (chapter 3.1.2). The most characteristic feature of all members of the *herpesviridae* is the unique architecture of their virions. A typical herpesvirion is about 200 nm in diameter and consists of four structural elements: the core containing the viral DNA, the capsid, the tegument and the envelope (chapter 3.1.3). The double stranded DNA genome of herpesviruses ranges between 125 kb for the Varicella-Zoster Virus (VZV) and 230 kb for the cytomegaloviruses (CMV) (Chee et al., 1990; Rawlinson et al., 1996), which are the largest vertebrate viruses. Up to 200 open reading frames can be predicted within the genomes encoding basic structural components as well as virus-specific enzymes and other factors, which are involved in nucleic acid synthesis (e.g. DNA polymerase, helicase, primase) and nucleotide metabolism (e.g. thymidine kinase, dUTPase) (Roizman and Pellett, 2001). In addition, herpesviruses carry a variable number of genes, which influence the host anti-viral response. After infection of the host cell the herpesvirus genomes can undertake two different feats: either they initiate virus multiplication or enter into latency. If multiplication occurs, DNA replication and the first steps of virus maturation, namely formation of capsids and packaging of the genomes, take place in the nucleus. Infectious particles are then formed in the cytosol by acquisition of the tegument and the final envelope. The subsequent release of newly formed virus is frequently accompanied by the destruction of the host cell, hence this process is referred to as the lytic cycle. During latency, the virus genome remains present in the cell nucleus in a circular form and only a small subset of genes is expressed, if any. The viral genome is maintained mainly by cellular activities. Lytic replication causes specific lesions leading to a symptomatic infection in susceptible hosts, whereas the latent state of infection is not related to diseases. However, the program of lytic replication can be initiated from latency resulting in recurrent infections, which characterize the pathogenesis of most herpesviruses.

### 3.1.1. Evolution of herpesviruses

More than 50 herpesvirus genome sequences have been determined and were analysed in terms of their gene content and structure. Evolutionary studies based on protein sequence analysis, the study of gene families and gene clusters as well as structural analysis of the capsid have formed the current view of the herpesvirus origin.

The virion structure (Figure 2) and a conserved set of genes provide strong evidence for a common ancestor for all herpesviruses. This ancestral virus is assumed to be at least 400 million years old (McGeoch et al., 2005) and is believed to be most similar to the contemporary herpesvirus HHV-6 (Karlin et al., 1994). The current estimate is that this ancestral virus contributed 43 genes to modern herpesviruses (McGeoch, 1999). These so called core genes are located in the central region of the herpesvirus genome. Most core genes are involved in vital aspects of the viral life cycle such as cell entry, DNA replication and packaging as well as formation and transport of newly generated virions. Many genes involved in control of the life cycle, host–virus interactions and latency appear to have developed independently in the lineages.

Regarding the time scale of evolution, sequence comparisons lead to the assumption that the initial split into two highly diverged lineages occurred from the ancestor virus at least 200 million years ago and possibly even much earlier (Benton, 1997; Davison, 2002; McGeoch et al., 2006). The first lineage comprises the herpesviruses that infect poikilothermic animals like fish, reptiles or molluscs (Bernard and Mercier, 1993; Booy et al., 1996; Davison, 1992; Davison, 1998; Davison et al., 1999). Assuming a co-evolution with their host, this first lineage suggests a branching of the herpesviruses as early as 450 million years ago, since fish viruses would have diverged about that time and the invertebrate specific virus about a billion years ago (Kumar and Hedges, 1998; Wray, 1996). The second lineage comprises the three subfamilies of  $\alpha$ -,  $\beta$ - and  $\gamma$ -herpesviruses (chapter 3.1.2). From this lineage,  $\alpha$ -herpesviruses are assumed to have diverged earlier than  $\beta$ - and  $\gamma$ -herpesviruses. Figure 1 shows the suggested phylogenetic tree for some mammalian herpesviruses. It is believed that the  $\alpha$ -herpesviruses split from the  $\beta$ - and  $\gamma$ -herpesvirus branch more than 200 million years ago. The final branching point to form the  $\beta$ - and  $\gamma$ -herpesvirus subfamily is dated between 150 and 200 million years ago (McGeoch et al., 1995).

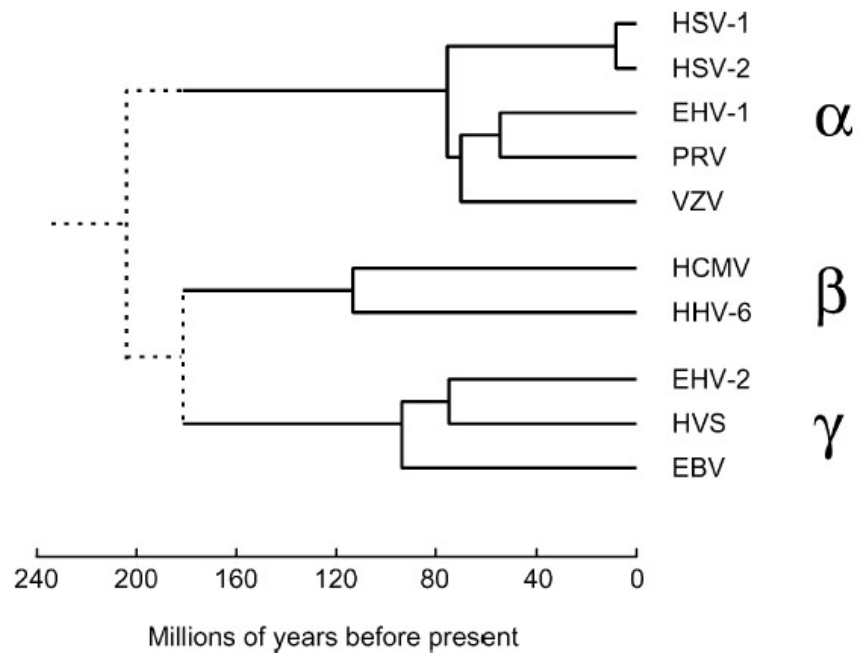


**Figure 1: Phylogenetic tree for mammalian herpesviruses.**

Simplified phylogenetic tree for mammalian herpesviruses. The timescale is based on the hypothesis that viruses co-speciate with their hosts. Broken lines indicate regions of lower confidence. Abbreviations for virus species: HSV: herpes simplex virus; EHV: equid herpes virus; PRV: pseudorabies virus; VZV: Varicella-Zoster virus, HCMV: human cytomegalovirus; HHV: human herpesvirus, HVS: herpesvirus saimiri; EBV: Epstein–Barr virus (modified from Davison, 2002;McGeoch et al., 1995).

The number of species specific genes in the genome termini of the herpesviruses suggests a co-evolution of herpesviruses with their host (Roizman and Pellett, 2001). Genes with a high similarity to cellular counterparts were most likely acquired directly or indirectly from the host cells by lateral gene transfer. Those genes were often shown to be involved in the manipulation of the host defence by anti-apoptotic and immune evasive functions. Well studied examples are the structural Bcl2 homologues of EBV or KSHV (BHRF1 and BALF1 in EBV, KSbc1-2 in KSHV) and the functional Bcl2 homologue of HCMV (UL37) that were shown to inhibit apoptosis (Goldmacher et al., 1999;Henderson et al., 1993;Marshall et al., 1999;Sarid et al., 1997;Goldmacher, 2005). Beside the lateral gene transfer, gene duplications, gene rearrangement or recombination contributed to the divergence of herpesviruses. An example for gene rearrangement is the pseudorabies virus (PrV), a pig herpesvirus, in which a substantial part of the genome is inverted relative to other  $\alpha$ -herpesviruses (Ben Porat et al., 1983;Davison and Wilkie, 1983). The plasticity of herpesvirus genomes is also evident in the adaptation of HCMV laboratory strains to cell culture and the cell lines, predominantly used for passaging. Adaptation occurred by deletion and inversion of large regions of the HCMV

genome (Hahn et al., 2004; reviewed in Prichard et al., 2001). Recombination of herpesviruses seems to be a rare event. Strains of HSV-1 and HSV-2, two  $\alpha$ -herpesviruses, can recombine in cell culture, however, the resulting viruses rarely survive (Timbury and Subak-Sharpe, 1973). In contrast, intra-species recombination is likely to have occurred for the studied strains of HHV-8 that appear as recombinational mosaics (Poole et al., 1999).

### 3.1.2. Herpesvirus subfamilies

On the basis of biological criteria such as the host range, length of replication cycle and cell tropism, herpesviruses of the second great lineage in herpesvirus evolution (chapter 3.1.1) are further classified into  $\alpha$ -,  $\beta$ - and  $\gamma$ -herpesvirus subfamilies.  $\alpha$ -herpesviruses exhibit a broad host range and a short replication cycle. Neurons are the main target of infection and latency is primarily, but not exclusively, established in sensory ganglia. The most prominent members of the  $\alpha$ -herpesviruses are VZV and the herpes simplex viruses, HSV-1 and HSV-2. In contrast,  $\beta$ -herpesviruses are characterized by a narrow host range and a long replication cycle. During infection with herpesviruses of this subfamily, host cells frequently become enlarged (cytomegalia) leading to the name of the cytomegaloviruses, the representative members of the  $\beta$ -herpesvirus subfamily. While  $\gamma$ -herpesviruses, similar to the  $\beta$ -herpesviruses, show a narrow host range, the length of their replication cycle varies between species.  $\gamma$ -herpesviruses infect cells of the lymphatic system, like T- and B-cells. Infection of such cells can be either lytic or latent, but rarely correlates with infectious progeny. When latent, viral genomes are detected in lymphoid tissue. The Epstein-Barr virus (EBV) is the prominent member of this subfamily.

Beside biological properties, herpesviruses can be grouped based on their genomic structure. The core genes that are highly conserved throughout all herpesvirus subfamilies are located in the centre of the linear DNA genome, flanked by genes shared by the subfamilies. The genes located towards the genome ends define the species specificity of the different viruses and are mainly involved in the cross talk with the host.

### 3.1.3. Structure of herpesviruses

The herpesvirus virion is built up by four distinct elements, the core, capsid, tegument and envelope (Figure 2). Mature virions range between 120 and 300 nm (Roizman and Pellett, 2001). The core, surrounded by the capsid, contains the viral DNA in the form of a torus, most likely stabilized by a proteinaceous scaffold. The capsid is an icosahedral shell of about 100-110 nm in diameter, built up by 162 capsomers, themselves complexes of structural proteins. The capsids are embedded in the tegument, a macromolecular meshwork containing about 20-30 different proteins, presumed to play a major role once the virus has entered the cell and during early gene transcription. Furthermore, both viral and cellular mRNAs can be detected in the tegument and can be translated immediately upon virus entry (Bresnahan and Shenk, 2000; Greijer et al., 2000). The tegument RNA may not only provide template for very early protein synthesis but also play a structural role in the virion. The virus envelope is formed by a lipid bilayer that originates from the host cell. The envelope contains spike-like virus encoded glycoproteins that allow virus attachment to receptor structures on host cells and are responsible for the fusion of the virion envelope to the host membranes during entry.

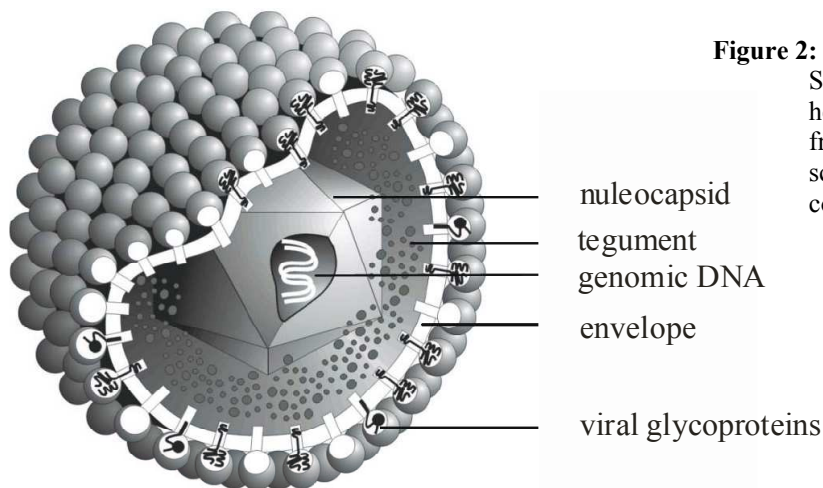


**Figure 2: The herpesvirus virion.**

Schematic representation of a herpesvirus virion (adapted from (modified from Reschke, 1994). Major virion components are indicated.

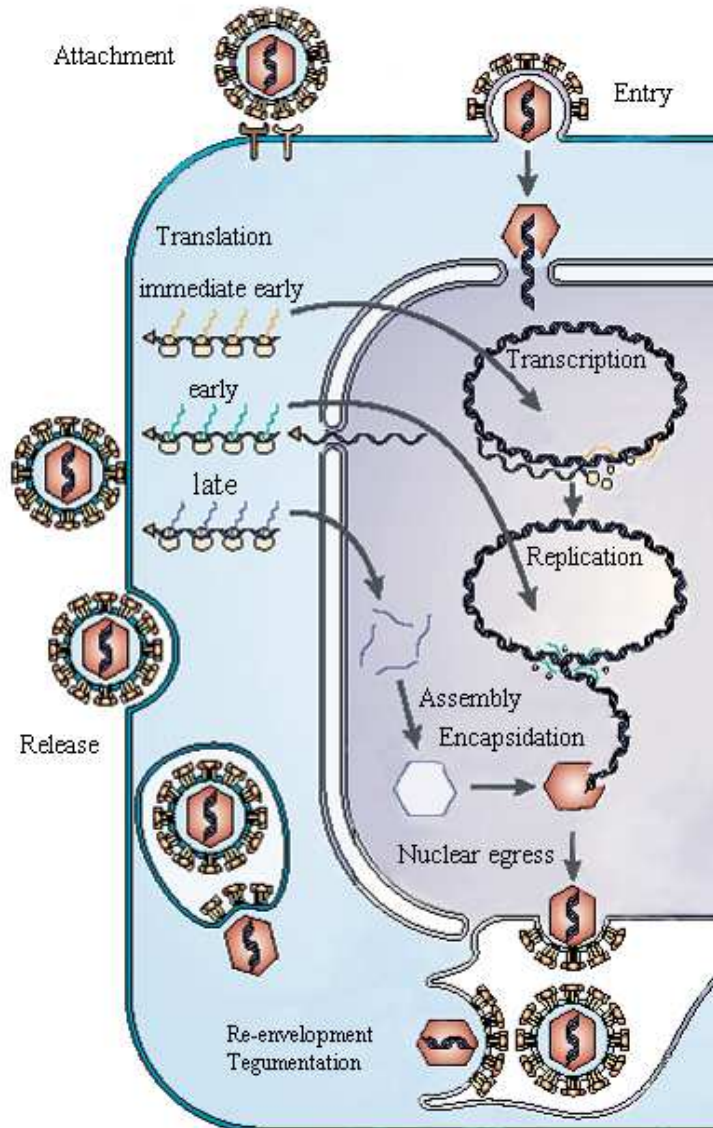
### 3.1.4. Replication of herpesviruses

The infection of the host cell begins with the adsorption of the virion on the cell membrane by a specific binding of the viral glycoproteins to their cell surface receptors (Figure 3), e.g. the binding of gB to heparan sulfate proteoglycans for HCMV (Compton et al., 1993) or gC to heparan sulfate for HSV-1 (WuDunn and Spear, 1989).

For many herpesviruses the receptors are unknown and multiple methods of attachment are assumed. After adsorption of the virions the viral envelope fuses with the cell membrane and the capsid containing the viral DNA is released into the cytoplasm. The capsids are transported to the nuclear pores and the viral genome is released into the nucleus where it circularizes. In the nucleus, transcription and replication occurs. Three groups of viral genes are transcribed, the immediate early (IE), early (E) and late (L) genes (Honest and Roizman, 1975) classified by their time of transcription during infection. The immediate early phase begins as soon as the viral genome enters the nucleus of a permissive cell. For the transcription of the IE genes no *de novo* synthesis of viral proteins is necessary. Parts of the transcripts are even thought to originate from the previous infection and brought to the new host by the tegument (Bresnahan and Shenk, 2000). IE proteins possess predominantly regulatory functions and are necessary for the initiation of the early phase (Honest and Roizman, 1975; Wathen and Stinski, 1982). The activation of the early genes takes place primarily on the transcriptional level (Godowski and Knipe, 1986). Early phase proteins are necessary for replication of the viral genome (e.g. viral DNA polymerase). The start of DNA replication defines the beginning of the late phase. During this phase mainly structural proteins are synthesized, which are necessary for the formation of the new generation of virions. DNA replication proceeds via high-molecular-weight concatameric intermediates, which are cleaved to genome length units during packaging into capsids. The nucleocapsids receive their primary envelope together with a few nuclear tegument proteins when budding at the inner nuclear membrane during the nuclear egress process (chapter 3.1.4.1). Following that, de-envelopment and subsequent re-envelopment of the immature virions is thought to occur for  $\alpha$ - and  $\beta$ -herpesviruses. The viral particles lose the primary envelope by fusion with the outer leaflet of the nuclear membrane or the ER. The naked, premature virions are released into the cytoplasm where they acquire most of their tegument. Viral re-envelopment occurs by budding into Golgi-derived vesicles that travel to the plasma membrane, where the mature virions are released by exocytosis (Gershon et al., 1994; Mettenleiter, 2002; Radsak et al., 1996; Sanchez et al., 2000; Siminoff and Menefee, 1966).

**Figure 3: Herpesvirus replication.**

Viral membrane proteins on virus particles bind to cellular receptors on the plasma membrane of the cell, which initiates fusion of the two membranes. Nucleocapsids containing the viral genome (red hexagons) are liberated into the cytoplasm and transported to nuclear pores. Viral DNA is released into the nucleus and circularizes. During transcription, three classes of viral genes are transcribed and translated into proteins. Immediate-early proteins (yellow) participate in further transcription. For replication, early proteins (green) synthesize new viral DNA molecules using circularized input DNA as a template. For encapsidation and nuclear egress, late proteins (blue) assemble into capsids, which incorporate newly replicated viral DNA. Nucleocapsids leave the nucleus by budding through the inner nuclear membrane into the perinuclear space. Through a complex process of de- and re-envelopment, mature virus particles reach exocytic vesicles, which fuse with the plasma membrane and release new virus particles into the extracellular space (modified from Coen and Schaffer, 2003).



## 3.1.4.1. The nuclear egress

DNA replication and encapsidation occurs in the nucleus of the herpesvirus infected cell. The cell nucleus is enveloped by two lipid membranes, the outer nuclear membrane (OMN) associated with the endoplasmic reticulum (ER) and the inner nuclear membrane (INM). The inner surface of the nuclear envelope is further covered by the nuclear lamina, a meshwork of lamins and other structural proteins. The intra-nuclear viral capsids with a diameter of about 100 nm exceed the size tolerated by the nuclear pores that interrupt the nuclear envelope and mediate the transport between the nucleus and the cytoplasm. Thus the export of herpesvirus capsids from the nucleus requires a unique process.



An early step in the nuclear egress is the destabilization of the nuclear lamina, followed by budding into the inner nuclear membrane. It has been suggested that cellular protein kinase C is recruited during the murine cytomegalovirus (MCMV) infection (Muranyi et al., 2002). Furthermore, binding of viral proteins to the nuclear lamins and lamine B receptor (LBR) was also detected (Lötzerich, unpublished observation). Two conserved herpesvirus proteins, members of the UL34 and UL31 protein family (Figure 4) are involved in this process. Members of these two protein families were studied in the  $\alpha$ -herpesviruses PrV, HSV-1, HSV-2 and EHV-1, the  $\beta$ -herpesviruses MCMV and HCMV and the  $\gamma$ -herpesvirus EBV. All studied members of the two protein families were shown to be important for efficient viral replication. They form a complex at the inner nuclear membrane, referred to as the nuclear egress complex (NEC), which is required for exporting viral capsids to the cytoplasm (Bubeck et al., 2004; Fuchs et al., 2002; Lake and Hutt-Fletcher, 2004; Neubauer et al., 2002; Reynolds et al., 2001; Yamauchi et al., 2001). The UL34 family members are type II C-terminally anchored membrane proteins, which are synthesised in the ER in the early to late phase of infection and transported to the inner nuclear membrane by diffusion. The UL31 family members were shown to be expressed late in infection and are transported to the nucleus by an N-terminal nuclear localization signal (NLS) (Lötzerich et al., 2006). The co-expression of both proteins in the absence of other viral proteins leads to the co-localization of the two proteins at the inner nuclear membrane. Furthermore, an alteration of the nuclear membrane was observed in cells expressing UL34 and UL31 of HSV-1 (Liang and Baines, 2005). Figure 4 shows the similarity blot obtained by an alignment of the UL34 and UL31 family members of six herpesviruses, representing two species from each subfamily. The set of previously studied members of the UL34 and UL31 families was supplemented by the respective gene product of the  $\gamma$ -herpesvirus MHV68 (murine herpesvirus 68). The blots show highly conserved amino acids in both protein families suggesting a structural, as well as functional and positional homology across the protein families. Conserved amino acids are distributed in small patches over the UL34 proteins with conservation peaks at about 80% similarity for some regions of the protein. While the UL31 family shows an overall lower conservation with peaks at 60% similarity, the similar residues are grouped in distinct conserved regions.

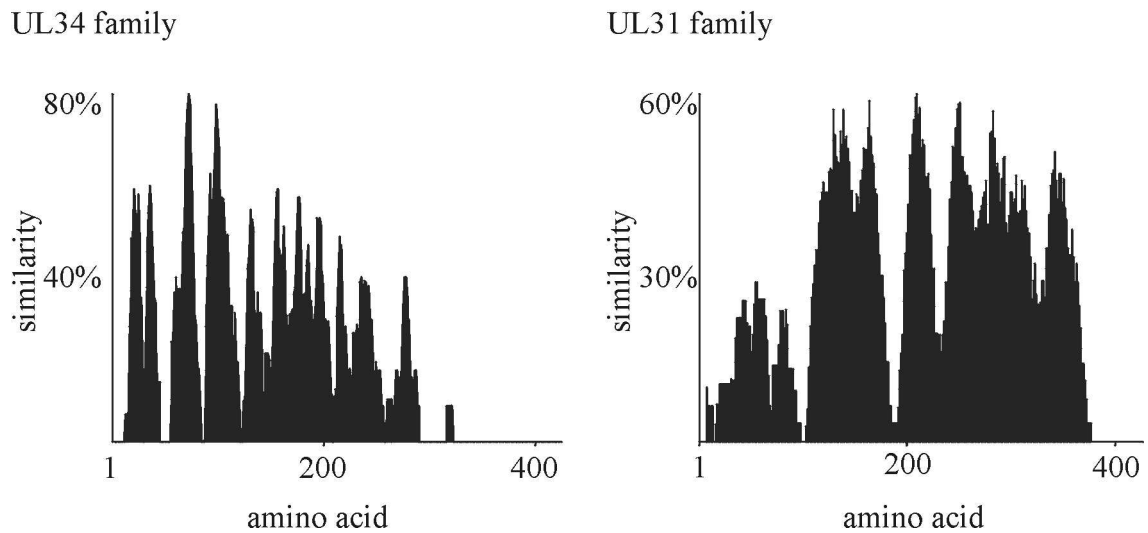


**Figure 4: Similarity blots of the UL34 and UL31 protein families.**

The similarity blot in **A**) shows the pattern obtained by the alignment of the UL34 family members UL34 of HSV-1 and PrV, M50 of MCMV, UL50 of HCMV, Orf67 of MHV68 and BFRF1 of EBV. The similarity blot in **B**) shows the pattern obtained by the alignment of the respective UL31 family members UL31 of HSV-1 and PrV, M53, UL53, Orf69 and BFLF2. Numbers on the y-axis indicate the percentage of homology for the amino acid position, indicated on the x-axis.

#### 3.1.4.2. The nuclear egress complex (NEC) in MCMV

M50 and M53, the UL34 and UL31 family members of MCMV, were studied extensively in our group. The two proteins form a complex by a non-obligatory interaction (Muranyi et al., 2002) and play an essential role in the nuclear stage of viral replication. It was recently shown that the interaction between M50 and M53 is essential for their function (Bubeck et al., 2004; Lötzerich et al., 2006). M50 is expressed by early-late kinetics. It is inserted into the ER after synthesis, reaching the nuclear membranes by diffusion. Its partner, M53, is expressed with similar kinetics and targeted to the nucleus through the nuclear pores by a canonical NLS. In the nucleus, M50 binds to M53 forming the nuclear egress complex (NEC) at the inner nuclear membrane (Bubeck et al., 2004; Lötzerich et al., 2006; Muranyi et al., 2002). The NEC is involved in destabilisation of the nuclear lamina and/or remodelling of the nuclear membranes, preparing them for primary budding of viral capsids. The NEC proteins might also act as a docking station for the viral capsids, guiding their nuclear egress process (Figure 5). For that, at least one additional viral protein, the primary tegument protein M94, is suggested to act as an adaptor protein between the nucleocapsids and the NEC (Ruzsics, unpublished

observation). Another protein, M51, was shown to bind to M53 in a yeast two-hybrid screen (J. Haas, unpublished observation), as it was assumed for its homologues from other herpesviruses (Uetz et al., 2006).

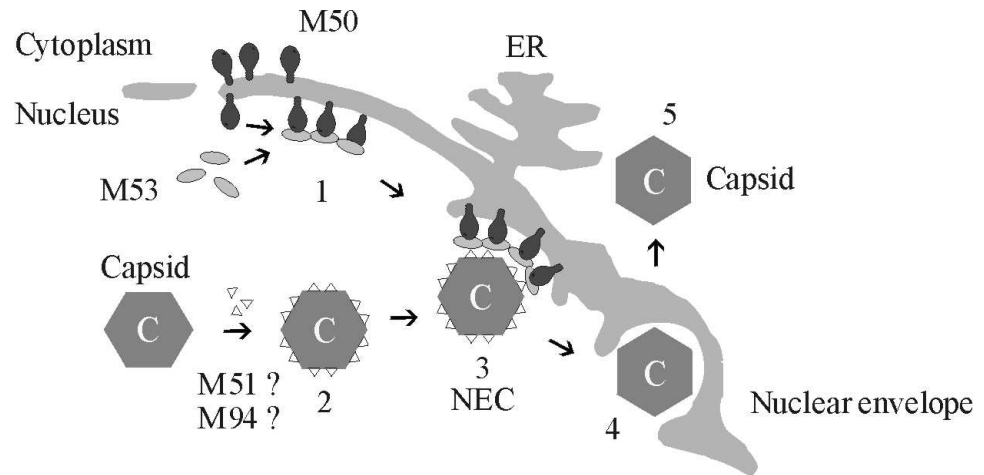


**Figure 5: Working model of the NEC in MCMV.**

The DNA genome is replicated in the nucleus and packed into the preformed capsids (C). M50 and M53 form a complex at the inner nuclear membrane (1) that might act as a docking station for the DNA filled capsids (2), with M94 as an adaptor protein. This configuration forms the nuclear egress complex (NEC) (3). The capsids bud in the membrane (4) and are released into the cytoplasm (5).

### 3.1.5. Studying herpesviruses

#### 3.1.5.1. MCMV and MHV68 infection of mice as an animal model

$\beta$ - and  $\gamma$ -herpesviruses show a high species specificity. Therefore, in order to study the entire spectrum of their infection biology, closely related viruses of animals that can serve as a laboratory model for human herpesvirus infections are needed. Murine cytomegalovirus belongs to the  $\beta$ -herpesvirus subfamily and when used to infect mice serves as an animal model for the human cytomegalovirus (HCMV) infection. The two viruses are closely related, showing high similarity in their biology and pathogenesis of infection and subsequent disease development in immunocompromised hosts (Brody and Craighead, 1974; Mayo et al., 1977; Reddehase et al., 1985) or the establishment of latency in immunocompetent hosts (Ho, 1982; Hudson, 1979; Jordan, 1991). MHV68, a member of the  $\gamma$ -herpesvirus subfamily, serves as a model for the infection by EBV and KSHV (Kaposi's sarcoma associated herpesvirus), two important human pathogens. Although not as closely related to the other  $\gamma$ -herpesviruses as MCMV is to HCMV,

MHV68 allows efficient and easy propagation in cell culture and the exploration of the lytic cycle of the viruses.

### 3.1.5.2. Mutagenesis of herpesviruses

Genetic analyses of viruses are facilitated by the establishment of a reverse genetic system, which allows targeted mutagenesis of the genes of interest in their genomic context. For herpesviruses this was achieved by cloning herpesvirus genomes as infectious bacterial artificial chromosomes (BAC) (Messerle et al., 1997). One copy of the herpesvirus genome is stably maintained in *E.coli* after insertion of the BAC cassette (approximately 8 kb) containing a chloramphenicol resistance gene as a selection marker and the origin of replication from the bacterial fertility factor (F-factor). The BAC technology allows rapid manipulation of the herpesvirus genome in bacteria, using well established and efficient methods of genome engineering within *E. coli*. The deletion of genes from the viral BAC is usually achieved by homologous recombination during which the targeted gene is replaced by a cassette carrying a resistance gene (Wagner et al., 2002). For the rapid and efficient introduction of mutant or foreign genes, site specific recombination mediated by the Flp recombinase can be applied. The Flp recombinase directs the site specific recombination event between two FRT sites (McLeod et al., 1986). One FRT site can be introduced into the viral BAC at a neutral position, for example between the MCMV genes m16 and m17 (Bubic et al., 2004). The second FRT site is placed on a shuttle plasmid, which carries the genetic element to be introduced. The general flow of this mutagenesis approach is depicted in Figure 6, exemplified by the exchange of a wild type (wt) with a mutant (mt) gene. The wt gene was deleted from the m16/17FRT-MCMV BAC by ET cloning (Wagner et al., 2002) and the resulting deletion genome was maintained as a BAC in *E.coli* (DH10B). The bacteria were transformed with pCP20, an Flp recombinase expressing plasmid (Cherepanov and Wackernagel, 1995), and subsequently with a shuttle plasmid. The shuttle plasmid contains the gene of interest under the control of an appropriate promoter, a resistance gene for bacterial selection, an FRT site and an origin of replication that is not recognized by the DH10B strain. The origin of replication of pO6T or pOriR6K-zeo-*ie* (Bubeck et al., 2004; Miller and Mekalanos, 1988) requires for its function the  $\pi$ -protein, a prophage derived gene, which is only expressed by the *E.coli* strain Pir (Kolter et al., 1978) and not the strain DH10B. The in DH10B inactive origin leads to a loss of the shuttle plasmid if it is not integrated in the BAC. The Flp recombinase unifies the BAC and the

shuttle plasmid. Subsequent selection with chloramphenicol and zeocin identifies BACs with the inserted shuttle plasmid. BAC-DNA is isolated and checked for correct insertion by restriction pattern analysis. For virus reconstitution, BAC-DNA is transfected into mouse embryonic fibroblasts (MEF). Cells are cultured until virus progeny is observed by plaque formation in the cell monolayer. Once reconstituted, the virus loses the BAC cassette over the first few passages due to the short homology sequences flanking the BAC cassette (Wagner et al., 1999).

The BAC technology has been adapted to HSV-1, PrV, HCMV, EBV and many other herpesviruses (Adler et al., 2000; Borst et al., 1999; Delecluse et al., 1998; Saeki et al., 1998; Smith and Enquist, 1999).

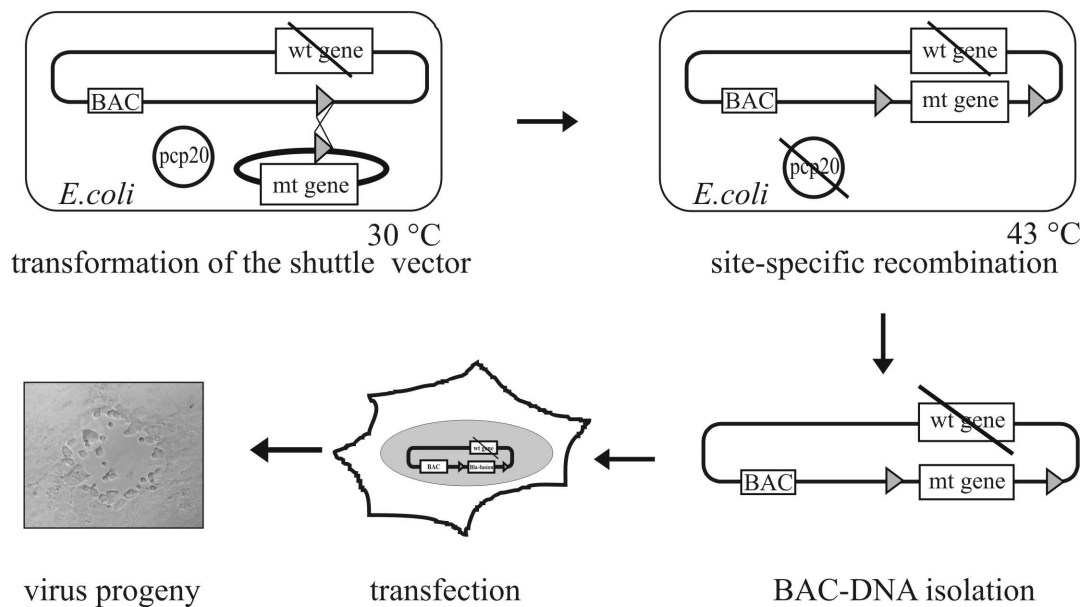


**Figure 6: BAC mutagenesis.**

Schematic representation of the MCMV BAC mutagenesis process. The MCMV genome, here deficient for one wild type gene, is maintained as BAC in *E. coli*. The bacteria are transformed by pCP20, the expression plasmid for the Flp recombinase and the expression plasmid containing the gene of interest. After Flp mediated recombination between the FRT sites at the permissive temperature of 30 °C, bacteria are cultured at 43 °C to remove the temperature sensitive pCP20. BAC-DNA is isolated, checked for correct insertion by restriction pattern analysis and transfected into MEF cells. Cells are cultured until virus progeny is observed by plaque formation in the cell monolayer.

### **3.2. Clinical relevance of herpesviruses in humans**

Humans are the host for at least eight herpesviruses, namely the two herpes simplex viruses HSV-1 and HSV-2, Varizella-Zoster Virus (VZV), human cytomegalovirus (HCMV), human herpesvirus 6 and 7 (HHV6 and HHV7) and two  $\gamma$ -herpesviruses, KSHV and EBV.

Herpesvirus infections follow three different phases, firstly the acute infection, followed by a latent stage and finally an eventual reactivation from latency. All viruses can cause acute, highly prevalent but mainly asymptomatic infections during early childhood, associated with life long latency. In contrast to the mild infection in immunocompetent patients, herpesviruses can provoke fatal diseases in susceptible individuals such as newborns and immunocompromised patients either in the context of primary infection or after reactivation from latency (Mocarski et al., 2001; Rickinson and Kieff, 2001; Whitley, 2001). During acute infection,  $\alpha$ -herpesviruses cause epithelial lesions as well as disseminated disease, e.g. conjunctivitis and encephalitis in children. In immunocompromised patients, primary infection can further lead to pneumonitis and hepatitis. HCMV, a  $\beta$ -herpesvirus, targets a variety of cell types and can lead to mononucleosis and sometimes hepatitis in immunocompetent hosts, but retinitis, encephalitis, hepatitis and pneumonitis in immunocompromised patients. The  $\gamma$ -herpesvirus, EBV, can lead to severe mononucleosis and encephalitis. In contrast to  $\alpha$ - and  $\beta$ -herpesviruses, EBV and KSHV are furthermore associated with a variety of cancers such as Kaposi's sarcoma, Castleman disease, Burkitt's and Hodgkin's lymphomas, nasopharyngeal carcinoma and other B-cell lymphomas (Rickinson and Kieff, 2001).

#### 3.2.1. Chemotherapy of herpesvirus infection

Herpesvirus related diseases are mainly self-limiting in immunocompetent host, however, the increase of the human life span combined with the number of organ transplantations and the spread of AIDS have all contributed to an increased occurrence of symptomatic disease and have enforced the urge of antivirals and vaccines against herpesviruses. In the large DNA genomes of herpesviruses, more than 50 essential genes code for viral replication. Different stages of the viral life cycle represent possible targets for blocking herpesvirus infection, such as virus attachment and cell entry, gene transcription, DNA replication and finally morphogenesis. Although several drugs have been approved for the treatment of herpesvirus infections, their utility is limited by problems

with pharmacokinetics, toxicity and development of resistance, as will be discussed in the following chapters.

### 3.2.1.1. Targeting virus entry

One strategy to target herpesviruses is to block virus attachment and entry. An advantage of early interference is the avoidance of later viral proteins that might alter cellular functions or exhibit cytotoxic effects. Furthermore, drugs inhibiting virus attachment would not need to enter the cell. Compounds were identified that bind glycoproteins of HSV-1, thereby inhibiting its initial attachment (Orozco-Topete et al., 1997; Pertel and Spear, 1996). A major drawback of drugs targeting the attachment process is a low bioavailability of existing compounds. Furthermore, alternative entry pathways of many herpesviruses reduce the effect of drugs, targeting one specific receptor.

### 3.2.1.2. Targeting the herpesvirus DNA replication and gene expression

Any essential process involved in the viral replication cycle represents a potential drug target, however, nearly all clinically used drugs interfere with viral DNA synthesis. Most popular are nucleoside analogues (De Clercq and Holy, 2005). After discovery and approval of idoxuridine in the early 1960s (Prussof, 1959), targeting the  $\alpha$ -herpesviruses HSV-1 and HSV-2, related drugs were developed such as acyclovir and famciclovir, both targeting the herpes simplex viruses and VZV, or ganciclovir and cidofovir that target the  $\beta$ -herpesvirus HCMV. The drugs, acyclic nucleoside homologues or acyclic nucleoside phosphonates, target the viral DNA polymerase indirectly and are administered as so called pro-drugs. The compounds are phosphorylated by viral thymidine kinase or serine/threonine kinase UL97 for HCMV (Chee et al., 1989), and are subsequently converted into active triphosphates by cellular kinases. The modified triphosphates then compete with the normal dNTPs as substrate for the viral polymerase and lead to termination of DNA elongation or enzyme inactivation. While these drugs are very specific, safe and efficient, a number of problems are associated with their use. The spectrum of viruses targeted by the drugs is narrow, meaning that although one herpesvirus species can be efficiently inhibited, others remain unaffected. Also since all these types of drugs target the same site in the kinase as well as in the DNA polymerase, few mutations are necessary to give rise to resistant strains. As a consequence, high doses of the drug have to be administered. Finally, the incorporation of the modified triphosphates also results in termination of cellular DNA elongation. This makes nu-

cleoside analogues mutagenic, inducing DNA breakage and chromosomal aberrations (Tomicic et al., 2002).

A non-nucleoside substrate analogue of the herpesvirus DNA polymerase is foscarnet, which binds in the pyrophosphate binding site of the polymerase. This drug allows the treatment when resistance against acyclovir or derivatives occurs, however, its high cytotoxicity leads to numerous side effects (Chrisp and Clissold, 1991). Recently non-nucleoside inhibitors of the viral DNA polymerase were discovered by high-throughput screens (Loregian and Coen, 2006). Inhibitory compounds were selected to target a site other than the substrate binding sites, thus representing new chemotherapeutics for resistant strains. Furthermore, it was shown that the viral DNA polymerase of several herpesviruses was targeted, whereas human DNA polymerases were barely disrupted. Preclinical trails are ongoing for the compound PNU-183792, an inhibitor belonging to the 4-oxo-dihydroquinoline class, which was reported to exhibit antiviral activity against the polymerase of HCMV, HSV and VZV (Brideau et al., 2002; Oien et al., 2002).

A novel strategy to inhibit viral replication is based on the disruption of virus protein-protein complexes by peptides or peptidomimetic compounds. Such compounds mimic one of the interacting subunits thereby interfering with the formation of an active viral protein assembly (Loregian et al., 2002; Loregian and Coen, 2006). Enzymes that consist of several subunits might be inhibited from forming the active holoenzyme. The first example studied was the inhibition of the tetrameric ribonucleotide reductase of HSV-1. This multimeric enzyme was disrupted in the presence of a nonapeptide resulting in specific inhibition of virus replication (Cohen et al., 1986; Dutia et al., 1986). Studies of the interaction surfaces in the DNA polymerases of HSV-1, HSV-2, VZV and HCMV are ongoing (Loregian and Palu, 2005).

New anti-HSV agents were developed that target the helicase-primase complex (Crute et al., 2002; Kleymann et al., 2002). The agent BAY-57-1293 (Betz et al., 2002) appears to increase the affinity of the trimeric viral complex to the DNA with a negative effect on DNA replication.



### 3.2.1.3. Targeting virus morphogenesis

An alternative strategy for targeting herpesviruses is to block a process further downstream in the replication cycle, the morphogenesis of virions. From the viral DNA packaging to the formation of the next generation of infectious particles several morphogenesis steps that consist of processes not present in the host cell provide numerous possibilities for an effective and specific inhibition. Four different classes of compounds that interfere with herpesvirus morphogenesis have been identified. All interfere with the viral DNA cleavage and encapsidation.

Thiourea inhibitors, such as WAY-150138, appear to inhibit the portal protein UL6 and at least one other protein in HSV-1, blocking DNA entry into the preformed capsids (Newcomb and Brown, 2002;van Zeijl et al., 2000). The other compounds, such as acridones, phenylenediamine-sulfonamides and ribosylbenzimidazoles interfere with cleavage of the DNA concatamers into a single genome-length DNA molecule or DNA encapsidation but the detailed mode of action and the target protein is not known (Akanitapichat et al., 2000;Krosky et al., 2002;Weber et al., 2001).

Maribavir, a ribosylbenzimidazole derivate that inhibits virus maturation by acting on the HCMV protein kinase UL97, is the most promising compound for possible clinical use. UL97 plays an important role not only during DNA replication (chapter 3.1.4) but also during DNA encapsidation (Wolf et al., 2001). One group has reported that maribavir inhibits viral DNA replication (Biron et al., 2002), whereas another has reported that maribavir blocks HCMV replication at the stage of nuclear egress (Krosky et al., 2003).

Virus morphogenesis depends on plenty of interactions involving solely viral proteins. As it will be later discussed, a big potential is seen in the inhibition of those interactions as they might be inhibited specifically. One focus of this work was the elucidation of an crucial interaction during viral morphogenesis.

### 3.2.1.4. Targeting cellular proteins

Although large DNA viruses, such as herpesviruses, show a low rate of adaptive mutations, resistance to certain drugs, especially the frequently used nucleoside analogues, is a serious problem. Since drugs designed to target viral proteins ensure specificity and low cytotoxicity, little effort has been made to target cellular proteins for antiherpesviral chemotherapy. However, blocking cellular proteins that interfere with the viral life cycle would reduce the chance of developing resistance and eventually more than one spe-

cies of herpesviruses could be inhibited. One example is the inhibition of the cycline dependant kinase (CDK), which is up regulated during herpesvirus infection (Jault et al., 1995). All viruses that replicate in the cell nucleus might be targeted by this mode of inhibition. One successful drug is the purine derivative roscovitine (Meijer et al., 1997) which binds in the ATP-binding site of CDKs and was shown to inhibit HSV-1, HSV-2, VZV and HCMV (Bresnahan et al., 1997; Schang et al., 1998; Schang et al., 2002; Taylor et al., 2004).

Targeting host kinases might even allow the control of latent infections by herpesviruses. Experiments performed by Cooper and Longnecker (Cooper and Longnecker, 2002) showed that the inhibition of the Syk threonine kinase by picaetanol (Geahlen and McLaughlin, 1989) resulted in induced apoptosis in LMP2 expressing cells and decreased the outgrowth of B cells in IL-7 containing methylcellulose. LMP2, the latent membrane protein 2, is thought to be essential for maintaining of latency in EBV infected cells and has been reported to directly interact with several kinases. Syk autophosphorylation and kinase activity is increased in LMP2A expressing cell lines and the interaction of LMP2A with Syk is essential for the ability of LMP2A to block B cell signal transduction (Fruehling and Longnecker, 1997; Merchant et al., 2000; Miller et al., 1995). The treatment of latent EBV infections in high risk patients might inhibit the development of EBV-associated cancers by the reduction of infected B-cells or influence progression and tumour survival.

### 3.2.2. Approaches in drug development

Strategies applied for the development of antiherpesviral drugs described in the previous chapter focused primarily on the anti-metabolite research for nucleoside analogues. Development of such drugs requires a modification to the known structure of the polymerase substrate such that the affinity to the substrate binding cleft is retained while other functions in the metabolic pathway are lost. The rational design of drugs requires knowledge of the structure of either the basic molecule of a potential inhibitor or the 3D structure of the protein or protein complex, which is targeted by the drug. This information can be obtained by crystallographic or NMR analyses of the proteins or by comparison to previously described structures of homologous proteins. Drugs can be designed rationally by the prediction of binding properties of certain molecules, designed *in silico* by bioinformatic tools. One example for structure assisted development of anti-viral drugs are SARS protease inhibitors. After elucidation of the protease structure

(Anand et al., 2003) effort was put in the design of inhibitory compounds (Yang et al., 2005). While results from the rational drug design are mainly hypothetical and require experimental validation, such an approach can drastically shorten the discovery process. The recent elucidation of the crystal structures of several glycoproteins of HSV-1 and UL44, a subunit of the HCMV polymerase (Appleton et al., 2006; Carfi et al., 2001) may serve as a basis for the rational design of antiherpesviral drugs that focus on blocking initial attachment or DNA replication of the virus.

Another effective approach is high-throughput screening (HTS) in which very large libraries of chemical compounds are screened for an inhibitory effect on a specific enzyme activity or protein-protein interaction. Information about the structure and properties of the interaction surfaces are helpful but not essential for the establishment of a HTS. The prerequisite of a HTS is a simple and fast readout for the targeted activity such as a colorimetric assay for an enzyme reaction or a yeast two-hybrid (Y2H) based assay. For HTS the yeast three-hybrid system, which evolved from the classical Y2H can be employed. Here, the inhibition of an interaction can be assayed in contrast to a basic interaction screen in an original yeast-two hybrid system (reviewed in Drees, 1999; Licitra and Liu, 1996).

Examples for antiviral drugs discovered by high-throughput screens are HSV-1 helicase inhibitors (Spector et al., 1998) and HCMV polymerase inhibitors (Loregian and Coen, 2006). The high-throughput helicase screen was based on a labelled primer displacement assay, where an  $\alpha$ - $^{33}\text{P}$ -labeled primer was annealed to an M13 template and pure baculovirus-expressed UL5/8/52 HSV-1 helicase complex was added together with ATP and  $\text{Mg}^{2+}$ . The extent to which the helicase enzyme complex could displace the labelled primer, in the presence of the test compound, was measured by counting the radioactivity that remained associated with the M13 substrate (Spector et al., 1998) For the compounds, disrupting interaction of the accessory subunit of the HCMV polymerase (UL44), and residues of the catalytic subunit (UL54), libraries were screened by an HTS, based on fluorescence polarization (Dandliker et al., 1981). A peptide of UL54 was labelled by a fluorophore. Alterations in the conversion of polarized light after excitation indicate the status of interaction with UL44, possibly inhibited by the screened compounds (Loregian and Coen, 2006).

### **3.3. Protein-protein interactions**

At present, protein-protein contact areas are considered to be new prospective drug targets. Most biological processes depend not on single proteins but specific protein assemblies, which can be influenced by external compounds. Beside the view of protein-protein interactions as drug targets, the understanding of complexes formed by proteins gives important insights into processes under study, such as virus morphogenesis or virus replication. Knowledge about interaction partners of proteins or the sites of interaction often help to embed processes that are understood on an isolated but detailed level into a comprehensive picture.

#### 3.3.1. Tools for monitoring protein-protein interactions

The most popular and frequently used method to monitor and reveal protein-protein interactions is the yeast-two hybrid (Y2H) system (Fields and Song, 1989). For this method, a transcription factor is split into its DNA binding and transcription activation domains. The two domains, which are not active when separated, are independently fused to a “bait” protein and the potential interaction partners, the “prey” proteins. Interaction of prey and bait proteins allow DNA binding and alignment of the other domain, enabling subsequent transcriptional activation of a reporter gene, such as the lacZ. The easy handling and low costs made the Y2H a tool for large screens to set up maps of interacting proteins, so called interactomes. Recently a comprehensive analysis of interacting proteins within VZV and KSHV was published which might serve as a platform for the discovery of protein-protein interactions in other herpesviruses (Uetz et al., 2006). Limitations of the Y2H concern the possible miss folding and subsequent instability of the hybrid proteins, their inappropriate sub-cellular localization, the absence of certain post-translational modifications such as phosphorylation or glycosylation, the lack of physiological context and the inability to screen a large variety of potential protein-protein interactions. Protein interactions identified by the Y2H system need to be validated further by techniques that allow detailed studies of the interactions in their biological context. Classical biochemical techniques used to validate the outcome of a Y2H screen are co-immunoprecipitation and pull-down assays. Both methods are based on affinity purification of the bait protein, which binds to a matrix either directly, or by an additional tag. Protein complexes involving the bait protein are retained by the matrix material and can be co-purified with the bait. A recent development is the tandem

affinity purification (TAP) technique that uses a complex tag fused to the bait protein for two consecutive purification steps in yeast (Puig et al., 2001; Rigaut et al., 1999).

### 3.3.2. Protein complementation assay

Based on the yeast-two hybrid assay, the protein complementation assay (PCA) evolved as a new method to monitor protein-protein interactions. In contrast to the Y2H system, the PCA allows real time monitoring and is not limited by the nuclear localization of the proteins of interest. The PCA can be applied to cytoplasmatic or even membrane anchored proteins in their native context.

In a PCA, two fragments of a reporter protein are fused to two known or putative interaction partners. The individual fragments are non functional by themselves and ideally cannot bind to each other. However, putting the split fragments in proximity by interaction of the proteins they are fused to, allows proper folding leading to the reconstitution of activity (Figure 7). As reporter proteins, enzymes or fluorescent proteins are used. The first PCA, developed in 1994 by Johnsson and Varshavsky, used N- and C-terminal halves of ubiquitin fused to interacting proteins. Interaction lead to the reassembly of the two ubiquitin halves and the subsequent cleavage by ubiquitin specific proteases produced a free reporter. A more direct readout can be achieved by the use of reporter enzymes in the PCA, such as the dihydrofolate reductase in bacteria (Pelletier et al., 1999) or the  $\beta$ -galactosidase and  $\beta$ -lactamase in eukaryotic cells (Rossi et al., 1997; Wehrman et al., 2002); chapter 3.3.3). The complementation of the two fragments leads to an active reporter enzyme that can be detected and quantified after substrate application. The time between the actual interaction and the detection can be shortened further by the use of fluorescent proteins as reporter. This type of PCA is also known as BiFC, the bimolecular fluorescence complementation, and was established for fluorescent proteins like GFP or YFP (Ghosh et al., 2000; Hu et al., 2002). Interacting proteins can be directly detected by fluorescence - even non-invasive in living animals (Paulmurugan et al., 2002) - however, one drawback is that a stable complex is formed once the fragments have been complemented, thus making the system irreversible.

PCAs attracted interest for mapping biochemical pathways, for example involved in cell differentiation and proliferation, apoptosis, stress response or secretion. (Nyfeler et al., 2005; Subramaniam et al., 2001). The PCA can be more widely applied as tool for genomic networking, which might be realised by the proposed GFP-PCA based, functional cDNA library screen (Remy and Michnick, 2004). Here a genome wide screen is

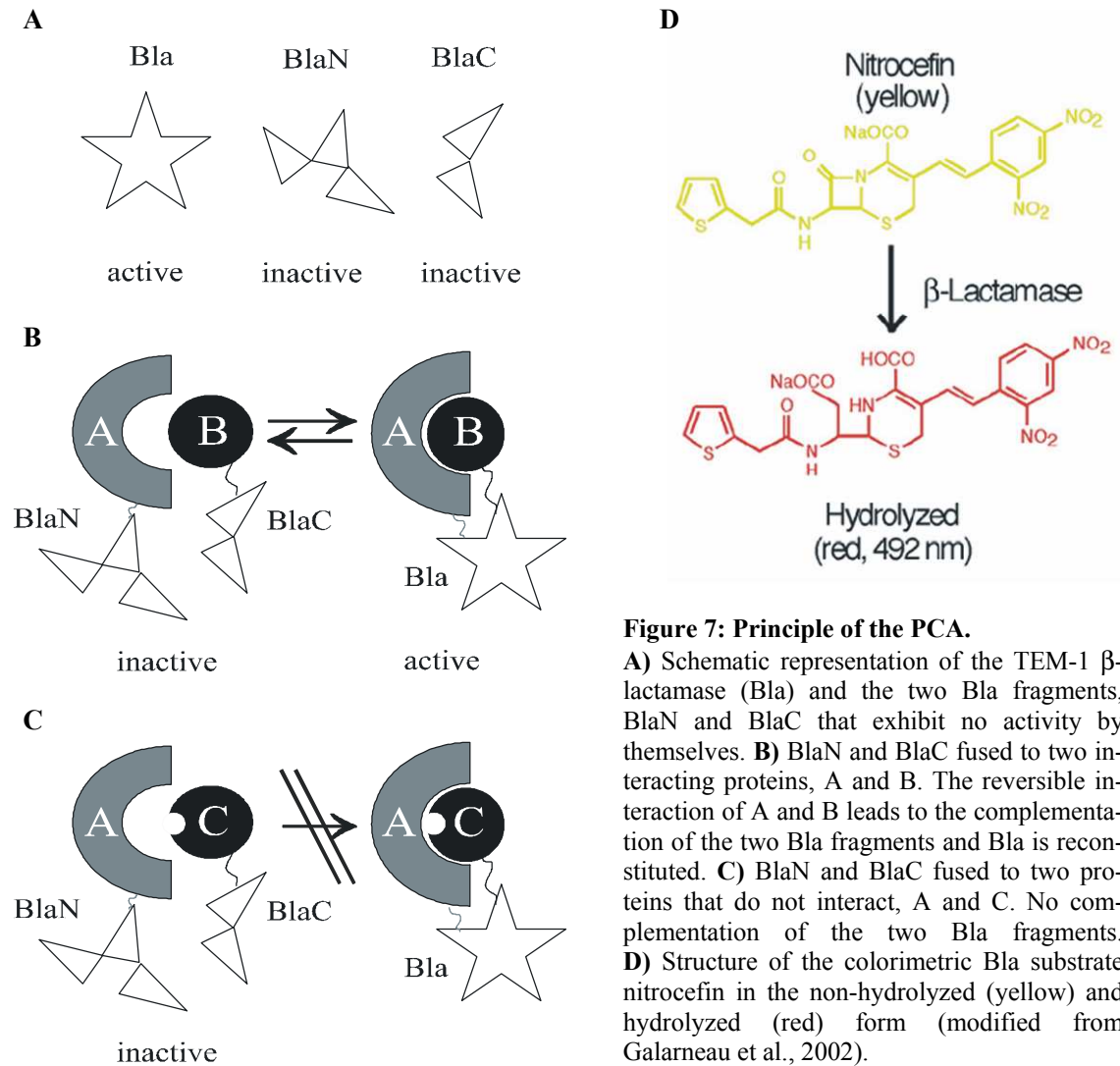
combined with functional validation experiments. As proof of principle the interaction partners of the protein kinase PKB/Akt were identified. PCAs were further suggested as tool for the validation of drugs and high-throughput screens for inhibitory compounds (Luker et al., 2004). Reichel and colleagues (Dirnberger et al., 2006) recently proposed the adaptation of the ubiquitin-PCA (Johnsson and Varshavsky, 1994) to a small molecule three-hybrid system. Two receptors (A and B), one of them (A) the designated drug target, are fused to the ubiquitin halves. Interaction, followed by the PCA readout, might be induced by addition of a bivalent hybrid organic molecule, binding to one receptor (B) and potentially to the second (A). This alternative three-hybrid technology for the detection of protein-small molecule interactions can be adapted to a HTS but keeps the flexibility of a PCA.

### 3.3.3. The TEM-1 $\beta$ -lactamase in the PCA

The TEM-1  $\beta$ -lactamase of *Escherichia coli* (EC 3.5.2.6.) combines most of the features desired for a PCA. The enzyme, a product of the ampicillin resistance gene Amp<sup>r</sup>, is small and monomeric (Sutcliffe, 1978). It is normally secreted in the periplasmic space but accumulates in the cytoplasm of bacteria when the signal sequence of 23 amino acids is deleted (Kadonaga et al., 1984). The TEM-1  $\beta$ -lactamase (Bla) used in the PCA lacks the signal peptide for secretion and has a size of 29 kDa (Philippon et al., 1998). The small size of the protein fragments may prove crucial for many applications where the major risk is impaired folding of the interacting proteins. The Bla is not toxic and can be expressed in both eukaryotic cells and bacteria making the Bla-PCA applicable to both classes of organisms (Moore et al., 1997). Bla, as a bacterial enzyme, has no orthologues in eukaryotic cells, which reduces the background and subsequently improves the sensitivity of the assay. Finally, the structure and function of Bla is well characterized which facilitates the design of suitable fragments and has led to a remarkably variety of available substrates for the enzyme. Most suitable for a PCA are chromogenic or fluorescent substrates, like nitrocefin (O'Callaghan et al., 1972) or CCF2/AM (Zlokarnik et al., 1998). Both substrates are cell permeable, allowing Bla activity to be studied in whole cells as well as in cell lysates. The chromogenic substrate nitrocefin (Figure 7D) changes from yellow to red (absorption at 495 nm) when hydrolyzed by Bla.

Galarneau and Wehrman (Galarneau et al., 2002; Wehrman et al., 2002) were the first to establish a PCA using the TEM-1  $\beta$ -lactamase (Bla) as a reporter enzyme. They studied

the ideal sites for enzyme cleavage and possible protein fragments were examined for successful complementation to restore reporter enzyme activity (Figure 7B). Furthermore, the fragments were tested for the lack of activity by themselves and the lack of affinity to each other (Figure 7A).



### **3.4. Aims of this work**

Among other features, a potential drug for herpesviruses would ideally target all eight herpesviruses infecting humans even though they differ in several aspects from each other. Viruses belonging to the three subfamilies differ in their target cell types and in the duration of their replication cycle but share processes such as virus entry, replication and morphogenesis. Any essential interaction of viral proteins, which leaves cellular processes untouched, might serve as a potential drug target. Most favourable would be interactions conserved throughout all three herpesvirus subfamilies.

The aim of this work was to undertake a detailed study of the conserved UL34/UL31 interaction of different herpesviruses. The interaction of the two proteins is important and in some viruses even essential for the nuclear egress of the newly formed viral nucleocapsids. The interaction between the UL34 and UL31 family members seems to be crucial for their activity. The fact that they are involved in a herpesvirus specific process, which is not found in the host cell but strictly conserved among all known herpesviruses, make them interesting for evaluation as a potential and novel drug target. In addition, a study of their interaction in a comparative manner should result in a better understanding of their structure and function. Therefore, the protein complementation assay using the TEM-1  $\beta$ -lactamase (Bla) was chosen to establish a protein-protein interaction assay that would allow a detailed and comprehensive, but simple study of UL34/UL31 interaction.

#### **3.4.1. Establishment of the PCA**

The initial step was the establishment and validation of the PCA for MCMV M50 and M53, which are representative members of the UL34 and UL31 families, respectively. Both proteins and their interaction have been well studied (Bubeck et al., 2004; Lötzerich et al., 2006; Muranyi et al., 2002). Information on the binding motifs involved in the M50/M53 interaction and the tolerance of inserted tags has already been determined. Also deletion and point mutants of both proteins have been constructed and well characterized to enable the efficient design of the PCA with necessary controls. The work of Michnik and colleagues (Galarneau et al., 2002) was followed with minimal modifications for the design of suitable Bla<sub>N</sub> and Bla<sub>C</sub> fragments.

In order to validate the PCA, experiments were planned to determine the background of the Bla-PCA, as well as the specificity and functionality of the proteins. For determin-



ing the background, mutants of M50, shown to be deficient in binding to M53, were included in the PCA. The specificity of the assay was to be tested by competition experiments in the presence of wild type M50 while the functionality of the fusion proteins should be proved by replacing the native M50 and M53 with the Bla-fusion constructs in the MCMV virus context.

### 3.4.2. Study of the UL34/UL31 interaction in herpesviruses

Once established and validated for the MCMV proteins M50 and M53, the next step planned was to expand the PCA to accommodate homologues of other herpesviruses. All three subfamilies were to be included in the study, represented by PrV and HSV-1 as two  $\alpha$ -herpesviruses, HCMV and MCMV from the  $\beta$ -herpesvirus subfamily and EBV and MHV68 as representatives from the  $\gamma$ -herpesvirus subfamily. For characterization of the UL34/UL31 interaction, the primary goal was to evaluate the degree of protein conservation at a functional level. The data gained from replacement studies in isolated expression were aimed to be applied in the virus context. Successful replacement of conserved core proteins would allow them to be studied in the herpesvirus context even for proteins originating from viruses lacking suitable animal models. Furthermore, the aim was to use the PCA as a tool for identifying the binding sites within the members of both protein families.

### 3.4.3. Establishment of a potential high-throughput screen using the PCA

The final aim was to establish a PCA in a cell free system. UL50 and UL53, the M50 and M53 homologues of HCMV, were selected for expression in bacteria to study the minimal binding sites in the protein and to establish a purification protocol. Both HCMV proteins were to be expressed as fragments of the wild type proteins or as constructs for the PCA, thus fused to Bla-fragments. Successful Bla complementation of purified proteins in a cell free system would supply a cheap system for testing large numbers of small molecules for an inhibitory effect on the UL50/UL53 interaction.

## 4. Material

### 4.1. Devices

Bio-Photometer	Eppendorf, Germany
Centrifuge 5417 R	Eppendorf, Germany
Centrifuge Avanti™ J-20xp	Beckman Coulter GmbH, Germany
Centrifuge L8-55M	Beckman Coulter GmbH, Germany
Crystal Screen 1	Hampton Research, USA
Crystal Screen 2	Hampton Research, USA
EagleEye	Bio-Rad, Germany
Gene Pulser™	Bio-Rad, Germany
Incubator (B5050E)	Heraeus Instruments, Germany
Incubator BB16CU	Heraeus Instruments, Germany
Incubator shaker ISF- 1- W	Kühner, Adolf AG, Switzerland
Light microscope Axiovert 25	Zeiss Carl AG, Germany
Luminometer	Perkin Elmer, Germany
Mini-PROTEAN3 Cell (SDS-Page apparatus)	Bio-Rad, Germany
Multifuge 3 S-R	Heraeus Instruments, Germany
ND-1000 Spectrophotometer	Nanodrop, USA
PCR machine	Roche, Germany
Semi-Dry-Transfer Cell (Trans-BlotSD)	Bio-Rad, Germany
Sonifier 450	Branson, England
Thermomixer 5436	Eppendorf, Germany
Versamax	Molecular Devices
Vortex-Mixer	Bender/Hobein AG, Switzerland
Water Bath F10	Julabo, Germany

### 4.2. Reagents and Consumables

Acetic Acid	Merck, Germany
Agar	Becton Dickinson, Germany
Agarose	Invitrogen, Germany
Ammonium Persulfate	Sigma, Germany
Ampicillin	Sigma, Germany
Cell culture dishes (145 cm <sup>2</sup> )	Sarstedt, Germany
Cell culture dishes (20 cm <sup>2</sup> , 55 cm <sup>2</sup> )	Becton, Germany
Chloramphenicol	Sigma, Germany
Conical Tubes, Falcon	Becton Dickinson, Germany
Dimethylsulfoxid (DMSO)	Merk, Germany
DNA ladder (100bp, 1kbp)	NEB, Germany
dNTPs	NEB, Germany
Dulbecco´s modified Eagle medium DMEM)	Invitrogen, Germany
Electroporation cuvettes	Bio-Rad, Germany
Ethanol	Roth, Germany
Ethylen-Diamin-Tetra-Acetic acid (EDTA)	Fluka, Karlsruhe
Fetal calf serum (FCS)	Invitrogen, Germany

Glycerol	Roth, Germany
Glycin	Roth, Germany
Hybond P- membrane	Amersham, Germany
Hyperfilm ECL	Amersham Pharmacia, Germany
Imidazole	Roth, Germany
IPTG	Roth, Germany
Isopropanol	Merck, Germany
Kanamycin	Sigma, Germany
L-Glutamin	Invitrogen, Germany
Magnesiumchlorid (MgCl <sub>2</sub> x6H <sub>2</sub> O)	Fluka, Germany
β-Mercaptoethanol	Sigma, Germany
Methanol	Roth, Germany
Methylcellulose	Sigma, Germany
Microcentrifuge tubes	Eppendorf, Germany
Modified Eagle Medium (MEM)	Invitrogen, Germany
NaCl	Merck, Germany
New born calf serum (NCS)	Invitrogen, Germany
Ni <sup>2+</sup> - NTA	Quiagen, Germany
Nitrocefin	Oxoid, Germany
PBS (Phosphate buffered saline)	Invitrogen, Germany
Penicillin-Streptomycine	Invitrogen, Germany
Phenol/Chloroform	Roth, Germany
Pipettes (5 ml, 10 ml, 25 ml)	Sarstedt, Germany
Protein ladder, low range	Biorad, Germany
Rapamycin	Sigma, Germany
Reporter Lysis buffer	Promega, Germany
Restriction enzymes	New England Biolabs (NEB)
RNase, DNase free Uvette	Eppendorf, Germany
Rotiphorese Gel 30	Roth, Germany
RPMI 1640	Invitrogen, Germany
Skim milk powder	Roth, Germany
Superfect	Quiagen, Germany
T4 Ligase	New England Biolabs (NEB)
TEMED	Sigma, Germany
Tris	Roth, Germany
Trypsin/EDTA	Invitrogen, Germany
Trypton	Becton Dickinson, Germany
Tween-20	Sigma, Germany
Urea	Fluka, Germany
Whatman paper	Machery & Nagel, Germany
Yeast Extract	Becton Dickinson, Germany
Zeocin	Invitrogen, Germany

#### 4.2.1. Kits

ECL plus Western blotting detection System	Amersham Pharmacia, Germany
Expand High Fidelity PCR system	Roche, Germany
GFX PCR; DNA and Gel band purification Kit	Amersham Pharmacia, Germany
GFX Micro Plasmid Preparation Kit	Amersham Pharmacia, Germany
Nucleobond PC100	Macherey-Nagel, Germany

### 4.3. Plasmids

#### 4.3.1. Commercially available and published plasmids

pCP20	Cherepanov and Wackernagel, 1995
pOriR6K	Miller and Mekalanos, 1988
pUC19	NEB, USA
RC <sub>4</sub> RH <sub>1</sub> E	Ariad, USA
C <sub>4</sub> EN-F <sub>1</sub>	Ariad, USA
Litmus28	NEB, USA
pO6-IET-gfp	Rupp et al., 2005
pOriR6K-zeo-ie	Bubeck et al., 2004
pOriR6K-zeo-ie-M50	Bubeck et al., 2004
pOriR6K-zeo-ie-M50-aa52,	Bubeck et al., 2004
pOriR6K-zeo-ie-M50-aa114	Bubeck et al., 2004
pOriR6K-zeo-ie-M53	Lötzerich et al., 2006
pCDNA4/TO	Invitrogen, Germany
pSMfr3-16FRT17	Wagner et al., 1999
pSMfr3-ΔM50	Bubeck et al., 2004
pSMfr3-ΔM53	Lötzerich et al., 2006
pET-24b	Novagene, USA
bicistronic pET-28b	kind gift from A. Meinhart

#### 4.3.2. Plasmids constructed over the project.

##### 4.3.2.1. Basic Bla-fusion vectors

###### **pL-Spacer**

Two complementary synthetic oligonucleotide pairs, encoding for a 17 aa glycine/serine spacer (S1/S2 and S3/S4, see chapter 11.3.1) were annealed and joined by XbaI digestion followed by ligation (Galarneau et al., 2002). The resulting DNA fragment was inserted into the Litmus28 (NEB) vector by BglIII and AflIII.

###### **pL-BlaN**

The N-terminal part of TEM-1 β-lactamase (Bla; EC: 3.5.2.6) was PCR amplified from pUC19 by the primers BlaNfor and BlaNrev. The PCR fragment was cleaved by BspEI and AflIII and introduced in the respectively cleaved pL-Spacer.

###### **pL-BlaC**

The C-terminal part of Bla was PCR amplified from pUC19 using the BlaCfor and BlaCrev primers. The PCR fragment was cleaved by BamHI and ApaI and introduced in the respectively cleaved pL-Spacer.

###### **pL-HA-Spacer**

The pL-Spacer was cut with BspEI and AflIII and the annealed HA1 and HA2 oligonucleotides, encoding for the HA-tag, were inserted resulting in pL-HA-Spacer.

**pL-HA-N**

The coding sequence for the N-terminal part of Bla was PCR amplified from pUC19 (NEB) using the primer pair BlaNfor and BlaNrev. The N-terminal fragment of the Bla (aa24-aa194) was cloned into pL-HA-Spacer by BspEI/NheI resulting in pL-HA-N.

**pL-HA-C**

The coding sequence for the C-terminal part of Bla (aa196-aa286) was PCR amplified from pUC19 (NEB) using the BlaCfor/BlaCrev primer pair. The fragment was then cloned into pL-HA-Spacer by AflII/BspEI resulting in pL-HA-C.

**pL-C-ST**

The pL-Spacer was cut with NotI and BamHI and the annealed ST1 and ST2 oligonucleotides, encoding for the Strep-tag, were inserted resulting in pL-Spacer-ST. The C-terminal part of Bla (aa196-aa286) was cut from pL-HA-C by NheI and BspEI and cloned into the AgeI and XbaI sites of pL-Spacer-ST, resulting in pL-C-ST.

## 4.3.2.2. Expression plasmids

In the following chapter, the plasmids used for protein expression are listed with detailed information of their construction. Table 1 is a comprehensive list containing names of the proteins used in the result section and the expression plasmid described in this chapter.

**Table 1 : Proteins and their corresponding expression plasmids.**

Alphabetical list of proteins as referred to in the result section and the corresponding expression vector.

<b>Protein</b>	<b>Plasmid</b>
BlaS	pO6T-BlaS
C-BFLF2	pO6T-C-BFLF2
C-CG	pO6T-C-CG
C-CP	pO6T-C-CP
C-GM	pO6T-C-GM
C-GP	pO6T-C-GP
C-M53	pO6T-C-M53
C-MG	pO6T-C-MG
C-MP	pO6T-C-MP
C-Orf69	pO6T-C-Orf69
C-PG	pO6T-C-PG
C-PM	pO6T-C-PM
C-UL31(HSV)	pO6T-C-UL31(HSV)
C-UL31(PrV)	pO6T-C-UL31(PrV)
C-UL53	pO6T-C-UL53
CUL53_His	pET24-CUL53-His
F-C	pO6T-F-C
M53-C	pO6T-M53-C
N-BFRF1	pO6T-N-BFRF1
N-M50	pO6T-N-M50
N-M50DM	pO6T-N-M50DM
N-M50DM*	pO6T-N-M50DM*
N-M50i114	pO6T-N-M50i114
N-M50i52	pO6T-N-M50i52
N-Orf67	pO6T-N-Orf67
N-R	pO6T-N-R
N-UL34(HSV)	pO6T-N-UL34(HSV)
N-UL34(PrV)	pO6T-N-UL34(PrV)
N-UL34DM	pO6T-N-UL34DM
N-UL34DM*	pO6T-N-UL34DM*
N-UL50	pO6T-N-UL50
NUL50_His	pET24-NUL50-His
NUL50DM_His	pET24-UL50DMHis
UL50_His	pET24-UL50-His
UL50_His and UL53_1	pET28-UL50His/UL53_1
UL50_His and UL53_2	pET28-UL50His/UL53_2
wt M50	pOriR6K-zeo-ie-M50
wt M53	pOriR6K-zeo-ie-M53

### **pO6T**

Vector elements of pOri6K-zeo-ie (Bubeck et al., 2004) and pCDNA4TO (Invitrogen) were combined to add a tet-operator regulation cassette to the HCMV promoter of the expression plasmid pOri6kie. Both vectors were cleaved by NdeI and EcoRV. The 550 bp fragment obtained from pCDNA4T was ligated to the vector fragment of pOri6kie resulting in pO6T.

### **pO6T-BlaS**

The N-terminal part of Bla was PCR amplified from pUC19 by the primers BlaNfor and BlaNrev. The PCR fragment was cleaved by BspEI and AflII and introduced in the respectively cleaved pL-BlaC, resulting in pL-BlaS. The coding sequence of BlaS was removed from the Litmus28 backbone and transferred to the expression plasmid pO6T by cleaving pL-BlaS with AflII and SnaBI and subsequent insertion into pO6T, linearized by AflII and EcoRV.

### **pO6T-N-R**

The coding sequence for FRB (R) was isolated from pC<sub>4</sub>-R<sub>H</sub>E by a BamHI and EcoRI cleavage and introduced in the equally treated Litmus28, resulting in pL-R. The FRB coding sequence was combined with BlaN by insertion into pL-BlaN. For that, pL-BlaN was cleaved by BglII und AvrII and ligated with the smaller fragment of pL-R after XbaI and BamHI cleavage, resulting in pL-R-N. The R-N sequence was transferred to the expression plasmid pO6T by cleaving pL-R-N with AflII and SnaBI followed by insertion into pO6T, linearized by AflII and EcoRV.

### **pO6T-F-C**

The coding sequence for FKBP12 (F) was isolated from pC<sub>4</sub>EN-F<sub>1</sub> by a BamHI and EcoRI cleavage and introduced in the equally treated Litmus28, resulting in pL-F. The F-fragment was removed from the Litmus28 vector by SpeI and BsiWI cleavage and inserted into pL-BlaC in between the BsiWI and NheI sites, resulting in pL-F-C. The F-C part was transferred to the expression plasmid pO6T by cleaving pL-F-C with AflII and SnaBI followed by into pO6T, linearized by AflII and EcoRV.

### **pOriR6K-zeo-ie-M50D**

The M50 mutant M50D was generated by inverse PCR on the pOriR6K-zeo-ie-M50 using the primers delmo-NheI-for and delmo2-Nhe-rev resulting in pOriR6K-zeo-ie-M50D. The PCR fragment obtained contained the vector backbone and the two parts of the M50 ORF, lacking nine amino acids that were defined as the M50 binding motif to M53 (Bubeck et al., 2004). The fragment was cleaved by NheI and religated.

### **pO6T-N-M50**

For construction of the BlaN-M50 fusion, the wt M50 fragment was PCR amplified from pOriR6K-zeo-ie-M50 using the primer pair M50for and M50rev. The PCR fragment obtained was inserted into pL-HA-N by SapI and AgeI. Fusion constructs were isolated from the Litmus28 vector after AflII and BspEI digest, filled-in and cloned into expression plasmid pO6T between the EcoRV and AflII sites.

#### **pO6T-N-M50DM, pO6T-N-M50i52, pO6T-N-M50i114**

The ORFs of M50D, M50i52 and M50i114 were amplified by the primers M50for and M50rev on the respective expression plasmids pOriR6K-zeo-ie-M50D, pOriR6K-zeo-ie-M50-aa52 and pOriR6K-zeo-ie-M50-aa114. The PCR fragments obtained were cleaved by SapI and AgeI and inserted into the adequately opened pL-HA-N. Fusion constructs were isolated from the Litmus28 vectors by AflII and BspEI digest, filled-in and cloned into the expression plasmid pO6T between the EcoRV and AflII sites. The constructs were named pO6T-N-M50DM, pO6T-N-M50i52 and pO6T-N-M50i114, respectively.

#### **pO6T-C-M53**

To generate the BlaC-M53 fusion, the M53 ORF was amplified from pOriR6K-zeo-ie-M53 (Lötzerich et al., 2006) using the primers M53for and M53rev. The fragment was inserted into pL-HA-C by the BamHI and ApaI sites. Fusion constructs were isolated from the Litmus28 vectors by AflII and BspEI digest, filled-in and cloned into the expression plasmid pO6T between the EcoRV and AflII sites.

#### **pO6T-M53-C**

The M53 ORF was amplified from pOriR6K-zeo-ie-M53 (Lötzerich et al., 2006) using the primers M53Aflfor and M53Saprev, cleaved by AflII and SapI and inserted into the AflII/SapI opened vector pL-BlaC. From there the M53 ORF was transferred into pL-C-ST by BamHI and AflII, resulting in pL-M53-C-ST. For the transfer from the Litmus28 backbone to the pO6T expression vector, M53-C-ST was removed by a SnaBI and AflII digest and cloned into the AflII and EcoRV sites in pO6T.

#### **pO6T-N-UL34(HSV)**

UL34 of HSV-1 was fused to the N-terminal Bla fragment. The ORF was PCR amplified on BAC-DNA by the primers HSVUL34for and HSVUL34rev. The resulting fragment was inserted into pL-HA-N by the XhoI and AgeI sites. The fusion construct was transferred into pO6T by AgeI and NheI, generating pO6T-N-UL34(HSV).

#### **pO6T-N-UL34(PrV), pO6T-N-UL50, pO6T-N-BFRF1, pO6T-N-Orf67**

UL34 of PrV, UL50 of HCMV, Orf67 of MHV68 and BFRF1 of EBV were fused to the N-terminal Bla fragment. ORFs were PCR amplified on viral DNA, BAC-DNA or plasmids (see chapter 4.9 for DNA and virus strains) by the primer pairs UL34PrVfor/UL34PrVrev, UL50for/UL50rev, ORF67for/ORF67rev and BFRF1for/BFRF1rev, respectively. The resulting fragments were inserted into pL-HA-N by the BamHI and AgeI sites. The fusion constructs were then transferred into pO6T by AgeI and NheI, generating pO6T-N-UL34(PrV), pO6T-N-UL50, pO6T-N-Orf67 and pO6T-N-BFRF1.

#### **pO6T-C-UL31(HSV)**

UL31 of HSV-1 was fused to the C-terminal Bla fragment. The ORF was PCR amplified on BAC-DNA by the primer pair HSVUL31for/HSVUL31rev. The resulting fragment was inserted into pL-HA-C by BamHI and NotI. The fusion fragment was removed from the Litmus28 vector by AflII/BspEI cleavage, filled-in and inserted into pO6T between the EcoRV and AflII sites, resulting in pO6T-C-UL31(HSV).



**pO6T-C-UL31(PrV), pO6T-C-UL53, pO6T-C-Orf69, pO6T-C-BFLF2**

UL31 of PrV, UL53 of HCMV, Orf69 of MHV68 and BFLF2 of EBV were fused to the C-terminal Bla fragment. ORFs were PCR amplified on viral DNA, BAC-DNA or plasmids (see chapter 4.9 for DNA and virus strains) by the primer pairs UL31PrVfor/UL31PrVrev, UL53for/UL53rev, ORF69for/ORF69rev and BFLF2for/BFLF2rev, respectively. The resulting fragments were inserted into pL-HA-C by BamHI and ApaI. The fusion constructs were removed from the Litmus28 vectors by AflIII/BspEI cleavage, filled-in and inserted in pO6T between the EcoRV and AflIII sites, resulting in pO6T-C-UL31(PrV), pO6T-C-UL53, pO6T-C-Orf69 and pO6T-C-BFLF2.

**pO6T-C-MP**

A chimeric UL31 fusion protein was constructed by the fusion of the variable region (V) and the first conserved region (CR1) of M53 (aa1-aa175) and the second to the fourth conserved region (CR2-CR4) of UL31 of PrV (aa92-aa271). The M53-fragment was PCR amplified from pO6T-C-M53 with the primer pair MP-Mfor and MP-Mrev and cleaved with BsrDI. The PrV UL31 fragment was PCR amplified from pO6T-C-UL31(PrV) with the primer pair MP-Pfor and MP-Prev and cleaved with BsrDI and NotI. Both fragments were ligated to the vector fragment of pO6T-C-M53 after BsrDI and NotI cleavage, resulting in pO6T-C-MP.

**pO6T-C-MG**

The V and CR1 of M53 (aa1-aa175) were fused to the CR2-CR4 of Orf69 of MHV68 (aa112-aa292). The Orf69 fragment was PCR amplified from pO6T-C-Orf69 by the primer pair MG-Gfor and MG-Grev and cleaved by BstAPI and NotI. The PCR fragment was inserted between the BstAPI and NotI sites of pO6T-C-M53, resulting in pO6T-C-MG.

**pO6T-C-PM**

The V and CR1 of UL31 (aa1-aa91) were fused to the CR2-CR4 of M53 (aa176-aa333). The UL31 fragment was PCR amplified from pO6T-C-UL31(PrV) by the primer pair PM-Pfor and PM-Prev and cleaved by BspMI and BsrDI. The PCR fragment was inserted between the BspMI and BsrDI sites of pO6T-C-M53, resulting in pO6T-C-PM.

**pO6T-C-GM**

The V and CR1 of Orf69 (aa1-aa111) were fused to the CR2-CR4 of M53 (aa176-aa333). The Orf69 fragment was PCR amplified from pO6T-C-Orf69 by the primer pair GM-Gfor and GM-Grev and cleaved by BspMI and BsrDI. The PCR fragment was inserted between the BspMI and BsrDI sites of pO6T-C-M53, resulting in pO6T-C-GM.

**pO6T-C-CP**

The V and CR1 of UL53 (aa1-aa125) were fused to the CR2-CR4 of UL31 of PrV (aa92-aa271). The UL53 fragment was PCR amplified from pO6T-C-UL53 by the primer pair CP-Cfor and CP-Crev and cleaved by BsrDI. The UL31 fragment was PCR amplified from pO6T-C-UL31(PrV) by the primer pair GP-Pfor and MP-Prev and cleaved by BsrDI and NotI. The PCR fragment was inserted between the NotI and BsrDI sites of pO6T-C-UL53, resulting in pO6T-C-CP.

### **pO6T-C-CG**

The V and CR1 of UL53 (aa1-aa125) were fused to the CR2-CR4 of Orf69 of MHV68 (aa112-aa292). The Orf69 fragment was PCR amplified from pO6T-C-Orf69 by the primer pair CG-for and MG-Grev and cleaved with DraIII and NotI. The PCR fragment was inserted between the NotI and BsrDI sites of pO6T-C-UL53, resulting in pO6T-C-CG.

### **pO6T-C-GP**

The V and CR1 of Orf69 (aa1-aa111) were fused to the CR2-CR4 of UL31 of PrV (aa92-aa271). The Orf69 fragment was PCR amplified from pO6T-C-Orf69 by the primer pair GM-Gfor and GP-Grev and cleaved by BsrDI. The UL31 fragment was PCR amplified from pO6T-C-UL31(PrV) by the primer pair GP-Pfor and MP-Prev and cleaved by BsrDI and NotI. The PCR fragment was inserted between the NotI and BsrDI sites of pO6T-C-M53, resulting in pO6T-C-GP.

### **pO6T-C-PG**

The V and CR1 of UL31 (aa1-aa91) were fused to the CR2-CR4 of Orf69 (aa112-aa292). The Orf69 fragment was PCR amplified from pO6T-C-Orf69 by the primer pair PG-Gfor and MG-Grev and cleaved by SapI and NotI. The UL31 fragment was PCR amplified from pO6T-C-UL31(PrV) by the primer pair PG-Prev and PM-Pfor and cleaved by SapI and BsrDI. The PCR fragment was inserted between the NotI and BsrDI sites of pO6T-C-M53, resulting in pO6T-C-PG.

### **pO6T-N-UL34DM**

The homologous nine aa of the binding motif in M50 (Bubeck et al., 2004) were deleted in UL34. For that, a part of the UL34 ORF of HSV-1 was PCR amplified from pO6T-N-UL34(HSV) by the primer pair UL34DMfor and UL34DMrev and cleaved by PpuMI and BsrDI. The PCR fragment was inserted into the equally treated expression vector from pO6T-N-UL34(HSV), resulting in pO6T-N-UL34DM.

### **pO6T-N-UL34DM\***

The 45 aa of the predicted binding motif in UL34 (Liang and Baines, 2005) were deleted in UL34. For that, two parts of the UL34 ORF of HSV-1 were PCR amplified from pO6T-N-UL34(HSV). The first fragment was amplified by the primer pair HSVUL34for and UL34DM\*rev and treated with SapI and XhoI. The second fragment was amplified by the primer pair UL34DM\*for and HSVUL34rev and treated with SapI and AgeI. Both fragments were ligated to the XhoI/AgeI opened vector pL-HA-N, resulting in pL-HA-NUL34DM\*. The coding sequence of NUL34DM\* was transferred to the expression vector by the exchange of NUL34 against NUL34DM\* in pO6T-N-UL34(HSV) between the XmnI and AgeI site, resulting in pO6T-N-UL34DM\*.

### **pO6T-N-M50DM\***

The homologous 47 aa of the binding motif in UL34 (Liang and Baines, 2005) were deleted in M50. For that, a part of the M50 ORF was PCR amplified from pO6T-N-M50 by the primer pair M50DM\*for and M50rev and treated with BssSI and AgeI. The PCR fragment introduced the mutation in the M50 ORF by fragment exchange between the BssSI and AgeI sites of pO6T-N-M50, resulting in pO6T-N-M50DM\*.

#### 4.3.2.3. Shuttle plasmids for BAC mutagenesis

##### **pO6ieUL34(HSV), pO6ieUL34(PrV), pO6ieUL31(HSV), pO6ieUL31(PrV)**

The UL34 and UL31 ORFs of HSV-1 and PrV were PCR amplified from pO6T-N-UL34(HSV) and pO6T-N-UL34(PrV) by the primer pairs HSVUL34(pOri)for/HSVUL34(pOri)rev, PrVUL34(pOri)for/PrVUL34(pOri)rev, HSVUL31(pOri)for/HSVUL31rev and PrVUL31(pOri)for/PrVUL31(pOri)rev, respectively. The PCR fragments were cleaved by KpnI and EcoRV and inserted into the correspondingly treated pori6K-zeo- ie.

##### **pO6ieUL50 and pO6ieUL53** (constructed by Anja Bubeck, unpublished)

The UL50 and UL53 ORF were PCR amplified from the AD169 BAC by the primer pairs 5'KpnIUL50/3'XhoIUL50 and 5'KpnIUL53/3'XhoIUL53, respectively. The PCR fragments were cleaved by KpnI and XhoI and inserted into the correspondingly treated pOriR6K-zeo-ie, resulting in pO6ieUL50 and pO6ieUL53.

##### **pO6ieOrf69**

The Orf69 ORF was PCR amplified from pO6T-C-Orf69 by the primer pair. Orf69(pOri)for and MG-Grev. The PCR fragment was cleaved by KpnI and NotI and inserted into the correspondingly treated pO6ieM53.

##### **pO6ieGP**

The GP coding sequence was removed from pO6T-C-GP by a NarI and NotI digest and inserted into the NarI/NotI treated pO6ieOrf69.

##### **pO6ieCP and pO6ieCG**

The CP and CG coding sequence was removed from pO6T-C-CP and pO6T-C-CG by an ApaI and BsiWI digest and inserted into the ApaI/BsiWI treated pO6ieUL53.

#### 4.3.2.4. Plasmids for bacterial expression

##### **pET24-UL50-His**

A fragment of UL50 (aa1-aa172) was PCR amplified from pO6T-N-UL50 by the primer pair UL50-Hisfor and UL50-Hisrev. The fragment was cleaved by NdeI and NotI and inserted between the NdeI and NotI sites in pET-24b.

##### **pET28-UL50His/UL53\_1**

The two ORFs coding for UL50His and UL53\_1 were introduced into a modified pET-28b expression vector for bicistronic expression (provided by A. Meinhart). A fragment of UL50 was PCR amplified from pO6T-N-UL50 by the primer pair UL50-Hisfor and UL50-Hisrev and introduced into the equally treated bicistronic vector, resulting in pET28-UL50His. The UL53\_1 ORF was PCR amplified from pO6T-C-UL53 by the primer pair UL53\_1for/ UL53\_1rev, cleaved by HindIII and NcoI and inserted into the HindIII/NcoI opened pET28-UL50His, resulting in pET28-UL50His/UL53\_1.

**pET28-UL50His/UL53\_2**

The UL53\_2 ORF was PCR amplified from pO6T-C-UL53 by the primer pair UL53\_1for/ UL53\_2rev, cleaved by HindIII and NcoI and inserted into the HindIII/ NcoI opened pET28-UL50His (see construction of pET28-UL50His/UL53\_1), resulting in pET28-UL50His/UL53\_2.

**pET24-NUL50-His and pET24-CUL53-His**

Parts of the N-UL50 and C-UL53 ORF were PCR amplified by the primer pairs HAfor/UL53\_PCAREV and HAfor/UL50-Hisrev on pO6T-N-UL50 and pO6T-C-UL53, respectively. The PCR fragments were cleaved by NdeI and NotI and inserted between the NdeI and NotI sites in pET-24b.

**pET24-NUL50DM-His**

First, the BlaN fragment was introduced into pET-24b. BlaN was amplified from pO6T-N-UL50 by the primer pair BlaNbactfor and BlaNbactrev, treated with BamHI and NdeI and introduced into the respective sites in pET-24b, resulting in pET24BlaN. To introduce the deletion of the UL50 binding motif, the N- and C-terminal part of UL50 were PCR amplified by the primer pairs UL50\_PCAfor/UL50DMrev and UL50DMfor/UL50-Hisrev. The N-terminal fragment was treated with BamHI and SapI, the C-terminal fragment was treated with SapI and NotI. Both fragments were ligated into the BamHI and NotI cleavage sites of pET24BlaN, resulting in pET24BlaN-UL50DM. For the addition of the HA-tag, the UL50 in pET24-NUL50-His was exchanged by UL50DM of pET24BlaN-UL50DM between the BamHI and NdeI sites, resulting in pET24-NUL50DM-His.

## 4.3.2.5. MCMV BACs

Mutant MCMV BACs were generated by insertion of pO6T or pOriR6K-zeo-ie derived expression plasmids into pSM3fr-16FRT17 (wt MCMV BAC) or pSMfr3- $\Delta$ M50 and pSMfr3- $\Delta$ M53. Table 2 shows the summary of constructed BAC mutants by the Flp mediated recombination of FRT sites present in the viral BAC and the insertion plasmids (chapter 5.5.1).

**Table 2 : BACs constructed during this study.**

<b>BAC -backbone</b>	<b>Inserted plasmid</b>	<b>resulting mutant BAC</b>
pSM3fr-16FRT17	pO6T-N-M50	wt/N-M50
pSM3fr-16FRT17	pO6T-C-M53	wt/C-M53
pSM3fr-16FRT17	pO6ieUL34(HSV)	wt/UL34(HSV)
pSM3fr-16FRT17	pO6ieUL31(HSV)	wt/UL31(HSV)
pSM3fr-16FRT17	pO6ieUL34(PrV)	wt/UL34(PrV)
pSM3fr-16FRT17	pO6ieUL31(PrV)	wt/UL31(PrV)
pSM3fr-16FRT17	pO6ieOrf69	wt/Orf69
pSM3fr-16FRT17	pO6T-N-UL34(HSV)	wt/N-UL34(HSV)
pSM3fr-16FRT17	pO6T-C-UL31(HSV)	wt/C-UL31(HSV)
pSM3fr-16FRT17	pO6T-N-UL34(PrV)	wt/N-UL34(PrV)
pSM3fr-16FRT17	pO6T-C-UL31(PrV)	wt/C-UL31(PrV)
pSM3fr-16FRT17	pO6ieMP	wt/MP
pSM3fr-16FRT17	pO6ieMG	wt/MG
pSM3fr-16FRT17	pO6ieGP	wt/GP
pSM3fr-16FRT17	pO6iePG	wt/PG
pSM3fr-16FRT17	pO6ieCG	wt/CG
pSM3fr-16FRT17	pO6ieCP	wt/CP
pSMfr3- $\Delta$ M50	pO6T-N-M50	$\Delta$ M50/N-M50
pSMfr3- $\Delta$ M50	pOieUL50	$\Delta$ M50/UL50
pSMfr3- $\Delta$ M50	pO6ieUL34(HSV)	$\Delta$ M50/UL34(HSV)
pSMfr3- $\Delta$ M50	pO6ieUL34(PrV)	$\Delta$ M50/UL34(PrV)
pSMfr3- $\Delta$ M50	pO6ieUL50	$\Delta$ M50/UL50
pSMfr3- $\Delta$ M53	pO6T-C-M53	$\Delta$ M53/C-M53
pSMfr3- $\Delta$ M53	pO6ieUL53	$\Delta$ M53/UL53
pSMfr3- $\Delta$ M53	pO6ieUL31(HSV)	$\Delta$ M53/UL31(HSV)
pSMfr3- $\Delta$ M53	pO6ieUL31(PrV)	$\Delta$ M53/UL31(PrV)
pSMfr3- $\Delta$ M53	pO6ieOrf69	$\Delta$ M53/Orf69
pSMfr3- $\Delta$ M53	pO6ieMP	$\Delta$ M53/MP
pSMfr3- $\Delta$ M53	pO6ieMG	$\Delta$ M53/MG

**4.4. Cells**

NIH3T3	murine fibroblasts	ATCC CRL 1658
293T	human kidney carcinoma cells	ATCC CRL 11268
M2-10B4	bone marrow stroma cells	ATCC CRL 1972
A549	lung epithelium	ATCC CCL-185
MEF	Mouse embryonic fibroblasts	BALB/c mice (Serrano et al., 1997)

**4.5. Bacteria**

DH10B (recA <sup>-</sup> )	Invitrogen, Germany
Pir1	Invitrogen, Germany
BL21-CodonPlus (DE3)-RIL	Stratagene, Netherlands

**4.6. Viruses**

The MCMV wild type (wt) and mutant viruses used in this study were derived from the bacterial artificial chromosomes (BACs) pSM3fr (Wagner et al., 1999), pSMfr3- $\Delta$ M50 (Bubeck et al., 2004) and pSMfr3- $\Delta$ M53 (Lötzerich et al., 2006) and constructed BACs, summarized in Table 2. For virus reconstitution, BAC-DNA was transfected into MEF cells (chapter 5.5.2).

**4.7. Oligonucleotides**

Oligonucleotides were synthesized by Metabion (Martinsried, Germany). For sequences see supplementary tables in chapter 11.3.

**4.8. Antibodies**

The M50 specific polyclonal antiserum was obtained from W. Muranyi (Muranyi et al., 2002). The Anti-HA-Peroxidase High Affinity antibody was purchased from Roche, Germany.

**4.9. Viral template DNA**

Template DNA for amplification and subsequent cloning was obtained as BACs or plasmids with subcloned ORFs of UL34 or UL31 homologues. The DNA originated from following strains:

PrV	Kaplan strain	viral DNA, kind gift from P.Sondermeier
HSV-1	Strain 17	subcloned ORFs, kind gift from J. Haas
MCMV	Smith strain	Messerle et al., 1997
HCMV	Strain AD169	Borst et al., 1999
EBV	Strain B95-8	subcloned ORFs, kind gift from J. Haas
MHV68		Adler et al., 2000

## 5. Methods

If not specifically mentioned, the methods used for this work conform with the protocols published by Sambrook and Russel in the Molecular Cloning manual (Sambrook and Russel, 2001). When commercially available kits were used, manufacturer's instructions were followed. For details see the user protocol of the according kit.

### 5.1. Isolation and purification of DNA

#### 5.1.1. Small scale isolation of plasmid DNA

Bacteria were cultivated over night (o.n.) at 37 °C on agar plates containing the adequate antibiotics for selection of the plasmids of interest. For small scale plasmid analysis (mini-preparation), single clones were picked and 3 ml of LB medium, with the respective antibiotics added, were inoculated and cultured at 37 °C either for 5-6 h or o.n. To isolate DNA, the GFX Micro Plasmid Preparation Kit (Amersham Pharmacia) was used and manufacturer's instructions followed. Plasmid DNA was recovered from the DNA binding columns of the kit by 100 µl distilled water. 5 µl were analysed by restriction pattern analysis (chapter 5.2.1).

#### *LB-medium (1l)*

10 g Bacto tryptone  
5 g Bacto yeast extract  
5 g NaCl

#### *Antibiotics*

zeocin: 30 µg/ml  
kanamycin: 50 µg/ml  
chloramphenicol: 25 µg/ml  
ampicillin: 50 µg/ml

#### *LB-agar (500 ml)*

7,5 g agar in 500 ml LB

#### 5.1.2. Large scale isolation of plasmid DNA

Large amounts of DNA necessary for cloning or transfection experiments were isolated from bacteria by the use of Nucleobond PC100 kit (Macherey-Nagel). DNA was isolated from 200 ml o.n. cultures that were inoculated with drops of the culture used for the plasmid analysis (mini-preparation) or a scratch of a glycerol culture of the bacteria bearing the plasmid of interest. For the preparation, the manufacturers instructions were followed. Dried DNA precipitates were resuspended in 150 µl distilled water and stored at -20 °C.

### 5.1.3. Small scale isolation of BAC-DNA

For small scale BAC-DNA preparation (BAC-mini-preparation), single clones were picked and 10 ml of LB medium containing 25 µg/ml chloramphenicol (cam) were inoculated and cultured at 37 °C o.n. Bacteria were centrifuged in 15 ml falcon tubes at 3500 rpm for 15 min at RT (Haereus; 2600x g). The pellet was resuspended in 150 µl solution I (25 mM Tris/HCl, 10 mM EDTA, pH 8,0) and transferred to 2 ml Eppendorf tubes. For alkaline lysis 150 µl of solution II (0,2 M NaOH, 1% SDS) was added. The reaction was stopped by the addition of 300 µl solution III (3 M KAc, pH 4,8) that causes the precipitation of proteins and chromosomal DNA. After a 10 min centrifugation at maximal speed, DNA was extracted by addition of 1 ml phenol/chloroform, which accumulates DNA in the upper phase after an additional 5 min centrifugation step. DNA of the upper phase was precipitated by addition of 1 ml of isopropanol, followed by centrifugation at maximal speed for 20 min. After a washing step with 1 ml of 70% EtOH, the DNA pellet was dried and resuspended in 100 µl distilled water. 50 µl of the preparation were used for restriction pattern analysis (chapter 5.2.1)

### 5.1.4. Large scale isolation of BAC-DNA

Large amounts of BAC-DNA for virus reconstitution experiments were isolated from bacteria by the use of Nucleobond PC100 kit (Macherey-Nagel). As a variant of the manufacturer's instructions, the filtered bacterial lysate was applied twice to the DNA binding columns. Furthermore, the total volume of the washing buffer was applied in three steps instead of 12 ml at once and the elution buffer N5 was pre-warmed to 50 °C and applied in two steps. Dried DNA pellets after the last centrifugation step of the protocol were dissolved in 150 µl distilled water for 2 h at 37 °C or o.n. at 4 °C and stored at 4 °C. For pipetting BAC-DNA during or after the DNA preparation, pipette tips were cut with a sterile pair of scissors to minimize shear forces that might damage the large BAC-DNA molecules.

### 5.1.5. Determination of DNA concentration and purity

To determine the concentration and purity after DNA isolation the optical density (OD) at 260 nm and 280 nm was measured using the ND-1000 spectrophotometer (nanodrop, peclab) or Bio-Photometer (Eppendorf). The OD<sub>260</sub> allowed the calculation of nucleic acid concentrations of the samples, taking the OD of 1 equal to a concentration of



50 µg/ml double stranded DNA. The ratio between the two readings ( $OD_{260}/OD_{280}$ ) provided an estimation of sample purity and ranged between 1,8 and 2.

## **5.2. Analysis and cloning of DNA**

### 5.2.1. Restriction enzyme digest

For restriction pattern analysis of plasmids, 5 µl of the plasmid mini-preparation, corresponding to approximately 0,5-1 µg of DNA, were used. To a total volume of 20 µl, 2 µl of the recommended buffer, 2 µl of 10x BSA (if necessary), at least 2 units of the adequate restriction enzyme (1 µl) and distilled water was added and incubated for 1-2 h at the recommended temperature. The restriction pattern analysis of BAC-DNA was performed in a total volume of 70 µl, adding 7 µl of the recommended 10x reaction buffer, 7 µl of 10x BSA, at least 10 units of the respective restriction enzyme (1,5 µl) and distilled water to 50 µl of the BAC mini-preparation. BAC-DNA digests were incubated for 3 h at the recommended temperature. For restriction pattern analysis after large scale DNA preparations of either plasmids or BACs, 1,5 µg DNA were digested in a total volume of 30–40 µl, containing the recommended reaction buffer and BSA.

### 5.2.2. Agarose gel electrophoresis

DNA fragments obtained by restriction enzyme digests were separated and analysed by gel electrophoresis. Digested plasmid DNA was separated in a 1% agarose/TAE gel while digested BAC-DNA was separated in a 0,8% agarose/TBE gel. Before poring the gels, ethidium bromide was added to a concentration of 1 µl/ml. Gels were run for 30 min at 120 V or 16 h at 60 V, respectively. Stained DNA bands were visualized by UV light in a Eagle-Eye imaging system (Biorad).

*TAE-buffer (50x), pH 7,3*  
2 M Tris  
0,25 M Na-acetate  
50 mM EDTA

*TBE-buffer (10x):*  
900 mM Tris  
900 mM boric acid  
25 mM EDTA

### 5.2.3. Isolation of DNA fragments from agarose gels

If separated fragments were to be used for further cloning steps, the respective band was cut from the gel and purified using the GFX PCR/DNA and Gel band purification Kit

(Amersham) following manufacturer's instructions. To prevent UV induced DNA damage, weak UV light was applied for visualization of the fragments while cutting.

### 5.2.4. Dephosphorylation of DNA ends

To avoid re-circularization of cleaved, linearized vector DNA, the 5'-ends of DNA fragments were dephosphorylated. vector DNA was treated with the shrimp alkaline phosphatase (SAP) in a ratio of about 1 unit of SAP for 1 pmol of DNA. The enzyme was added after the restriction enzyme cut and incubated for another hour at 37 °C. The SAP was inactivated by 20 min of incubation at 65 °C.

### 5.2.5. Phenol/chloroform extraction and ethanol precipitation

Proteins were removed from DNA preparations by extraction with 1 volume phenol/chloroform. After vigorous vortexing for 10 s the solution was centrifuged at 14000 rpm (microcentrifuge) for 1 min and the upper DNA containing phase was recovered. Then 0.1x volume 3 M NaAc pH 5,2 and 2.5x volumes 100% EtOH (cold) were added and samples were incubated at -80 °C for 20 min. The precipitated DNA was centrifuged at 14000 rpm for 30 min (4 °C). The pellet was washed once with 70% EtOH (cold). After another centrifugation step (14000 rpm, 15 min, 4 °C, microcentrifuge) the EtOH was carefully removed, the pellet air-dried at RT and finally resuspended in water.

### 5.2.6. Annealing of synthetic oligonucleotides

For insertion of short DNA fragments into a vector, complementary oligonucleotides were synthesized (Metabion) and annealed to form a double stranded DNA fragment. Oligonucleotides were flanked by suitable overhangs as usually obtained after restriction enzyme cuts to allow the insertion into a respectively cut vector. Two complementary oligonucleotides were mixed to a concentration of about 40 µM each, incubated at 75 °C for 5 min and cooled down at RT for 30 min. 1 µl of the annealed oligonucleotides, neat and diluted 1/50, were added to separate ligation reactions containing 100 ng of an adequately cut and purified vector fragment.

### 5.2.7. Amplification of DNA by Polymerase Chain Reaction (PCR)

DNA fragments were primarily amplified for cloning purposes. Since several reactions, using different templates and primer pairs were run at the same time, the touch down

function of the thermo cycler (Roche) was used. A decrease of annealing temperature in each of the first 10 cycles allowed a high specificity for the PCR, even if the main PCR cycles were performed at an annealing temperature lower than the optimal annealing temperature of most of the primer pairs.

PCR conditions:

	<b>Step</b>	<b>Temperature</b>	<b>Time</b>	
1	Denaturation	95 °C	5 min	
2	Denaturation	95 °C	5 min	
3	Primer annealing	65 °C – 55 °C	45 sec	-1 °C every cycle
4	Extension	72 °C	45 sec	10 x back to 2
5	Denaturation	95 °C	5 min	
6	Primer annealing	55°C	45 sec	
7	Extension	72 °C	45 sec	30 x back to 5
8	Final extension	72 °C	7 min	
9	End	4 °C	infinite	

In general the PCR reaction mix contained:

10 ng-100 ng template DNA  
 400 nM of each oligonucleotide-primer  
 240 µM dNTPs  
 0,1 Volume 10x Expand HF reaction buffer, including Mg<sup>2+</sup>  
 0,1 Volume DMSO (for BAC or virus DNA as template)  
 3,5 units Expand High Fidelity PCR system Polymerase

Most PCRs were run in a total volume of 100 µl. 10 µl of the PCR were tested for amplicon on a 1% agarose/TAE gel. The remaining 90 µl were purified using the GFX PCR/DNA and Gel band purification Kit (Amersham) following the manufacturers instructions.

5.2.8. Ligation of DNA fragments

DNA fragments were mixed in a molecular ratio of 1:3 of vector (100 ng) and insert. Ligations were performed in a total volume of 20 µl comprising 15 units of T4 ligase (2 µl), 2 µl of the supplied T4-ligase reaction buffer, DNA fragments and distilled water. Reactions were incubated for 1 h at RT or o.n. at 16 °C.

### 5.2.9. Preparation of electrocompetent bacteria

All preparation steps were done on ice or at 4 °C, using pre-cooled pipettes and solutions. 200 ml of LB were inoculated with 2 ml of an o.n. culture and cultivated at 30 °C or 37 °C up to an OD<sub>600</sub> of about 0,4 (2-3 h of cultivation). Cultures were then cooled on ice for 15 min and centrifuged for 10 min at 7000x g. To eliminate salts and medium components bacteria were washed by resuspension in 100 ml of 10% glycerol and subsequent centrifugation for three times. Thereafter, the pellet was resuspended in 1 ml of 10% glycerol and aliquots of 65 µl were snap frozen in liquid nitrogen and stored at –80 °C.

### 5.2.10. Transformation of electrocompetent bacteria

To introduce plasmids into electrocompetent bacteria, 2 µl of the ligation mix were added to 65 µl of electrocompetent bacteria, thawed on ice. The bacteria were transferred to a pre-cooled electroporation cuvette (Biorad; 0,2 µm in diameter) and inserted into a GenePulser (Perkin Elmer). Bacterial membranes were destabilized for the uptake of DNA by 2,5 kV, 400 Ω and 25 mFD. Immediately after electroporation 1 ml antibiotic free LB medium was added and the bacteria were transferred to a 1,5 ml tube for incubation at 37 °C or 30 °C. After 1 h, 75-200 µl were plated on pre-warmed agar plates, containing the adequate antibiotic, and incubated at 37 °C/43 °C o.n.

### 5.2.11. Preparation of chemocompetent bacteria

All preparation steps were done on ice or at 4 °C using pre-cooled pipettes and solutions. 100 ml of LB were inoculated with 1 ml of an o.n. culture and cultivated at 37 °C up to an OD<sub>600</sub> of about 0,5. Bacteria were then centrifuged in 50 ml falcon tubes for 15 min at 3500 rpm (Heraeus, 2600x g), the supernatant discarded and the pellet resuspended in 10 ml Tfb I buffer. After 50 min incubation on ice, bacteria were pelleted again, resuspended in 2 ml Tfb II and snap frozen in liquid nitrogen as aliquots of 100 µl and stored at –80 °C.

*Tfb I (pH 5,2)*  
100 mM RbCl<sub>2</sub>  
50 mM MnCl<sub>2</sub>  
30 mM KAc  
10 mM CaCl<sub>2</sub>

*Tfb II (pH 7)*  
10 mM MOPS pH 7  
10 mM RbCl<sub>2</sub>  
75 mM MnCl<sub>2</sub>  
15% glycerol

### 5.2.12. Transformation of chemocompetent bacteria

To introduce plasmids into chemocompetent bacteria, 2 µl of the ligation mix or 20 ng of plasmid DNA were added to 100 µl of chemocompetent bacteria thawed on ice. After 30 min of incubation on ice, the samples were subjected to a heat shock of 1 min at 42 °C, followed by another 2 min on ice. Supplied with 1 ml antibiotic free LB, bacteria were kept on a shaker at 30 °C or 37 °C for 1 h. 300 µl were plated on pre-warmed LB agar plates containing the adequate antibiotics and cultured o.n. at 30 °C or 37 °C.

### 5.2.13. Glycerol cultures of bacteria

To keep bacteria bearing the plasmids of interest in a permanent culture, glycerol stocks were prepared by adding 400 µl of 50% glycerol to 700 µl of the bacterial culture. Glycerol cultures were stored at –80 °C.

### 5.2.14. Sequencing of DNA fragments

All constructs were checked for correct sequence by the company GATC (Germany). 35 µl of DNA samples diluted to 100 ng/µl and 10 µM primers flanking the region of interest were sent to the company for sequence analysis on an ABI sequencer.

## **5.3. Analysis of proteins**

### 5.3.1. SDS page gel electrophoresis

Proteins were separated by size using gel electrophoresis under denaturing conditions. Protein samples were obtained after isolated expression of proteins in 293T cells or from intermediate steps and elutions of protein purification experiments. After isolated expression, transfected cells were scraped from the plates and transferred to an eppendorf tube. After centrifugation at low speed, the cell pellet was washed with 500 µl PBS, centrifuged again and resuspended in 350 µl total lysis buffer. Aliquots of the intermediate steps and elutions of protein purification experiments were mixed with 4x sample loading buffer. The 12% separating gel was poured in a Protean II gel system (Biorad). During solidification, the gel surface was overlaid by 1 ml of water, decanted before the stacking gel was poured on top. Protein samples were prepared in a maximum volume of 20 µl with total lysis buffer or 4x sample loading buffer, and heated for 8 min at 95 °C prior to loading. The gel was run in 1x Laemmli buffer at 160 V for 60 min. After the run, separated proteins were either visualized by a stain of all proteins

by Commassie Blue (chapter 5.3.2) or defined proteins were detected in a subsequent Western Blot (chapter 5.3.3).

*separating gel (12% / 17,5 %)*

4 / 5,6 ml acrylamide (rotiphorese 30; 30:1)  
 2,5 ml 4x separating gel buffer  
 3,4 / 1,8 ml H<sub>2</sub>O  
 3 µl TEMED  
 100 µl APS

*stacking gel*

2,5 ml acrylamid (rotiphorese 30; 30:1)  
 3,75 ml 4x stacking gel buffer  
 9,75 ml H<sub>2</sub>O  
 20 µl TEMED  
 100 µl APS

*4x separating gel buffer (pH 8,8)*

1,5 M Tris  
 0,4% SDS

*10x Laemmli buffer*

25 mM Tris  
 10% SDS  
 250 mM glycine

*4x stacking gel buffer (pH 6,8)*

0,5 M Tris  
 0,4% SDS

*total lysis buffer (pH 6,8)*

62,5 mM Tris  
 2% (v/v) SDS  
 10% (v/v) glycerol  
 6 M urea  
 0,01% (w/v) bromphenolblue  
 0,01% (w/v) phenolred  
 5% (v/v) β-mercaptoethanol

*4x sample loading buffer (pH 6,8)*

160 mM Tris/HCl  
 20% β-mercaptoethanol  
 4% SDS  
 20% glycerol  
 0,01% (w/v) bromphenolblue

### 5.3.2. Commassie Blue Stain

For visualization of proteins in the SDS gel, gels were incubated in a staining solution for 20 min followed by destaining for several hours with 3-4 changes of the destaining solution. Protein bands appeared blue on a clear gel background.

*staining solution*

50% (v/v) methanol  
 10% (v/v) acetic acid  
 0.1% (w/v) Commassie blue R350

*destaining solution*

50% (v/v) methanol  
 10% (v/v) acetic acid

### 5.3.3. Western Blot

After the separation of proteins by SDS-page, proteins were transferred from the gel onto Hybond-P membranes (Amersham Biosciences) in the presence of blotting buffer. For that, the PVDF membrane was activated by brief inversion in methanol then washed in water and equilibration for several minutes in blotting buffer. The gel was placed on the membrane and covered on both sides by three layers of Whatmann filter paper

soaked in blotting buffer. Blotting conditions were 18 V for 30 min. The membrane was blocked for 30 min (at RT) or o.n. (at 4 °C) in TBS-T containing 5% nonfat dry milk. To detect the proteins, the membrane was incubated at RT for one hour with TBS-T containing Anti-HA-Peroxidase High Affinity antibody (Roche, 1:5000) or a specific polyclonal rabbit antiserum anti-M50 (Muranyi et al., 2002; 1:2000). After one hour of washing with TBS-T, blots for M50 detection were incubated with a secondary anti-rabbit, horseradish peroxidase conjugated, antibody (Dianova, Hamburg, Germany). Membranes were again washed with TBS-T and proteins were visualized with an ECL-Plus Western Blot detection system (Amersham Biosciences) and Hyperfilm ECL (Amersham) detection films.

### *Blotting buffer*

25 mM Tris  
192 mM glycine  
20% methanol

### *TBS-T (pH 8,0)*

150 mM NaCl  
10 mM Tris/HCl  
0,05% Tween-20

#### 5.3.4. Determination of protein concentration

The protein content of cell lysates was determined by Bradford assay. The principle of the Bradford assay is a shift of the absorption maximum of Coomassie-Brilliant blue from 465 nm to 595 nm upon binding to proteins, which can easily be monitored by photometric analysis. The Bradford reagent (Biorad) was diluted following the manufacturer's instructions and 1 ml was added to 1 µl of cell lysate. The samples were briefly mixed and transferred to a photometer cuvette. After 5 min incubation in the dark, the OD<sub>595</sub> was determined. Values or volumes of further experiments were adjusted relative to the measured OD<sub>595</sub> of the different samples. The protein concentration was calculated using a bovine serum albumin (BSA) standard curve. If only a rough estimation of the protein content was needed, the protein concentration was calculated by the following equation: protein concentration (µg/µl) = OD<sub>595</sub>/0,0657.

## 5.4. Tissue culture

### 5.4.1. Cultivation of cells

All cell lines were cultivated in an incubator (Haereus) at 37 °C in 5% CO<sub>2</sub> and 95% humidity. Cells were split every 3-6 days in a ratio between 1:3 and 1:8. To split the attached cell lines, the medium was removed, cells washed with 10 ml PBS and de-

tached from the plate bottom by incubation with few drops of trypsin/ETDA for 1-2 min at RT. The trypsin was inactivated by 10 ml of the adequate medium, cells were resuspended and the pertinent amount was brought to a plate with fresh medium. All cell lines were tested regularly to be negative for mycoplasma contamination.

**Table 3 : Cell lines used during this work**

List of Cell lines and culture media, prepared from the commercial available basic media and additives. In the last column the dilution of the cells for each split and the split interval.

Cell line	Basic medium	Additives	Split/interval
NIH3T3	DMEM	5% NCS, 0,6% (w/v) Pen., 1,3% (w/v) Strep	1:5/3-4 days
M2-10B4	RPMI	10% FCS, 0,6% (w/v) Pen., 1,3% (w/v) Strep	1:4 /3-4 days
MEF	DMEM	10% FCS, 0,6% (w/v) Pen., 1,3% (w/v) Strep	1:3/3-4 days
293T	DMEM	10% FCS, 0,6% (w/v) Pen., 1,3% (w/v) Strep,0,3 mg/ml Q	1:5/3 days
A549	DMEM	10% FCS, 0,6% (w/v) Pen., 1,3% (w/v) Strep,0,3 mg/ml Q	1:10/3-4 days

#### 5.4.2. Freezing of cells

To keep a stock of cells, which are low in passage number, cells were frozen as permanent cultures in liquid nitrogen. Cells were grown to 95% confluence and detached from the plates by trypsin. After centrifugation (5 min, 1200 rpm, Haereus, 315x g) the cell pellet was resuspended in one volume of media (0,5 ml as equivalent for one 10 cm dish) and mixed gently with 1 volume of 2x freezing medium. 1 ml aliquots were transferred to cryotubes (Nunc) and kept at -80 °C for 48-72 h before storage in liquid nitrogen. Isopropanol isolated cryo-boxes allowed gentle freezing of the cells (1 °C per hour).

#### *2x Freezing media*

50% FCS  
40% DMEM  
10% DMSO

#### 5.4.3. Determination of cell number

Cells were detached from the culture plate by trypsin and resuspended in 1 ml of PBS. 10 µl were applied to a Neubauer chamber and cells were counted in 3 squares of the grid. Taking into account that the volume in one square corresponds to 0,1 µl, the total cell number of the culture plate was the counted cell number per square x 10000.



### 5.4.4. Thawing of cells

Frozen aliquots were removed from the nitrogen tank and thawed in a 37 °C water bath. As soon as possible, cells were brought to 10 ml with the adequate medium and centrifuged for 5 min at 1200 rpm (Heraeus, 315x g). The pellet was resuspended in 12 ml of medium and transferred to culture dishes.

### 5.4.5. Transfection of eukaryotic cells using Superfect (Quiagen)

293T cells were split 1:3 to seed 6 well plates one day before transient transfection (60-70% confluence at day of transfection). DNA, serum free DMEM and Superfect was mixed and incubated for 15 min. Together with supplemented medium, the DNA/Superfect mix was added to the PBS washed cells. After 2,5 h the transfection mix was exchanged to supplemented, pre-warmed medium. As a variant to the manufacturers instructions, 5 µg instead of 3 µg DNA per well were used for transfection of 293T cells.

### 5.4.6. Transfection of eukaryotic cells using Ca<sub>2</sub>PO<sub>4</sub> precipitation

293T cells were split 1:3 to seed 6 cm dishes one day before transient transfection (60-70% confluence at day of transfection). 250 µl of 2x HBS was added to a 15 ml Falcon tube. In a second tube, 6 µg DNA was combined with 250 µl 250 mM CaCl<sub>2</sub>. The tube containing 2x HBS was vortexed while the DNA/CaCl<sub>2</sub> solution was added dropwise. The solution was incubated at RT for 15 min to allow the formation of the calcium-DNA precipitates. Subsequently, the suspension was mixed with 3 ml fresh medium and added to the cells after removal of the old medium. The next day, fresh medium was applied to the cells and protein expression was assessed the following day by Western Blot.

*2x HBS (pH 7,05)*

50 mM HEPES

1,5 mM Na<sub>2</sub>HPO<sub>4</sub> × 2 H<sub>2</sub>O

280 mM NaCl

12 mM glucose

## **5.5. Working with MCMV**

### 5.5.1. Generation of recombinant viral BACs

Electrocompetent DH10B, bearing an MCMV BAC and pcp20 plasmid (coding for the Flp recombinase) were electroporated with 50-80 ng of plasmid DNA with a por16-zeo origin. For Flp mediated recombination, bacteria were kept for 1 h under non-selective conditions at 30 °C. Thereafter, 150 µl were plated on Cam/Zeo plates and cultured at the non-permissive temperature of 43 °C o.n. The next day, colonies were picked for BAC-DNA mini-preparation to check for single insertions.

### 5.5.2. MCMV virus reconstitution

To reconstitute virus from mutagenized BACs, BAC-DNA was transfected into MEF cells by the use of Superfect. MEF cells were thawed and seeded on two 10 cm dishes. When they reached 100% confluence, cells were split 1:3 on 6 cm dishes one day before transfection. Since primary cultures are more sensitive than stable cell lines, the manufacturer's protocol of transfection was modified using less of the Superfect reagent. 1,5 µg of a BAC-DNA preparation was mixed with DMEM medium to a total volume of 150 µl and 10 µl of Superfect were added. After 15 min incubation at RT, 1 ml of pre-warmed supplemented medium was added and transferred to PBS washed MEF cells. After 2,5 h the Superfect/DNA mixture was replaced by 3 ml of supplemented medium. MEF cells were split to 10 cm dishes the next day and passaged with 1:2 splits every 7 days thereafter. After 5 days, first plaque formation was observed in the transfection with the wild type MCMV BAC. Plaque formation in transfections with mutant MCMV BACs first occurred after 10 to 30 days. After complete cell lysis, cells were harvested together with the supernatant and frozen at -80 °C.

### 5.5.3. MCMV virus stock preparation

For a high titre virus stock, M2-10B4 cells were infected. 20-30 dishes (14,5 cm) with 60% confluent M2-10B4 cells were infected with an MOI of about 0,1. After complete cell lysis, broken cells were harvested with the supernatant and collected in 250 ml centrifuge beakers. All following preparation steps were performed on ice or in centrifuges cooled to 4 °C. After 15 min of centrifugation (Beckmann; JLA 16-250, 6500x g), the supernatant was collected in fresh beakers and stored on ice. The cell pellet was resuspended in 5 ml of DMEM and homogenized in a glass homogenisator (douncer) by 20

strokes. Cell debris was removed by a second centrifugation (Beckmann; JA 25-50, 18000x g, 10 min) and the supernatant was combined with the retained supernatant from the first centrifugation step. To concentrate viral particles, samples were centrifuged for 3 h at 25000x g (Beckmann; JLA 16-250). The virus pellet obtained was resuspended in 4 ml DMEM and dounced 20 times before being loaded on a sucrose cushion of 15% sucrose in VSB (7 ml in SW28 centrifuge tubes). After 1 h ultracentrifugation (Beckmann; SW28, 20000 rpm), the pellet of purified viral particles was resuspended in 1-2 ml of VSB and treated again with a douncer. The virus stock preparation was stored in 50–100 µl aliquots at –80 °C.

*VSB (pH 7,8)*  
50 mM Tris/HCl  
12 mM KCl  
5 mM EDTA

#### 5.5.4. Growth curves

The growth kinetics of different mutant viruses were compared to each other and wild type MCMV in multi-step growth conditions. NIH3T3 fibroblasts were grown on 12 well plates (Nunc) one day before the start of the experiment to obtain cells numbers around  $3 \times 10^5$  per well at the day of infection. Cells were infected with a MOI of 0,1 in a volume of 1 ml. After 1 h of incubation at 37 °C to allow virus adsorption, the infectious supernatant was exchanged by 1 ml of supplemented medium. The supernatant after infection, as well as the supernatant collected from cells every day over a period of 5 days, was stored at –80 °C and virus titre determined. Samples were taken in triplicates for each day.

#### 5.5.5. MCMV virus titration

For determination of MCMV virus titres, MEF cells were plated 1:2 on 48 well plates one day before titration (95% -100% confluence at day of infection). MEFs were infected with 400 µl of serial dilutions ( $1:10^2$ - $1:10^7$  in supplemented DMEM) of the virus. Titrations were done in triplicates. After 1 h of incubation at 37 °C to allow virus adsorption, the infectious supernatant was exchanged by 300 µl of carboxymethylcellulose containing medium. Infectious particles won't diffuse in medium of such viscosity, thus

no secondary plaque formation occurs. After 5 days, plaques were counted by observation under a light microscope and the virus titre determined by the following equation:

$$\text{Virus titre (PFU/ml)} = \frac{\text{(counted plaques x dilution factor)}}{\text{vol. of infectious dilution (0,4 ml)}}$$

### *Carboxymethylcellulose containing medium (500 ml)*

3,75 g carboxymethylcellulose

388 ml H<sub>2</sub>O

to be autoclaved

25 ml FCS

50 ml 10 x MEM

5 ml L-glutamine

2,5 ml NEAS (non essential amino acids)

5 ml Penicillin/Streptomycin (0,6% (w/v) Pen., 1,3% (w/v) Strep)

24,7 ml NaHCO<sub>3</sub> (7,5%)

## **5.6. Bacterial expression**

### 5.6.1. Expression of heterologous proteins

The constructs for bacterial expression were cloned, analysed and subsequently isolated from DH10B. For expression 100 ng of plasmid DNA were transferred into BL21 (DE3) RIL (Stratagene) by electroporation. Bacteria were cultured o.n. at 37 °C on agar plates (Kan/Cam). The next day, 50-100 colonies were scraped from the plate to inoculate 50 ml of preculture. After 5-6 h at 37 °C, 10 ml of the preculture were used to inoculate 1 l of the main culture. When the OD<sub>600</sub> of the culture reached 0,6, culture flasks were cooled on ice for 15 min. The expression of the heterologous proteins was induced by IPTG, added to a final concentration of 0,5 mM and cultures were maintained in a shaking incubator at 20 °C o.n. The next morning cells were harvested by centrifugation at 4 °C and 3500x g for 30 min (Sorvall; SLC 6000). The supernatant was removed and the pellet resuspended in 35 ml lysis buffer, frozen in liquid nitrogen and stored at -80 °C.

### 5.6.2. Lysis of bacteria

The bacterial solution was thawed in a water bath at 37 °C and sonified (Sonifier 450; Branson) by 1 s pulses for 20 min, using a flat bottom tip. The lysate was cleared of membranes, DNA, still intact bacteria and eventual inclusion bodies by a 1 h centrifuga-

tion at 18000x g at 4 °C (Beckmann; JA 25-50). The pellet was dissolved in 6 M urea to analyse the solubility of the protein. The supernatant was applied to a Ni<sup>2+</sup>-NTA column.

### 5.6.3. Purification of His-tagged proteins

To avoid denaturation and degradation of proteins, all preparation steps were done on ice, in pre-cooled centrifuges or in the cold room. All buffers used for purification were cooled to 4 °C and mixed with either fresh  $\beta$ -mercaptoethanol or 1,4 dithiotreitol (DTT) to prevent possible oxidation. 1600  $\mu$ l of Ni<sup>2+</sup>-NTA (Quiagen) were cast into a 10 ml plastic column (Biorad) to sediment, resulting in a bed volume of 800  $\mu$ l. The column was washed with two column volumes (CV) of water and equilibrated with 1 CV of equilibration buffer. After centrifugation of the bacterial sample (see chapter 5.6.2), the supernatant was filtered and loaded on the Ni<sup>2+</sup>-NTA column. For preparing and loading of the column, a 5 cm flexible tube was attached to the column's bottom valve for capillary force induced suction. After loading of the lysate and collecting the flow through (FT), the column was washed with 2 CV of equilibration buffer (wash 1) and 4 ml of equilibration buffer containing 5 mM imidazole (wash 2). His-tagged proteins were eluted from the column by three applications of 1 ml elution buffer (equilibration buffer containing 250 mM imidazole). 15  $\mu$ l of the lysate, FT, washes, and elutions were analysed on a 12% SDS-page under denaturing conditions and subsequent Commassie Blue staining.

#### *equilibration buffer (pH 8)*

50 mM Tris

300 mM NaCl

10 mM  $\beta$ -MeOH

### 5.6.4. Purification by anion-exchange chromatography (MonoQ)

The principle of ion exchange chromatography is based on the interaction between charged proteins and the contrarily charged groups of the column matrix. Protein binding occurs under low salt conditions (buffer A). The continuous increase in anion concentration in a salt gradient (buffer B) leads to elution. Different binding properties of proteins result in a different elution profile, thereby allowing removal of impurities. Dilution of the pooled Ni<sup>2+</sup>-NTA elution fractions (1:5) with buffer A decreased the salt

concentration so that the protein solution could be loaded on the MonoQ resin using a 50 ml superloop.

### *Mono Q buffer*

50 mM Tris (pH 9 at RT)

1 mM EDTA

0 M (buffer A) or 1 M NaCl (buffer B)

to be degased

5 mM DTT

### 5.6.5. Purification by gel filtration (Superose 6)

This method is used to separate proteins according to their Stokes radius (size exclusion chromatography). Small molecules can easily diffuse in the interspaces, whereas larger molecules move more directly through the column and elute earlier. Large proteins, which have no access to the pores elute in the void volume. Considering this principle, the applied volume should be quite small (0,3-0,5 ml) to enable a good elution profile. The chromatogram should show a sharp, uniform peak. After analysis of the MonoQ fractions by SDS-PAGE, those with highest purity were pooled, concentrated by Amicon Ultra tubes (Millipore, MWCO 10 kDa) to a volume of about 500  $\mu$ l and injected on the equilibrated column. The flow rate was set to 1 ml/min and 0,5 ml fractions were collected.

### 5.6.6. Purification by an HA-matrix

As a further purification step after the Ni<sup>2+</sup>-NTA column, eluted proteins were treated by an HA-matrix to up concentrate HA-tagged proteins and loose impurities. 50  $\mu$ l of HA-matrix (Roche) and 2,5  $\mu$ l of a complete protease inhibitor cocktail (PIC, Roche, 100x) were added to 200  $\mu$ l of the elution from the Ni<sup>2+</sup>-NTA column. After 90 min incubation on a roll incubator in the cold room, the samples were washed four times. For that, the beads were dispersed in 1 ml of equilibration buffer (chapter 5.6.3) containing protease inhibitors and subsequently centrifuged for 2 min at full speed. To elute the protein bound to the HA-matrix, 50  $\mu$ l of HA-peptide (1 mg/ml) was added and the samples incubated for another 40 min at 4 °C. After a 2 min centrifugation, the supernatant containing the eluted protein (1. elution) was removed. To ensure complete recovery of the matrix bound protein, another 50  $\mu$ l of HA-peptide was applied to the samples, incubated o.n. and gathered after centrifugation (2. elution). Both elutions

were analysed by SDS-PAGE / Western Blot and in a nitrocefin assay (see chapter 5.7.3).

### 5.6.7. Concentration of proteins

The protein solutions were transferred to an Amicon Ultra-4 Centrifugal Filter Device with a cutoff at 10 kDa. Centrifugation was performed at 4 °C and 2500 rpm until the desired concentration was reached.

### 5.6.8. Edman sequencing

For identification of proteins in Commassie stained SDS–PAGE, bands were cut and partially sequenced by Edman sequencing. Samples were prepared with the passive adsorption method. The protein band was excised from the SDS gel and dried in a heating block at 45 °C for 1 h. The dried gel piece was then reswollen in 50 µl swelling buffer for 1 h. In the next step, 200 µl of distilled water were added to set up a concentration gradient. A small piece of pre-wet (100% methanol) PVDF membrane was added and allowed to adsorb. Once the solution started to turn blue from the dye, 25 µl of methanol were added as a transfer catalyst and the mixture was incubated for several days at RT. The membrane was washed five times with 1 ml 10% methanol, dried and analysed by Edman sequencing (AG Cramer, Gene Center, Munich, Germany).

*swelling buffer (pH 8,5)*

200 mM Tris-HCl

2% SDS

### 5.6.9. Crystallization

The hanging drop method, based on vapour diffusion, was used for crystallization setups. Thereby small volumes of precipitant and protein are mixed together and the drop equilibrates against a larger reservoir of mother solution through evaporation. The experiments were carried out at 20 °C under temperature control. In order to determine initial crystallization conditions, commercial screens from Hampton Research were used. Around each well of the 24 well plate, a ring of grease was applied with a 5 ml plastic syringe. Then each reservoir was filled with 200 µl of buffer. 1 µl of concentrated protein was pipetted in the middle of a plastic cover slide and subsequently mixed

with 1  $\mu$ l of the buffer, already in the reservoir. After that it was inverted and placed on the well containing the same buffer. The cover slide was pressed on the greased well and special care was taken to ensure that the set up was completely sealed in order to protect the drop from drying out. Four wells were done simultaneously and the whole plate was finished row by row.

### **5.7. Biochemical assays**

#### **5.7.1. Nitrocefin assay in cell lysates**

293T cells were co-transfected with Bla-fusion constructs. After 24 h, cells were detached from the plates by trypsin, washed with 500  $\mu$ l PBS and lysed in 75  $\mu$ l 1x luciferase reporter lysis buffer (Promega). After 30 min incubation on ice, cell debris was removed by centrifugation for 30 min at full speed and 4 °C. To measure the  $\beta$ -lactamase activity, 50  $\mu$ l of the lysates were transferred to a 96 well plate and mixed with 120  $\mu$ l phosphate buffer (0,1 M, pH 7), 15  $\mu$ l H<sub>2</sub>O and 15  $\mu$ l nitrocefin (500 mg/ml, Oxoid). Hydrolysis of nitrocefin was observed in a Versamax Plate reader (Molecular Devices) by measuring the change in absorption every 5sec at 495 nm for 20 min at 37 °C. The maximal change in absorption was determined by the data points in the linear range and expressed in milliabsorption units/min. Data were normalized by the protein content of the lysates determined by Bradford assay (chapter 5.3.4). This protocol was optimized for the M50/M53 PCA by preliminary experiments, testing different lysis buffers (Luciferase lysis buffer (Promega) or a lysis buffer with 150 mM NaCl, 20 mM Tris and 1% TritonX, pH 8) and different time points for cell lysis (16h, 24h and 48h after transfection) as well as different normalization methods (quantification of co-expressed SEAP (secreted alkaline phosphatase) or luciferase and the measure of the total protein concentration).

#### **5.7.2. Rapamycin induced FRB/FKBP12 interaction**

293T cells were seeded on 10 cm dishes the day before transfection with pO6T-N-R or pO6T-F-C by the Superfect method (chapter 5.4.5). 24 h post transfection the cells were lysed in 1 ml of luciferase reporter lysis buffer. 25  $\mu$ l of both lysates, N-R and F-C expressing cells, were mixed and rapamycin was added at different concentrations. Bla reconstitution was determined as described in chapter 5.7.1.



### 5.7.3. Nitrocefin assay with purified proteins

Proteins purified by a Ni<sup>2+</sup>-NTA column or HA-matrix were tested for Bla reconstitution in the presence of 120 µl phosphate buffer (0,1 M, pH 7) and 15 µl nitrocefin (500 mg/ml, Oxoid). The reaction mix was filled up to 200 µl by different volumes of the eluted proteins. Hydrolysis of nitrocefin was observed in a Versamax Plate reader (Molecular Devices) by measuring the change in absorption every 5sec at 495 nm for 20 min at 37 °C.

### 5.8. Statistical analysis

Nitrocefin hydrolysis rates in cell lysates after co-expressions, as well as mean virus titres, were tested for statistical significance. Mean values were subjected to an analysis of variance test (ANOVA). In an ANOVA, it is analysed as significant, if means of groups that are formed by values of the independent variable are different enough not to have occurred by chance. As a threshold for significance a p-value of 0,05 was chosen, meaning that there is a 5 in 100 chance the result occurred by chance. The lower the p-value, the more likely it is that the difference between groups was caused by treatment.

### 5.9. Bioinformatics

Secondary structure predictions of the UL50 ORF were performed by the PHD (Rost and Sander, 1994) programme offered by the “Network of protein sequence analysis” of the “Pôle BioInformatique Lyonnais” (<http://pbil.univ-lyon1.fr/>). DNA or protein sequence analyses were analysed by different programmes of the VNTI series (Invitrogen). Protein sequences were aligned by the use of the Vector NTI AlignX program (Infomax, Bethesda, Md.) via the BLOSUM62 similarity matrix.

---

## 6. Results

### 6.1. Establishment of the protein complementation assay (PCA)

#### 6.1.1. TEM-1 $\beta$ -lactamase in the PCA

The TEM-1  $\beta$ -lactamase of *E. coli* (Bla, Figure 8A) was reported as an attractive candidate for a reporter enzyme used in a protein complementation assay (PCA). Wehrmann and Galarneau (Galarneau et al., 2002; Wehrman et al., 2002) established a PCA using the TEM-1  $\beta$ -lactamase as a reporter enzyme, studying the ideal sites for the cleavage of the enzyme. According to their findings, the Bla fragments used for the constructs in this work were obtained by a cleavage of the Bla ORF between the amino acids (aa) 194 and 196. In addition, the signal sequence consisting of the first 23 amino acids (Zlokarnik et al., 1998) was deleted from the N-terminal fragment (Galarneau et al., 2002) and the expression of the bacterial lactamase in mammalian cells was improved by an exchange of aa180 from M to T (Genblazer, Invitrogen).

#### 6.1.2. Insertion of a flexible spacer into the Bla ORF

As a positive control for the Bla-PCA, the Bla ORF was not cleaved into two fragments but interrupted by a flexible 17 aa glycine/serine stretch ((S<sub>1</sub>G<sub>4</sub>)<sub>2</sub>S<sub>2</sub>G<sub>4</sub>S), which was later used as a spacer (S) between either of the two Bla fragments and the proteins of interest. The linker was inserted between amino acids 194 and 196 of Bla (Figure 8A and B). The construct was named BlaS and inserted into the expression vector pO6T (pO6T-BlaS; Figure 8C). The pO6T expression vector (2500 bp) originates from the modified pOriR6K-zeo-ie (Bubeck et al., 2004) and exhibits features that are suitable for the project: beside elements for replication (oriR6K) and selection (zeocin resistance) in bacteria, the vector contains an FRT site for insertion into viral BACs (chapter 6.4). The transcription unit of this vector consists of an HCMV immediate early (IE) promoter/enhancer, which is modified with tetracycline responsive elements and has a poly adenylation signal from the bovine growth hormone gene located downstream from the multiple cloning site.

#### 6.1.3. Determination of Bla activity

The Bla is a well studied enzyme commonly used in microbiology in a wide variety of applications. While there are many substrates available to measure the enzyme activity, chromogenic or fluorescent substrates like nitrocefin (O'Callaghan et al., 1972) and

## Results

CCF2/AM (Zlokarnik et al., 1998), respectively, have been found to be suitable for a PCA. Both substrates are cell permeable and water soluble, which enables to measure Bla activity in intact cells as well as in cell lysates. The chromogenic substrate nitrocefin changes from yellow to red (absorption at 495 nm) when hydrolyzed by Bla. Using the positive control BlaS, nitrocefin was tested for the visualization and quantification of Bla activity in our experimental setting.

293T cells were transfected in a 6 well plate with pO6T-BlaS using different DNA concentrations. After 24 h the cells were trypsinated, washed and lysed, using 1x Luciferase reporter lysis buffer (Promega). Nitrocefin was added and the hydrolysis rate was determined by a kinetic readout over 30 min, measuring the absorption at 495 nm every 10 seconds. To express the relative amount of Bla in the cell lysates the maximal hydrolysis rate of nitrocefin was determined, defined as the change of absorption at 495 nm during the linear phase and expressed in milliabsorption units/min (Figure 8D).

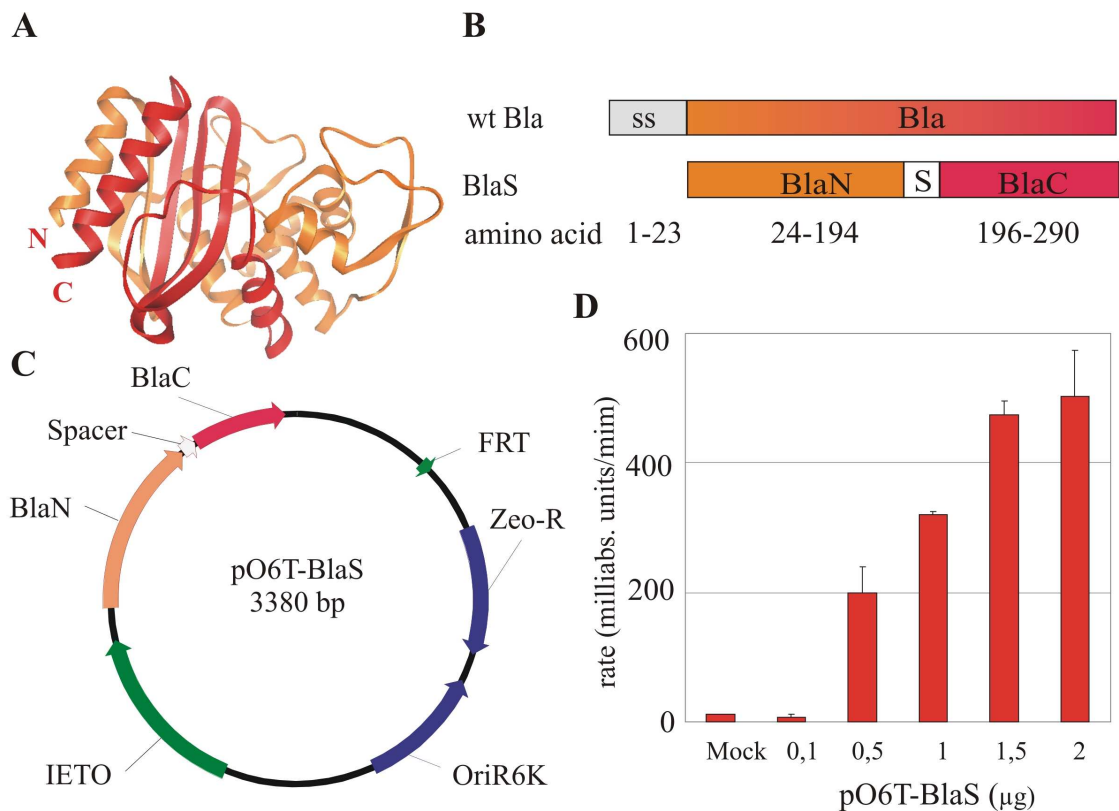


**Figure 8: Establishment of the PCA.**

**A)** Structure model of TEM-1  $\beta$ -lactamase (Jelsch et al., 1993), modified and visualized by “3D-Molecule Viewer” of VNTI (Invitrogen). Indicated are the BlaN and BlaC fragment in orange and red. **B)** Schematic representation of the Bla ORF (wt Bla) and BlaS with the inserted spacer. **C)** Schematic representation of BlaS inserted into the expression vector pO6T. Indicated the Bla ORF, in blue the bacterial regulation elements (zeocin resistance gene and OriR6K) and in green elements for eukaryotic expression and insertion into the BAC genome (IETO and FRT). **D)** 293T cells were seeded on 6 well plates and transfected with the indicated amount of pO6T-BlaS. Mean hydrolysis rates of nitrocefin were determined (chapter 5.7.1). Error bars indicate the standard deviation.

### 6.1.4. Bla complementation induced by the interaction of FKBP12 and FRB

To test whether our Bla fragments and constructs are suitable for the PCA, fusion proteins with well characterized binding partners, FKBP12 and FRB (Brown et al., 1994), were constructed to serve as positive controls for complementation. The two fragments of Bla designated as BlaN, which covers the N-terminal amino acids (aa24-aa194 of TEM-1  $\beta$ -lactamase) and BlaC, covering the C-terminal amino acids (aa196-aa286 of TEM-1  $\beta$ -lactamase) were fused to FRB and FKBP12, respectively. The two cellular proteins interact only in the presence of rapamycin, a so called dimerizer (Figure 9B). BlaN was fused N-terminally to the ORF of FKBP12 (R) and BlaC was fused C-terminally to the ORF of FRB (F), giving rise to the fusion proteins N-R and F-C, respectively (Figure 9A). To allow proper folding of the interacting proteins and spatial flexibility of the Bla fragments, the 17 aa spacer (chapter 6.1.2) was introduced between the Bla fragments and the proteins under study.

The expression vectors pO6T-N-R and pO6T-F-C were transiently transfected into 293T cells using Superfect transfection reagent. After 24 h, the cells were harvested and lysed. The lysates were mixed one to one and rapamycin was added at different concentrations. Finally, nitrocefin was added to the assay to test for Bla reconstitution by the rapamycin-induced interaction of FRB and FKBP12. The colour change provoked by the hydrolysis of nitrocefin was followed over time in a Versamax plate reader at 495 nm. As a measure for Bla activity, the hydrolysis rate was calculated and expressed as the change of absorption in milliabsorption units per minute (Figure 9C).

Without rapamycin a hydrolysis rate of about 5 milliabsorption units/min was measured defining the base line. The hydrolysis rate increased with increasing concentrations of rapamycin. The maximal hydrolysis rate, which was more than 10 fold above the background Bla activity, was achieved with rapamycin concentrations of at least 7,5 nM. This is comparable to the observation made by the Michnick group (Galarneau et al., 2002).

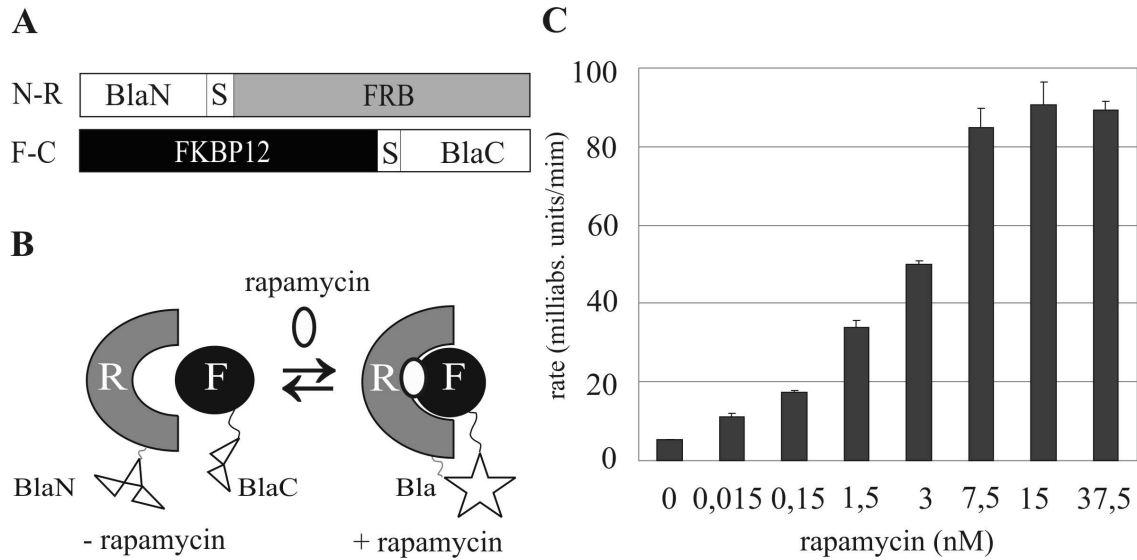


**Figure 9: FRB and FKBP12 in the PCA.**

**A)** Schematic representation of the Bla-fusion constructs. BlaN was fused to the N-terminus of FRB (N-R) and BlaC was fused to the C-terminus of FKBP12 (F-C). The coding sequences for the Bla fragments were separated from the ORFs coding for the interacting proteins by the 17 aa glycine/serine spacer (S). **B)** Schematic representation of the inducible interaction of FRB (R) and FKBP12 (F) with the fused Bla tags. The two proteins only interact in the presence of rapamycin. The interaction of FRB and FKBP12 induced by rapamycin then leads to the complementation of the two Bla fragments BlaN and BlaC and Bla activity is restored. **C)** 293T were transfected with pO6T-N-R or pO6T-F-C. 24 h post transfection, mean hydrolysis rates of nitrocefin were determined in the presence of the indicated rapamycin concentrations (chapter 5.7.2). Error bars indicate the standard deviation.

### **6.2. The NEC-PCA**

#### 6.2.1. M50 and M53 in the PCA

The PCA was established for the two MCMV proteins M50 and M53, which are essential in the nuclear egress of viral capsids. M50 and M53 form a complex at the inner nuclear membrane that is believed to act as a docking station for the viral capsids to build up the nuclear egress complex (NEC). Mapping of the mutual interaction sites on both proteins by mutational analysis showed that these sites and the M50/M53 interaction are essential for the functionality of the NEC.

The Bla<sub>N</sub> fragment (N) was fused N-terminally to M50 (pO6T-N-M50). Since M50 is a type II membrane protein, its C-terminus is luminal. Only the N-terminus provided a site for Bla fragment fusion since it is accessible from the nucleoplasm where M53 is localized after isolated expression. For M53, which is a soluble nuclear protein, the Bla<sub>C</sub> was fused both to the N- and C-terminus (pO6T-C-M53 and pO6T-M53-C). An HA-tag was added to the N-terminal Bla-fusions. The C-terminal fusion of Bla<sub>C</sub> to M53 was Strep-tagged (Figure 10B).

The expression vector pO6T-N-M50 was co-transfected into 293T cells with either pO6T-C-M53 or pO6T-M53-C. 24 h after transfection the cells were harvested and lysed. Nitrocefin was added to the cell lysates and the hydrolysis rate of nitrocefin was determined. For both combinations the hydrolysis rates were more than 50 times higher than in mock transfected cells (Figure 10C). The N-terminal Bla<sub>C</sub>-fusion to M53 lead to high Bla activity of more than 120 milliabsorption units/min whereas, the C-terminal Bla<sub>C</sub>-fusion lead to a slightly weaker signal of about 90 milliabsorption units/min.

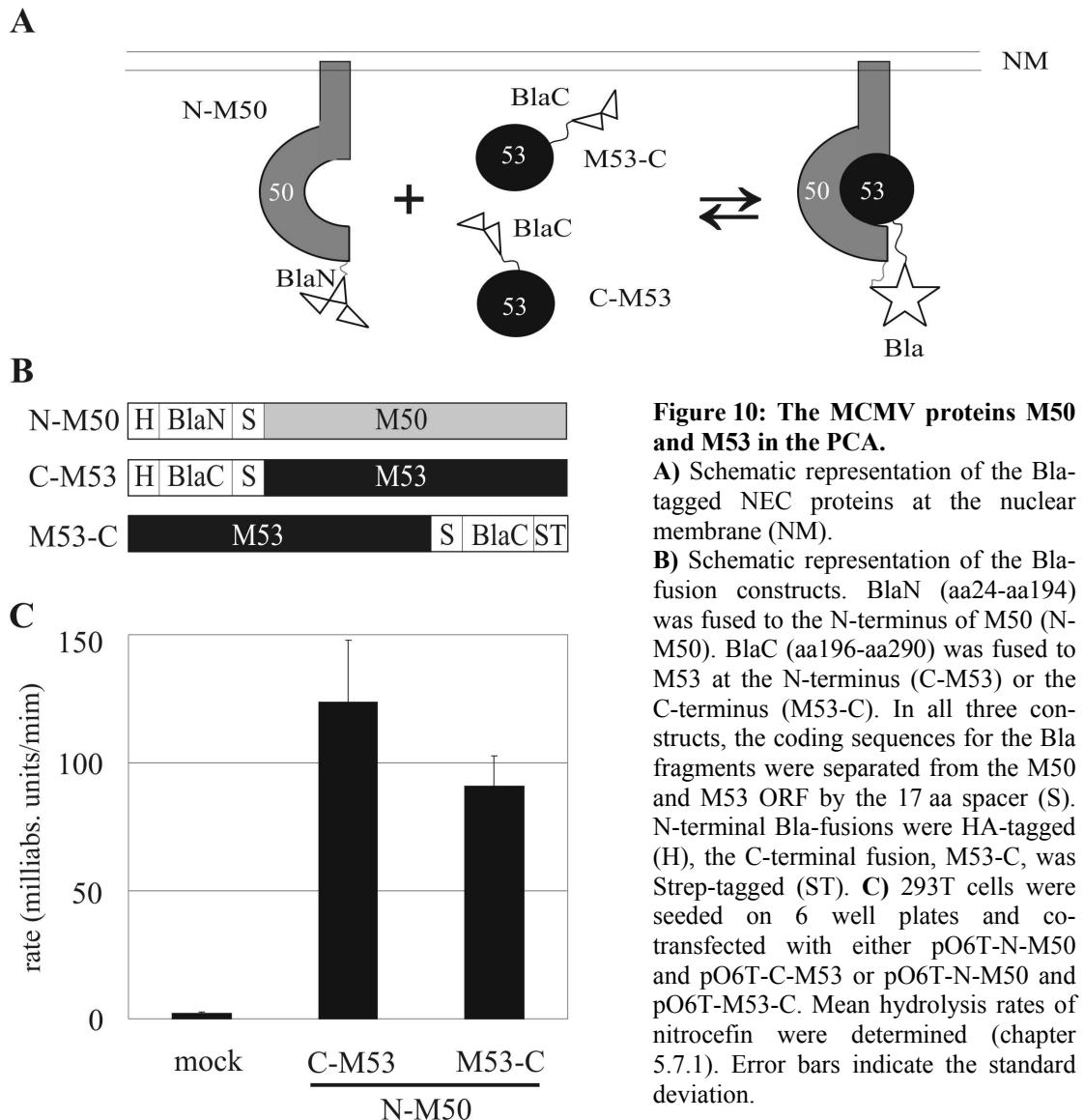


**Figure 10: The MCMV proteins M50 and M53 in the PCA.**

**A)** Schematic representation of the Bla-tagged NEC proteins at the nuclear membrane (NM).

**B)** Schematic representation of the Bla-fusion constructs. BlaN (aa24-aa194) was fused to the N-terminus of M50 (N-M50). BlaC (aa196-aa290) was fused to M53 at the N-terminus (C-M53) or the C-terminus (M53-C). In all three constructs, the coding sequences for the Bla fragments were separated from the M50 and M53 ORF by the 17 aa spacer (S). N-terminal Bla-fusions were HA-tagged (H), the C-terminal fusion, M53-C, was Strep-tagged (ST). **C)** 293T cells were seeded on 6 well plates and co-transfected with either pO6T-N-M50 and pO6T-C-M53 or pO6T-N-M50 and pO6T-M53-C. Mean hydrolysis rates of nitrocefin were determined (chapter 5.7.1). Error bars indicate the standard deviation.

For further experiments, the N-terminal BlaC-fusion C-M53 was used since previous studies revealed that C-terminal modifications of M53 can interfere with the functionality of the protein in the virus context, whereas mutations within the N-terminus do not.

### 6.2.2. Validation of the NEC-PCA

For validation of the PCA for M50 and M53, the Bla signal after complementation has to be significantly higher than the background signals. Further, increased hydrolysis rates have to be specific: induced exclusively when M50 and M53 interact. Finally, the fusion of the NEC proteins to the Bla fragments should not alter their functionality in the virus context.

### 6.2.2.1. Background of the NEC-PCA

The NEC-PCA background gives a measure for possible residual activity or affinity of the two Bla fragments or non-specific binding between the Bla fragments and the target proteins. To determine the background signal of the PCA, the BlaN fragment was fused to mutants of M50 (Figure 11A). These mutants were shown to be deficient in binding to M53 by co-immunoprecipitation and immunofluorescence after co-transfections (Bubeck et al., 2004). The mutants of M50 used for this study were obtained by either an insertion of a five aa transposon after the amino acids 52 or 114 of M50 (M50i52 and M50i114) or deletion of the nine amino acids, defined as the binding motif of M50 to M53 (aa51-aa59; M50DM).

When N-M50 and C-M53 were co-expressed, the hydrolysis rate of nitrocefin in the cell lysates was more than 130 fold higher than in lysates of mock transfected cells. The co-expression of C-M53 with the BlaN-fusions of M50 mutants resulted in a nitrocefin hydrolysis rate of less than 10% of the wild type N-M50/C-M53 complementation. The hydrolysis rate detected after co-transfection of the N-M50DM and C-M53 was about 12 times higher than mock and served as the background of the subsequent NEC-PCAs (detection limit; DL) (Figure 11B).

To ensure, that the low signal detected in the PCAs with non-binding M50 mutants was not due to poor protein expression, 293T cells were transfected with the individual M50 constructs. 24 h after transfection the cell lysates were probed with an anti-HA-antibody in a Western Blot. All mutants were detected at the predicted molecular weight of 56 kDa and expressed to the same level as the complementing N-M50 (Figure 11C).



## Results

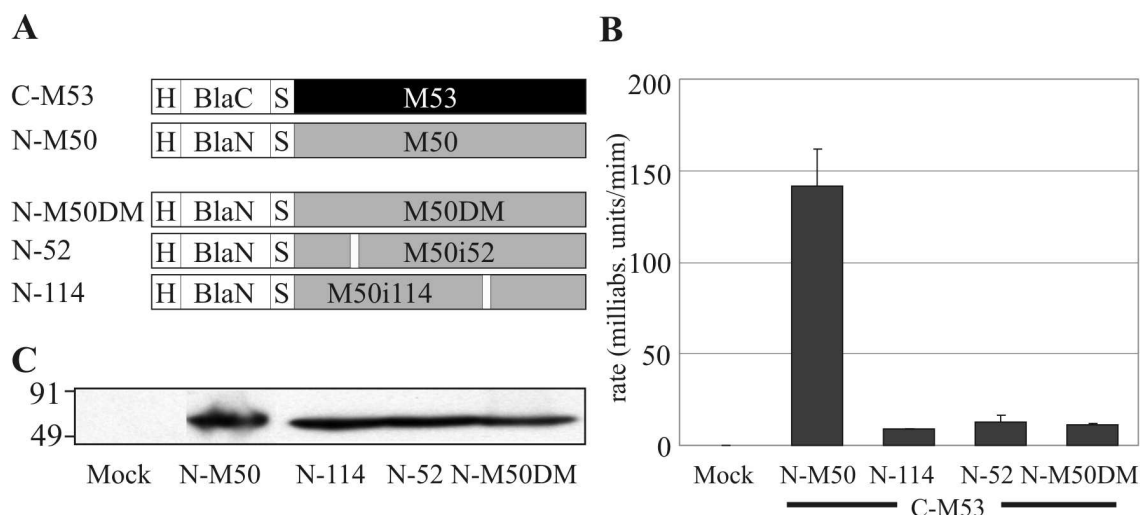


**Figure 11: Background of the NEC-PCA.**

**A)** Schematic representation of the HA (H)-tagged Bla-fusion constructs. BlaN (N) and a glycine/serine spacer (S) were fused to mutants of M50 that were shown to be deficient in binding to M53. **B)** Bla activity in cell lysates after co-expression in 293T cells. C-M53 was co-expressed with N-M50 and the N-M50 mutants (N-52, N-114 and N-M50DM). Mean hydrolysis rates of nitrocefin were determined (chapter 5.7.1). Error bars indicate the standard deviation. **C)** Steady state level of the expression of N-M50 and N-M50 mutants shown in a HA-specific Western Blot after isolated expression in 293T cells. Numbers indicate the position and size of the protein marker in kDa.

### 6.2.2.2. Specificity of the NEC-PCA

The specificity of the N-M50/C-M53-PCA was tested in the presence of increasing amounts of wt M50, which binds C-M53 but does not complement due to the lack of the complementary Bla fragment. If the PCA signal is only dependent on the M50/M53 interaction, the wt M50 would compete with N-M50 for C-M53, which then should result in the decrease of the PCA signal. Therefore, wt M50 was expressed by the expression construct pOriR6K-zeo-ie-M50 (Bubeck et al., 2004). The competitor pOriR6K-zeo-ie-M50 DNA was added to the co-transfections in increasing amounts from 0,5 to 3  $\mu$ g, whereas the amount and ratio of DNA coding for N-M50 and C-M53 was kept at a constant 1,5  $\mu$ g for all co-transfections. To ensure that any change in signal strength was not due to an overload of transfected DNA, the amount of transfected DNA was kept constant by an adequate addition of the carrier DNA pO6-IET-gfp coding for GFP, a protein, which is irrelevant in the assay.

As shown in Figure 12A, the PCA signal decreased in a wt M50 concentration dependent manner. The initial hydrolysis rate of 170 milliabsorption units/min in the absence of wt M50 was gradually reduced by more than three fold, reflecting the relative proportion of tagged and non-tagged M50. The amounts of N-M50 and wt M50 in the assay

## Results

were visualized by an anti-M50 probed Western Blot. N-M50 and wt M50 were detected at the predicted sizes of 56 kDa and 35 kDa, respectively (Figure 12B). Degradation products of M50 with lower molecular weights were detected in all lanes except for the first, where only N-M50 and C-M53 were present. This, and the slight decrease of detected N-M50 over the increase of wt M50, are presumably due to the instability of N-M50. The wt M53 stabilizes wt M50 (Bubeck et al., 2004) which also seems to be true for N-M50, if C-M53 is present. If C-M53 is competed out by wt M50, N-M50 becomes unstable.

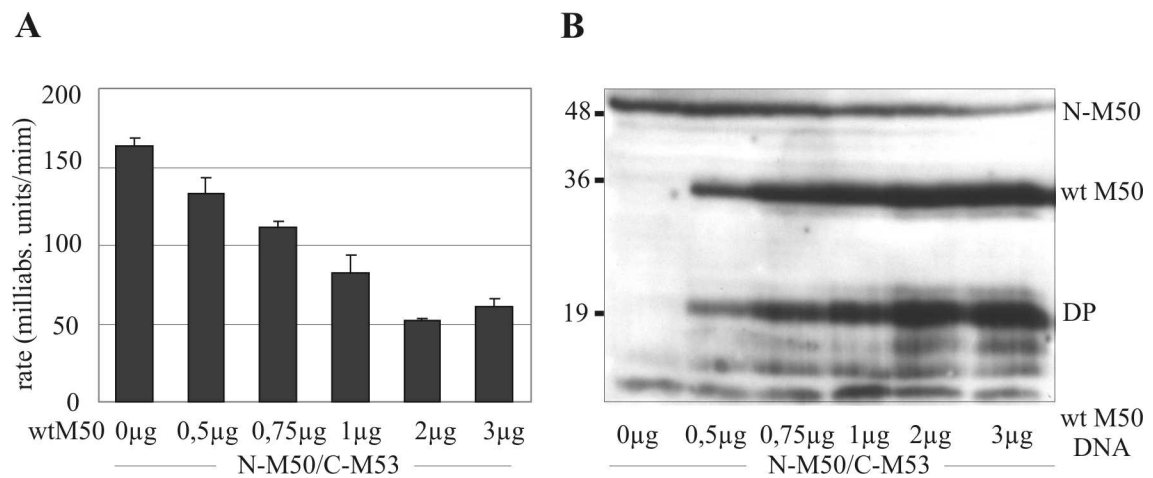


**Figure 12: Specificity of the NEC-PCA.**

**A)** Competition assay. Bla activity in cell lysates after co-expression in 293T cells. N-M50 and C-M53 (1,5 µg of each DNA) were co-expressed together with increasing amounts of wt M50. Carrier DNA was added in the transfections to maintain the constant amount of 6 µg total DNA. Mean hydrolysis rates of nitrocefin were determined (chapter 5.7.1). Error bars indicate the standard deviation. **B)** Steady state level of N-M50 and wt M50 expression shown by an M50-specific antibody in a Western Blot. Indicated on the right N-M50 (56 kDa), wt M50 (35 kDa) and lower sized degradation products (DP) of M50 (Muranyi et al., 2002). Numbers on the left indicate the position and size of the protein marker in kDa.

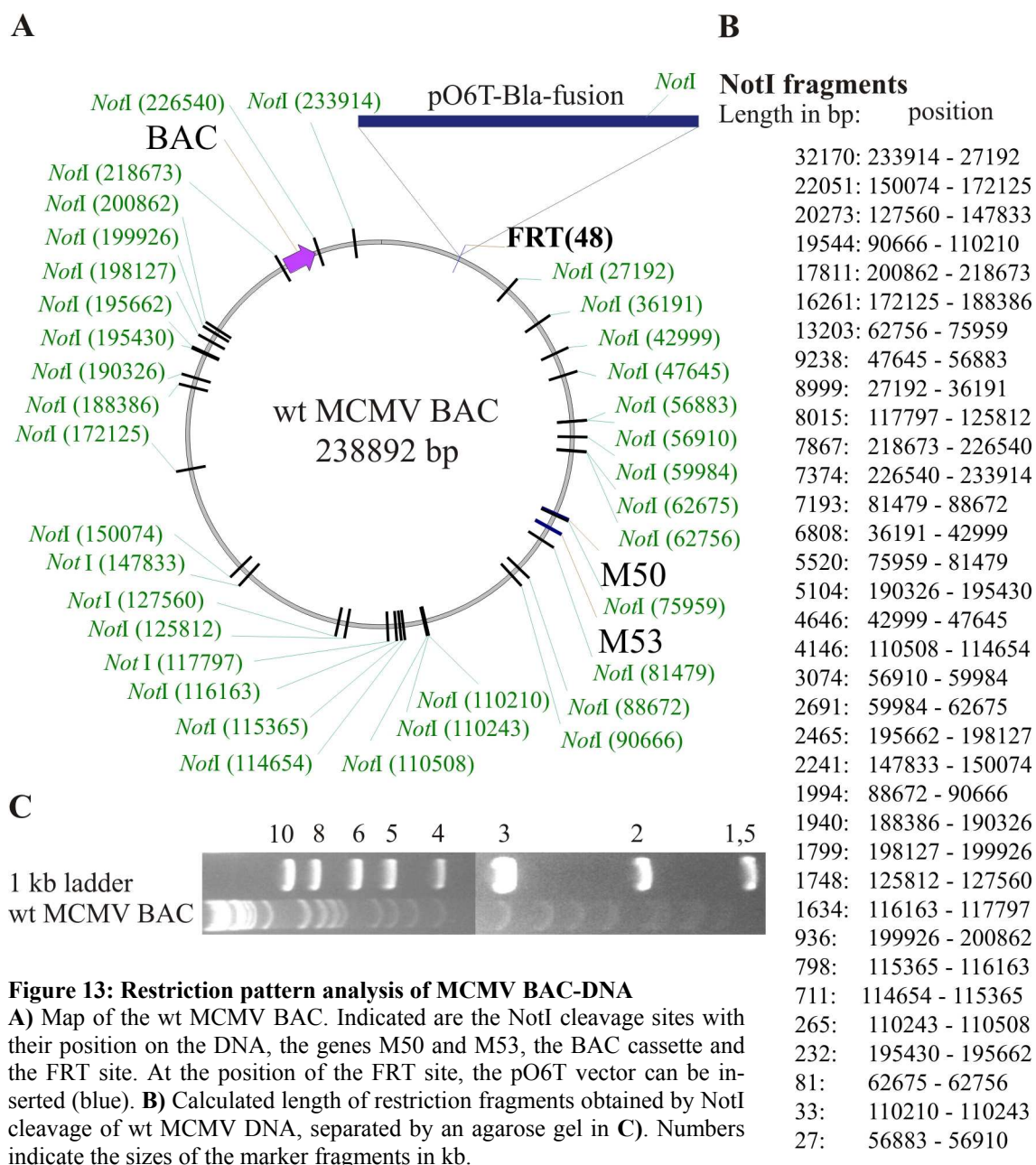
### 6.2.2.3. Functionality of the fusion proteins used in the NEC-PCA

N-M50 and C-M53 were tested for their functionality in the context of MCMV replication to show that their essential features were retained upon fusion to the Bla fragments. To this end, the fusion constructs were introduced into MCMV genomes lacking the native genes.

The N-M50 and C-M53 genes were inserted into  $\Delta$ M50 and  $\Delta$ M53 genomes, respectively. In these two MCMV BAC genomes, the ORF of wt M50 or wt M53 was deleted by homologous recombination and replaced by a kanamycin selection cassette. As a

further mutation to the wt MCMV genome, these BACs carry an FRT site between the m16 and m17 gene. The FRT site allows an efficient insertion of additional genetic elements at that position. In previous studies in which essential genes like M50 or M53 were deleted from the genome, the resulting null phenotype was rescued when the respective genes were re-inserted into the BAC at this position (Bubeck et al., 2004; Lötzerich et al., 2006). Insertion of genes at the m16/m17FRT locus requires the expression of Flp recombinase (McLeod et al., 1986) and the presence of a DNA fragment carrying another FRT site compatible with that in the BAC. The Flp recombinase is expressed from the temperature sensitive plasmid pCP20, which is introduced into the bacteria harbouring the BACs to be targeted. The second FRT site is located on the pO6T vector (chapter 6.1.2), thus not only serving as an expression vector but also as a shuttle plasmid for insertion into the FRT site of the MCMV BAC (chapter 3.1.5.2).

Figure 13A gives an overview of the wt MCMV BAC genome and the BAC-DNA restriction pattern. The NotI cleavage sites are indicated as it was used for characterization of the BAC-DNA constructs. The relatively low number of NotI recognition sites on the BAC-DNA (less than 40) made it the most suitable enzyme for restriction analysis. Detection of changes in the restriction pattern enabled distinction not only of wt BACs from BAC constructs with the inserted pO6T, but also of multiple copy inserts from the desired single insertion clones. While both single and multiple copy inserts result in the appearance of a new band at 11,8 kb, only the multiple copy clones display an additional 3000-3500 bp band. This additional band corresponds to the size of the pO6T constructs and their presence in the BAC as tandem repeats. Single insertion constructs lack this additional band due to a single NotI cleavage site in the pO6T vector backbone.



Bacteria carrying the BACs with the M50 or M53 deletion genomes ( $\Delta$ M50 and  $\Delta$ M53) together with pCP20 were transformed with pO6T-N-M50 or pO6T-C-M53, respectively. Flp mediated homologous recombination was performed for one hour at the permissive temperature of 30 °C, before the rise to cultivation temperature of 43 °C, the non-permissive temperature for pCP20. Bacterial clones were then selected for the insertion of the pO6T constructs on zeocin and chloramphenicol (Cam) containing agar plates. Bacteria harbouring the BAC with the inserted pO6T constructs are resistant to both antibiotics due to the Cam resistance gene in the BAC cassette and the zeocin re-

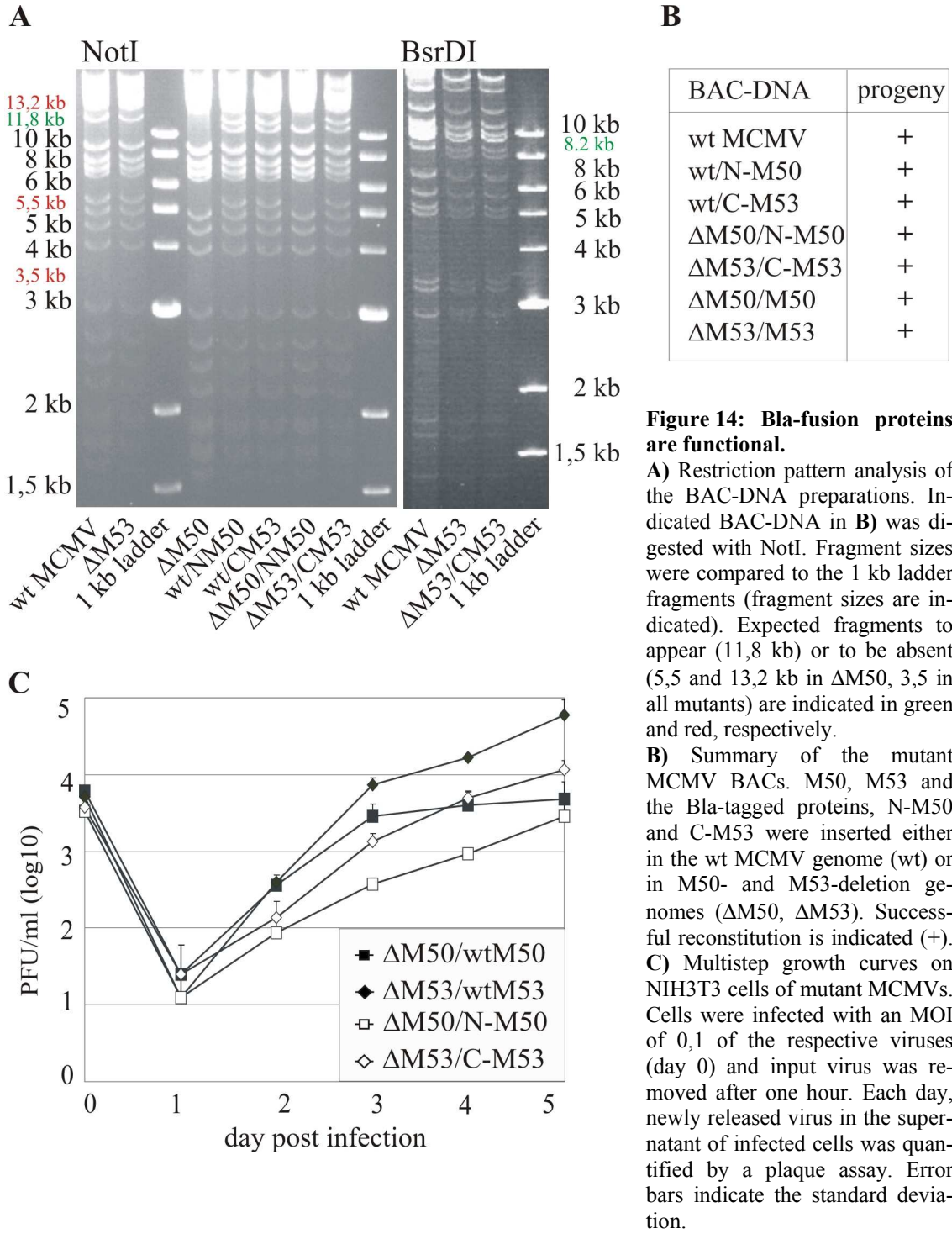
## Results

---

sistance in the pO6T vector. Co-existence of both DNA molecules in the same cell is excluded since the DH10B strain does not support the replication of the pO6T plasmids (Bubeck et al., 2004). The mutated MCMV BAC-DNA of  $\Delta$ M50/N-M50 and  $\Delta$ M53/C-M53 was isolated and analysed by restriction pattern analysis (Figure 14A). Compared to the wt MCMV BAC-DNA, an additional band at 11,8 kb showed the insertion of the expression vectors for the Bla-fusion proteins. Single copy inserts were selected by the absence of an additional band of about 3,5 kb. BACs with the  $\Delta$ M50-backbone lack the DNA fragments of 5,5 and 13,2 kb since a NotI site is located in the M50 ORF which is removed with the deletion of M50. Instead, an additional fragment of 18,9 kb appears which, however, cannot be distinguished from the neighbouring DNA fragments. All other fragments appeared in the constructed recombinant BACs as well as in the control DNA of the wt MCMV BAC, excluding other unwanted recombination events. To confirm the absence of the native M53 gene in constructs based on the  $\Delta$ M53-backbone, an additional BsrDI digest was performed. Deletion of the native M53 leads to an 8200 bp fragment in addition to an 8700 bp fragment from the wt MCMV genome.

The BAC-DNA of two clones, showing the expected restriction pattern, was isolated from bacteria and subsequently transfected into mouse embryonic fibroblasts (MEF) to allow virus reconstitution.

After transfection of MEF cells, both the  $\Delta$ M50/N-M50 and  $\Delta$ M53/C-M53 BAC, gave rise to infectious progeny (Figure 14B and C). Initial viral plaques were observed after two passages of the transfected MEFs, about 16-18 days after transfection of the BAC-DNA. Cells were harvested when the entire monolayer was lysed by the mutant viruses.



### 6.2.2.3.1. Fitness of the $\Delta$ M50/N-M50 and $\Delta$ M53/C-M53 virus

Multi-step growth curves were performed to compare the replication ability of the mutant viruses carrying the M50 and M53 Bla-fusions ( $\Delta$ M50/N-M50 and  $\Delta$ M53/C-M53) to MCMV mutant viruses carrying the wt M50 or wt M53 ( $\Delta$ M50/wtM50 and  $\Delta$ M53/wtM53) at the same ectopic position. NIH3T3 fibroblasts were infected with a multiplicity of infection (MOI) of 0,1 and incubated for one hour with the infectious supernatant. Thereafter the supernatants were replaced with fresh culture media. Newly produced infectious particles were quantified daily over a period of 5 days, including the titre of the inoculums (day 0).

The growth of  $\Delta$ M50/N-M50 and  $\Delta$ M53/C-M53 was comparable to  $\Delta$ M50/wtM50 (Bubeck et al., 2004) and  $\Delta$ M53/wtM53 (Lötzerich et al., 2006). The high virus titre at day 0 represents the titre of the infectious inoculums used to initiate the growth curves. The sudden decline in titre at day 1 indicates that the input virus was removed by the medium exchange since the generation time of the MCMV is longer than 24 h. Accordingly, release of infectious particles was detectable from the second day and reached its highest titre at day 5, the last day of the experiment (Figure 14C). A difference in peak titres of less than one log is usually considered to be not significant because of the logarithmic nature of titre determination. This was confirmed by an ANOVA test, calculating a p-value above 0,05 for the growth differences of  $\Delta$ M50/wtM50 and  $\Delta$ M50/N-M50 ( $p=0,37$ ) and the p-value of for the growth difference of  $\Delta$ M53/wtM53 and  $\Delta$ M53/C-M53 ( $p=0,07$ ).

These experiments validated the PCA for the NEC proteins M50 and M53. The background of the N-M50/C-M53-PCA, due to spontaneous folding of the Bla fragments was low as shown by co-expression of C-M53 with N-M50 mutants. The specificity of the PCA signal was confirmed by the competition experiment and the functionality of the Bla-fusion proteins was proven by their ability to replace the wt NEC proteins. Thus the NEC-PCA provides a tool to monitor and characterize the interaction of M50 and M53.

### 6.3. The UL34/UL31 interaction of different herpesviruses

Any essential interaction of herpesviral proteins, which leave cellular processes untouched, may serve as potential drug targets. Most favourable are interactions that are conserved throughout all three herpesvirus subfamilies. Homologues of M50 and M53, members of the UL34 and UL31 protein families, respectively, are present in all species of *herpesviridae* and are highly conserved in their amino acid sequence (Figure 19 and Figure 22). The aim of the work presented in this chapter was an extensive study of the two interacting proteins in the aspect of a universal drug target to fight herpesvirus related diseases.

In order to study the binding of M50 and M53 homologues, the NEC-PCA established for M50 and M53 was expanded to include representatives belonging to the  $\alpha$ - and  $\gamma$ -herpesvirus subfamilies and a second virus of the  $\beta$ -herpesvirus subfamily. The UL34 and UL31 family members of PrV, HSV-1, HCMV, MHV68 and EBV were fused to the Bla fragments in the same manner as M50 and M53. The N-terminus of Bla (BlaN; N), was fused N-terminally to the UL34 family members and the C-terminus of Bla (BlaC; C), was fused N-terminally to the UL31 family members of the representative herpesviruses (Table 4).

**Table 4 : Members of the UL31 and UL34 protein families of representative herpesviruses.**

List of the six UL34 and UL31 family members included in the study. Indicated in the first column the herpesvirus subfamily the virus (second column) belongs to, followed by the name, abbreviation and length of the proteins of the UL34 and UL31 protein family.

Subfamily	Virus	UL34 homologue	UL31 homologue
$\alpha$	HSV-1	UL34 (h); 275 aa	UL31 (H); 306 aa
$\alpha$	PrV	UL34 (p); 260 aa	UL31 (P); 271 aa
$\beta$	HCMV	UL50 (c); 397 aa	UL53 (C); 376 aa
$\beta$	MCMV	M50 (m); 316 aa	M53 (M); 333 aa
$\gamma$	EBV	BFRF1 (e); 336 aa	BFLF2 (E); 318 aa
$\gamma$	MHV68	Orf67 (g); 226 aa	Orf69 (G); 292 aa



## Results

To test the fusion constructs for expression, pO6TN-UL34 and pO6TC-UL31 homologues (Figure 15A) were transfected into 293T cells. Cells were lysed and the proteins analysed by an anti-HA probed Western Blot. N-UL34 fusion proteins were detected at the predicted molecular weight between 50 and 80 kDa (Figure 15B, upper panel) and C-UL31 fusion proteins at the predicted molecular weight between 33 and 50 kDa (Figure 15B, lower panel). All proteins were expressed to a comparable level. The two fusion proteins N-M50 and N-UL50 show lower molecular weight degradation products which were frequently observed in previous experiments where UL50 or M50 were expressed without the BlaN-tag (Bubeck et al., 2004).

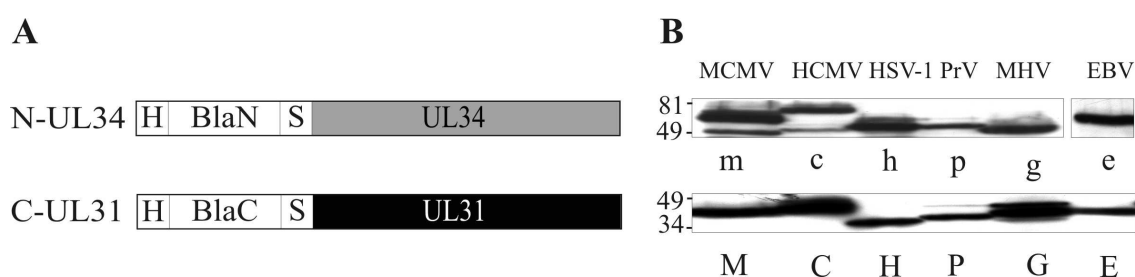


**Figure 15: Bla-fusions to members of the UL34 and UL31 family.**

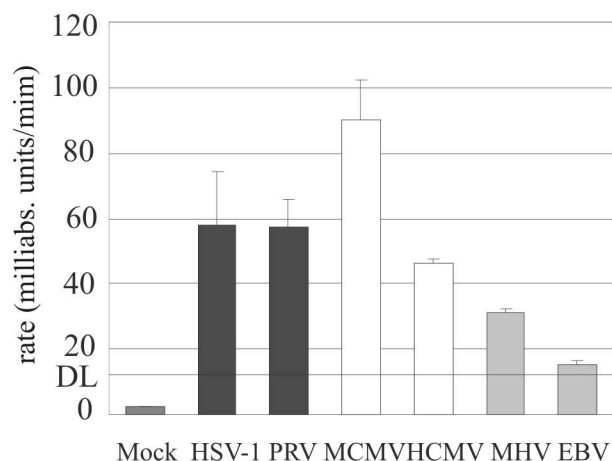
**A)** Schematic representation of the used HA (H)-tagged Bla-fusion constructs. The N- (BlaN) and C-terminal part (BlaC) of the Bla were fused to members of the UL34 and UL31 family, linked by a glycine/serine spacer (S). BlaN was fused to members of the UL34 family: M50 (m), UL50 of HCMV (c), UL34 of HSV-1 (h), UL34 of PrV (p), Orf67 of MHV68 (g) and BFRF1 of EBV (e). BlaC was fused to the members of the UL31 family: M53 (M), UL53 of HCMV (C), UL31 of HSV-1 (H), UL31 of PrV (P), Orf69 of MHV68 (G) and BFLF2 of EBV (E). **B)** Steady state level of expression of N-UL34 and C-UL31 fusion proteins shown in an HA-specific Western Blot. Numbers indicate the position and size of the protein marker in kDa.

### 6.3.1. UL34 and UL31 family members in the NEC-PCA

The NEC-PCA was performed by the co-expression of BlaN- and BlaC-fusions of each virus in 293T cells. After 24 h, cells were lysed and tested for reconstituted Bla activity induced by the interacting proteins. Specific signals were obtained for the NEC proteins of HSV-1, PrV, MCMV, HCMV and MHV68. For  $\gamma$ -herpesvirus MHV68 the detected signal was low but significant, however, in case of EBV the complementation induced hydrolysis rate was not significantly higher than the detection limit (p-value = 0,22) (Figure 16). The high hydrolysis rate obtained with the MCMV proteins in contrast to the lower signal of the homologues probably reflects the optimization of the assay towards that particular interaction (chapter 5.7.1).

**Figure 16: The NEC-PCA with members of the UL34 and UL31 family of different viruses.**

Interaction of N-UL34 and C-UL31 homologues after co-expression in 293T cells. From left to right: N-UL34/C-UL31 (HSV-1), N-UL34/C-UL31 (PrV), N-M50/C-M53 (MCMV), N-UL50/C-UL53 (HCMV), N-Orf67/C-Orf69 (MHV68) and N-BFRF1/C-BFLF2 (EBV). Mean hydrolysis rates of nitrocefin were determined (chapter 5.7.1). The indicated detection limit (DL) was defined by the hydrolysis of nitrocefin after co-expression of C-M53 and N-M50DM. Error bars indicate the standard deviation.



### 6.3.2. Cross-complementation within the UL34 and UL31 families

The development of a drug targeting the important interaction of UL34 and UL31 family members of several herpesviruses requires a high degree of protein homology. Analysis of translated sequence revealed both protein families were highly conserved (Figure 19 and Figure 22). In order to see whether the conserved NEC proteins of different viruses bind to each other, functional assays were performed. Proteins of both families were co-transfected in a heterologous manner to determine their ability for cross-complementation. The Bla-fusions of UL34 and UL31 family members from the three viruses PrV, HCMV and MHV68 were chosen as representatives for each of the three herpesvirus subfamilies and co-expressed with all six potential partners which have been tested for the native PCAs (Figure 16).

#### 6.3.2.1. Cross-complementation by UL31 family members

To measure the extent to which UL34 family members are able to interact with UL31 family members of other viruses, the N-UL34 homologue of PrV, HCMV or MHV68 was co-expressed with each C-UL31 fusion protein of the study. The corresponding plasmids were co-transfected into 293T cells and Bla activity was determined after 24 h (Figure 17).

N-UL34 of PrV resulted in a high Bla activity in combination with C-UL31 of either HSV-1 (H) or PrV (P), however no significant signal was obtained in combination with BlaC-fusions to UL31 homologues of other subfamilies represented by MCMV, HCMV, MHV68 or EBV proteins (Figure 17A). For all combinations of Bla-fusions in which crossing the subfamilies were tested, no significant signal was obtained. This revealed that N-UL34 of PrV is complemented by the UL31 family member of the same

herpesvirus subfamily, but not by homologues of the  $\beta$ - or  $\gamma$ -herpesvirus subfamily. A similar pattern was observed when either N-UL50 or N-Orf67 was co-expressed with the six BlaC-fusions (Figure 17B and C): N-UL50 and N-Orf67 were complemented to a high percentage by the homologue of their subfamily, either MCMV or EBV, but not by the Bla-fusions of the other two herpesviruses subfamilies. C-M53 complemented its HCMV homologue C-UL53 to nearly 100%. For the  $\alpha$ - and  $\gamma$ -herpesvirus subfamily, the heterologous combination of N-UL34 with C-UL31 (UL34/H) and N-Orf67 with C-BFLF2 (Orf67/E) gives an even higher signal in the PCA than the native combination of N-UL34 with C-UL31 (UL34/P) and N-Orf67 with C-Orf69 (Orf67/G). This might indicate a stronger interaction of the heterologous proteins or better accessibility of the Bla fragments to each other.

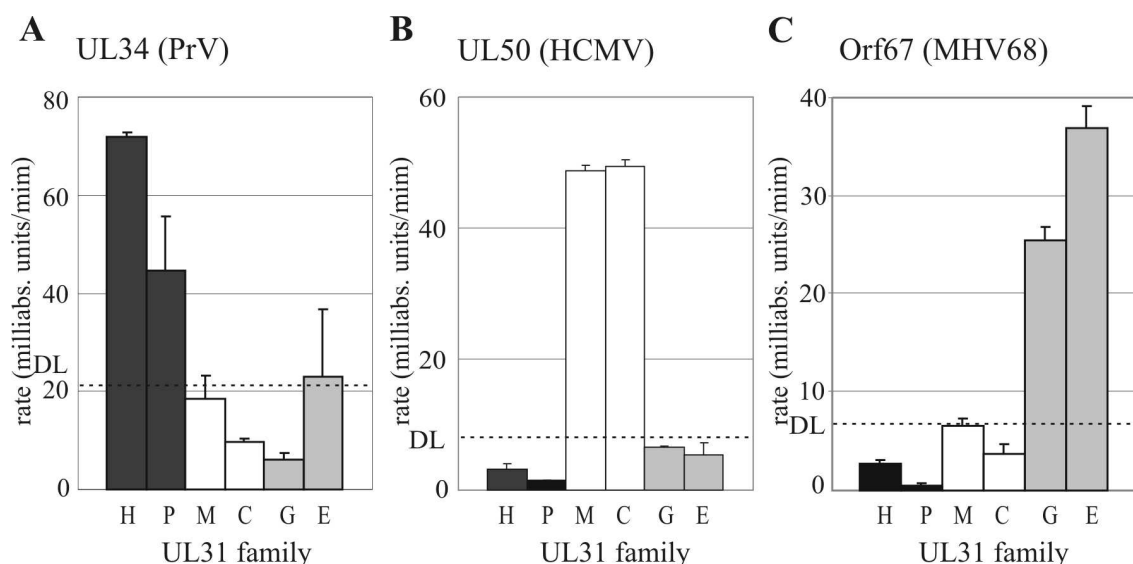


**Figure 17: Cross-complementation by UL31 family members.**

Members of the UL34 and UL31 protein families were co-expressed in heterologous combinations. The partners in the co-expressions were N-UL34 (A), N-UL50 (B) and N-Orf67 (C) in combination with C-UL31 of HSV-1 (H), C-UL31 of PrV (P), C-M53 (M), C-UL53 (C), C-Orf69 (G) and C-BFLF2 (E). Mean hydrolysis rates of nitrocefin were determined (chapter 5.7.1). The indicated detection limit (DL) is defined by the hydrolysis rate of nitrocefin after co-expression of C-M53 and N-M50DM. Black, white and grey indicate UL31 family members of  $\alpha$ -,  $\beta$ -, and  $\gamma$ -herpesviruses, respectively. Error bars indicate the standard deviation.

### 6.3.2.2. Cross-complementation by UL34 family members

Having shown the cross-complementation by UL31 family members, the extent to which UL34 family members of different viruses can replace each other in the PCA was measured. In the same manner as for the cross-complementation experiments in chapter

## Results

6.3.2.1, the C-UL31 homologue of PrV, HCMV or MHV68 was co-expressed with each N-UL34 fusion protein of the study.

Similar to the pattern already observed for cross-complementation with different BlaC-fusions (chapter 6.3.2.1), the reaction of C-UL31 of PrV with the six BlaN-fusions to UL34 family members was only positive in combination with N-UL34 of either PrV or HSV-1 (UL31/p and UL31/h) but not for fusion proteins of MCMV, HCMV, MHV68 or EBV, belonging to other herpesvirus subfamilies (Figure 18A). However, even N-UL34 of HSV-1 (h) complemented the C-UL31 of PrV only to an extent of 35% of the native PrV interaction (UL31/p, Figure 18A). When C-UL53 was co-expressed with the six N-UL34 fusions, the strength of the Bla signal obtained by the native combination of C-UL53 with N-UL50 (UL53/c) was only reached in the combination of C-UL53 with the partner of the same herpesvirus subfamily, N-M50 (UL53/m), but not with any BlaN-fusion of the other herpesviruses (Figure 18B). In contrast to the  $\alpha$ - and  $\beta$ -herpesvirus, C-Orf69 was not cross-complemented by any of the heterologous BlaN-fusions (Figure 18C).

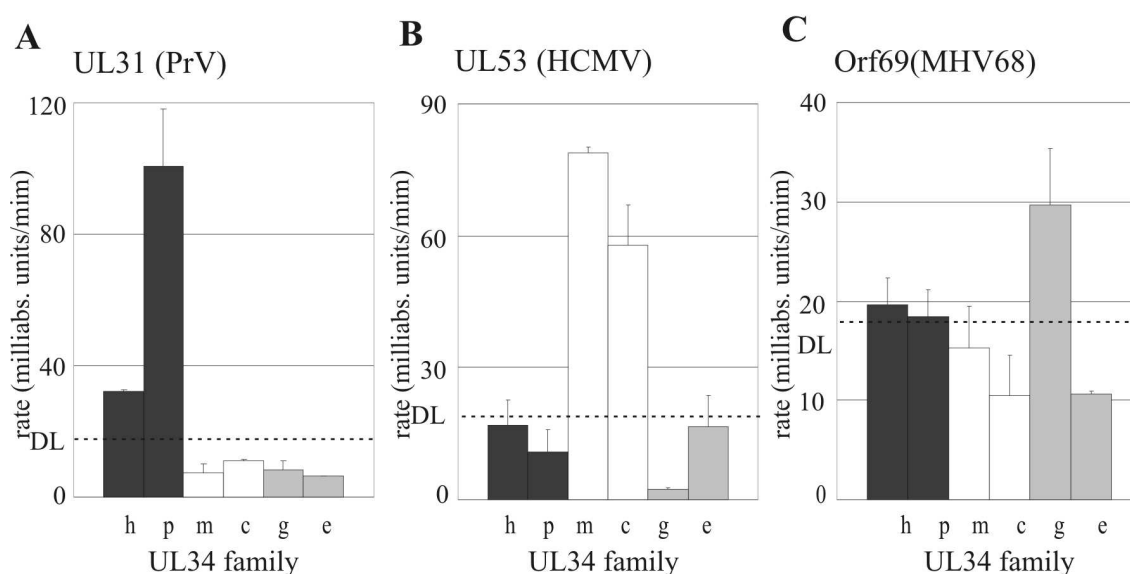


**Figure 18: Cross-complementation of UL34 family members.**

Members of the UL34 and UL31 protein families were co-expressed in heterologous combinations. The partners in the co-expressions were C-UL31 (A), C-UL53 (B) and C-Orf69 (C) in combination with N-UL34 of HSV-1 (h), N-UL34 of PrV (p), N-M50 (m), N-UL50 (c), N-Orf67 (g) and N-BFRF1 (e). Mean hydrolysis rates of nitrocefin were determined (chapter 5.7.1). The indicated detection limit (DL) is defined by the hydrolysis rate of nitrocefin after co-expression of C-M53 and N-M50DM. Black, white and grey indicate UL34 family members of  $\alpha$ -,  $\beta$ -, and  $\gamma$ -herpesviruses, respectively. Error bars indicate the standard deviation.

In summary, the PCA indicates cross-complementation is possible within the herpesvirus subfamilies, however, no cross-complementation was measured across subfamilies. BlaN-fusions within subfamilies were found to interact to nearly the same extent with the tested BlaC-fusions as they do with the natural NEC partner. Therefore, despite sequence conservation, the binding specificity has diverged with the subfamilies.

### 6.3.3. Study of the binding sites in the UL34 and UL31 protein family

As seen in the co-transfection experiments, binding of the UL34 and UL31 homologues is conserved, however the binding site of the UL34 and UL31 protein families diverged during evolution of the subfamilies.

#### 6.3.3.1. The binding site in the UL31 family

The UL31 family is highly conserved. A similarity blot, obtained by the alignment of the six UL31 family members used in this study, allows a simple subdivision of the proteins into four conserved regions, depicted in Figure 19A. Stretches of amino acid similarity of up to 60% are separated from each other by short interspaces of low conservation, thereby defining the borders of the conserved regions (CR). The N-terminal parts of the aligned proteins show a low level of conservation, indicating a species specific part of the protein, here depicted as variable region (V). It was recently shown by our group that the binding site of M53 to M50 is located in the first conserved region (CR1) of M53. The variable region carries a nuclear localisation signal (NLS) (Lötzerich et al., 2006) to direct the protein to the cell nucleus. For the three C-terminal conserved regions (CR2-CR4) no function has yet been assigned.

For other UL31 family members, binding to the UL34 homologues was reported but the binding domains have not been defined. Therefore, based on the findings in M53 and the similarity of the protein sequences (Figure 19A and B), all three herpesvirus subfamilies were tested to determine whether the CR1 harbours the binding site to members of the UL34 family. To this end, chimeric BlaC-fusions were constructed combining the variable region and the CR1 of one UL31 family member and the subsequent three conserved regions (CR2-CR4) of another (Figure 19C, Table 5). The variable region and CR1 of M53 were fused to CR2-CR4 of UL31 of PrV or Orf69 of MHV68 (C-MP and C-MG). Accordingly, the variable region and the CR1 of UL31 or Orf69 were fused to

## Results

CR2-CR4 of M53 (C-PM and C-GM). Expression of the chimeric proteins at the expected size (Table 5) was confirmed by an anti-HA probed Western Blot (Figure 19D).

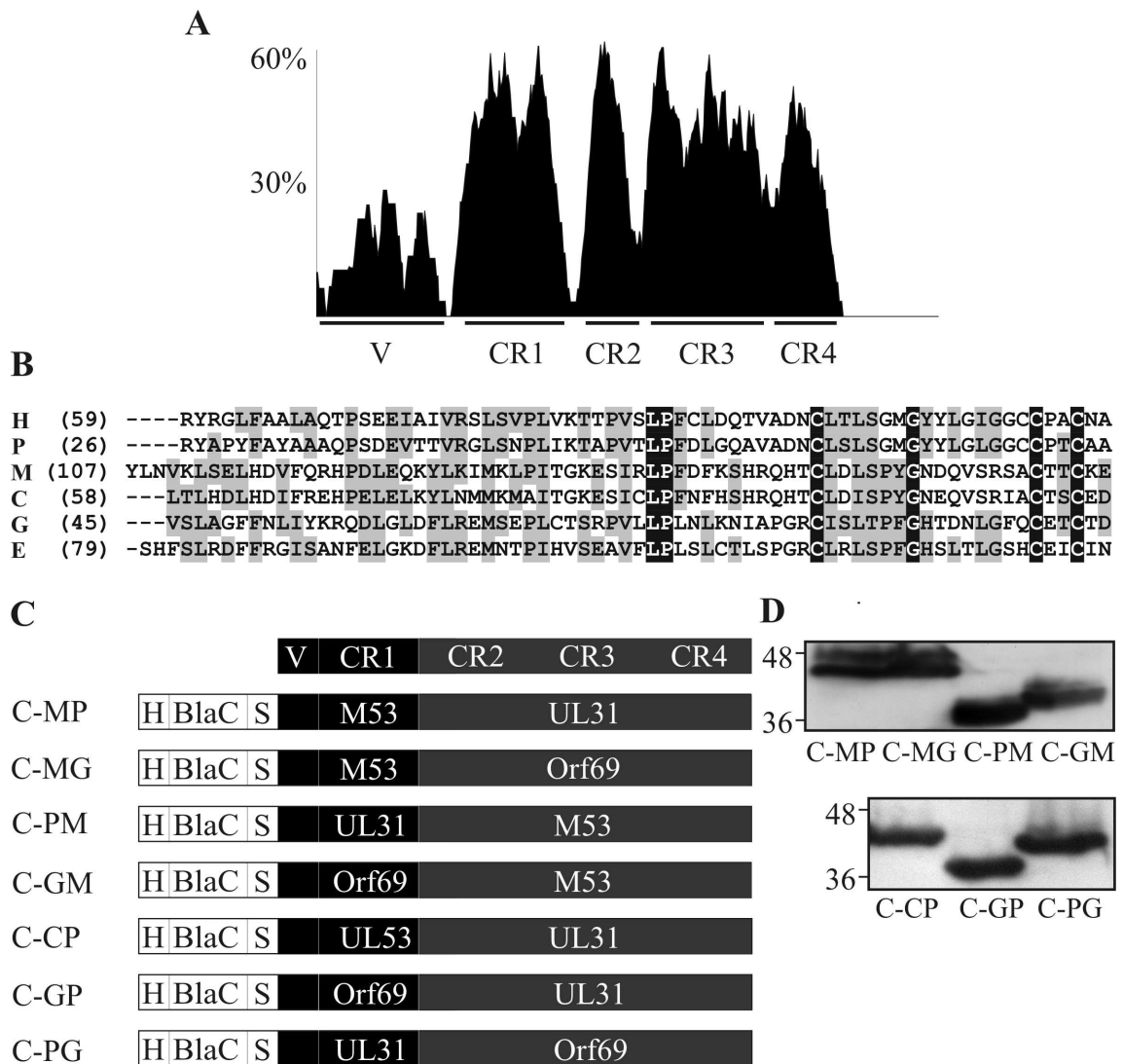


**Figure 19: BlaC-fusions to chimeric UL31 proteins.**

**A)** Similarity blot obtained by the alignment of the protein sequences of the six UL31 family members. Indicated are the variable region (V) and the four conserved regions, CR1–CR4. **B)** Alignment of the first conserved region (CR1) of the studied UL31 family members. Black indicates identical, grey similar residues. The capital letters stand for the UL31 homologues, UL31 of HSV-1 (H), UL31 of PrV (P), M53 (M), UL53 (H), Orf69 (G) and BFLF2 (E). The numbers in brackets stand for the number of the first aa of the depicted CR1. **C)** Schematic representation of the HA (H)-tagged constructs. The C-terminal part (BlaC) of Bla was fused to chimeras, built up by the variable region (V) and CR1 of one UL31 family member and the CR2-CR4 of another. The CR1 of M53 was combined with the CR2-CR4 of UL31 of PrV (C-MP) or CR2-CR4 of Orf69 (C-MG). The CR1 of UL31 of PrV and the CR1 of Orf69 were combined with the CR2-CR4 of M53, UL31 or Orf69 (C-PM, C-GM, C-GP and C-GP, respectively). The CR1 of UL53 was combined with the CR2-CR4 of UL31 (C-CP). **D)** Steady state expression levels of the chimeric fusion proteins shown in an HA-specific Western Blot after isolated expression. Numbers indicate the position and size of the protein marker in kDa.

## Results

**Table 5 : Chimeric UL31 proteins.**

List of chimeric UL31 proteins, obtained by the fusion of BlaC to UL31 proteins built up by the variable region (V) and CR1 of one UL31 family member and CR2-CR4 of another. Indicated are the amino acids defining the variable and conserved regions of the proteins used to construct the chimeras. The last column lists the calculated size of the BlaC-tagged chimeras.

Chimera	V and CR1	CR2-CR4	Protein size
C-MP	M53 (aa1-aa175)	UL31 (aa92-aa271)	53 kDa
C-MG	M53 (aa1-aa175)	Orf69 (aa112-aa292)	53 kDa
C-PM	UL31 (aa1-aa91)	M53 (aa176-aa333)	41 kDa
C-GM	Orf69 (aa1-aa111)	M53 (aa176-aa333)	43 kDa
C-CP	UL53 (aa1-aa125)	UL31 (aa92-aa271)	47 kDa
C-GP	Orf69 (aa1-aa111)	UL31 (aa92-aa271)	45 kDa
C-PG	UL31 (aa1-aa91)	Orf69 (aa112-aa292)	43 kDa

### 6.3.3.1.1. The binding site in UL31 homologues in $\beta$ -herpesviruses

To confirm that the CR1 of M53 bears the binding site to M50 (Lötzerich et al., 2006), the chimeric BlaC-fusion proteins were co-expressed with N-M50 (m) and tested for reconstituted Bla activity in the PCA (Figure 20). As seen previously, a high hydrolysis rate of about 100 milliabsorption units/min was obtained when the NEC proteins of MCMV were co-expressed (m/M) but no cross-complementation was observed in the combination with C-UL31 or C-Orf69 (m/P and m/G). However, if N-M50 was co-expressed with either of the two chimeric BlaC-fusions C-MP and C-MG, bearing the variable region and CR1 of M53 (m/C-MP and m/C-MG), binding to N-M50 was restored. C-MP complemented N-M50 to about 50% of the native MCMV interaction (Figure 20A), whereas C-MG fully complemented the C-M53/N-M50 interaction (M/m). In contrast, N-M50 co-expressed with the chimeric BlaC-fusion constructs bearing the heterologous CR1s, C-PM and C-GM, did not lead to complementation. For those combinations, the reconstituted Bla activity was below the detection limit, which was defined by the interaction of C-M53 and the non-binding M50 mutant, N-M50DM. These data confirm that the first conserved region of M53 is necessary and sufficient for binding to M50.

## Results

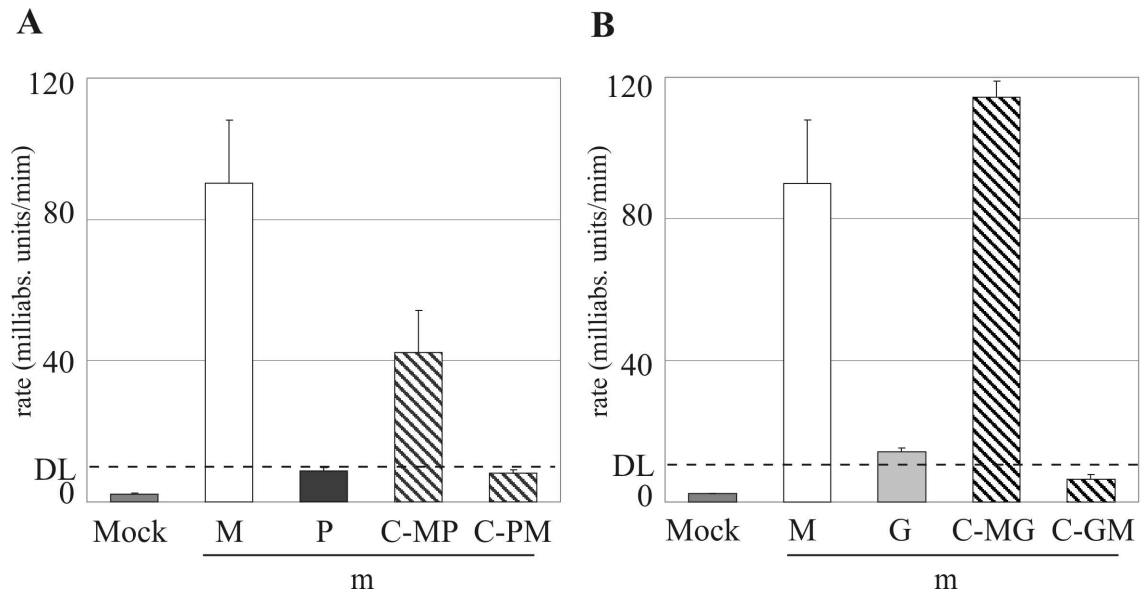


**Figure 20: Mapping the binding site in M53.**

Bla activity in cell lysates after co-expression in 293T cells. **A)** N-M50 (m) was co-expressed with C-M53 (M), C-UL31 of PrV (P) and the chimeric fusion constructs C-MP and C-PM. **B)** N-M50 was co-expressed with C-M53 (M), C-Orf69 (G) and the chimeric fusion constructs C-MG and C-GM. Mean hydrolysis rates of nitrocefin were determined (chapter 5.7.1). The indicated detection limit (DL) is defined by the hydrolysis of nitrocefin after co-transfection of C-M53 and N-M50DM. Error bars indicate the standard deviation.

Since UL31 family members can cross-complement each other within subfamilies (chapter 6.3.2.1), we wanted to confirm this cross-complementation was dependant on the CR1 region. Therefore, the chimeric protein C-MP was modified by replacing the variable region and CR1 of M53 by the respective parts of UL53, resulting in the chimeric protein C-CP (Table 5). C-UL53 complements N-M50 to more than 65% of the interaction of the MCMV proteins N-M50/C-M53. In contrast, co-expression of C-CP and N-M50 lead to only 15% of the native N-M50/C-M53 (m/M) interaction and 22% of the cross-complementing  $\beta$ -NEC proteins, N-M50/C-UL53 (m/C) (data not shown).

### 6.3.3.1.2. The binding site in UL31 homologues in $\alpha$ - and $\gamma$ -herpesviruses

Having confirmed the M53 binding site to M50 is located in the first conserved region, the chimeric proteins were then co-transfected with the Bla<sub>N</sub>-fusions to UL34 of PrV and Orf67 of MHV68 to test for the binding site in the proteins belonging to the  $\alpha$ - and  $\gamma$ -herpesvirus subfamilies. The findings obtained by these co-transfections were comparable to the data concerning M53 (chapter 6.3.3.1.1). An hydrolysis rate of about 75 milliabsorption units/min was obtained when the NEC proteins of PrV were co-expressed (p/P) but no cross-complementation was observed in combination with C-



## Results

M53 or the chimeric BlaC-fusion C-MP. However, the combination of N-UL34 with C-PM or C-PG, bearing the CR1 of UL31 of PrV (p/C-PM and p/C-PG), restored the binding and gave rise to a signal of about 65% and 56% of the native PrV interaction (p/P), respectively (Figure 21A for p/C-PM). Similarly, for co-transfection of MHV68 fusion proteins, a positive signal was only obtained for the combination of N-Orf67 (g) with proteins bearing the CR1 of Orf69, namely C-Orf69 (G) or the chimera C-GM. Proteins bearing the heterologous CR1, C-M53 (M) or C-MG, did not lead to a significant Bla signal after co-transfection (Figure 21B).

These data confirm that the binding site of UL31 family members of  $\alpha$ - and  $\gamma$ -herpesviruses is located in the first conserved region as expected after studies of the similarity to M53.

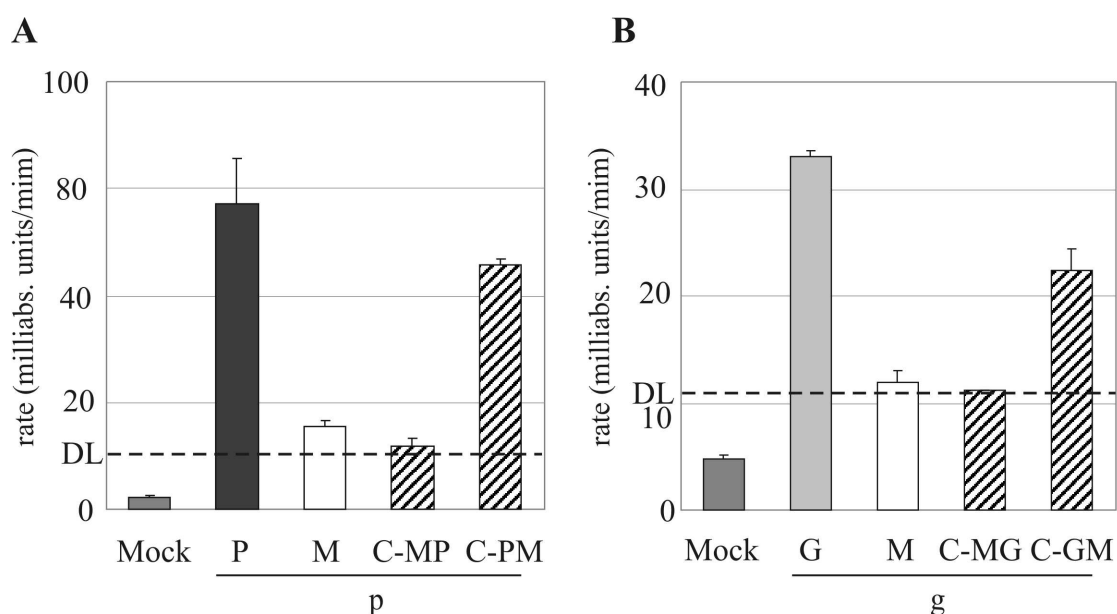


**Figure 21: Mapping of the binding site in UL31 family members of  $\alpha$ - and  $\gamma$ -herpesviruses.**

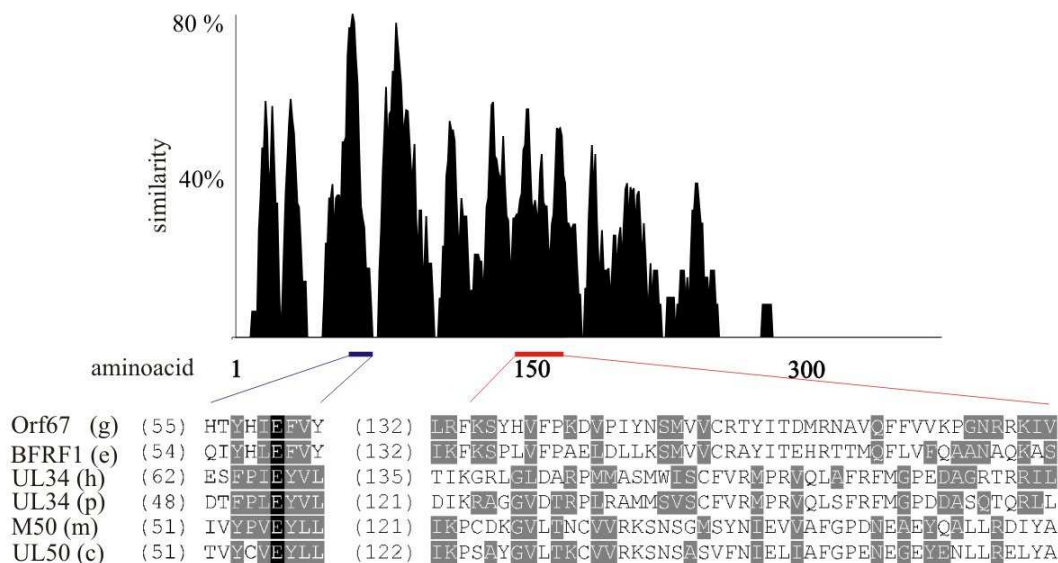
Bla activity in cell lysates after co-expression in 293T cells. **A)** N-UL34 of PrV (p) was co-expressed with C-UL31 of PrV (P), C-M53 (M) and the chimeric fusion constructs C-MP and C-PM. **B)** N-Orf67 (g) was co-expressed with C-Orf69 (G), C-M53 (M) and the chimeric fusion constructs C-MG and C-GM. Mean hydrolysis rates of nitrocefin were determined (chapter 5.7.1). The indicated detection limit (DL) is defined by the hydrolysis of nitrocefin after co-transfection of C-M53 and N-M50DM. Error bars indicate the standard deviation.

### 6.3.3.2. The binding site in the UL34 family

Having studied the binding of UL31 to UL34 family members for all three herpesvirus subfamilies, we also wanted to undertake a brief study of the binding site in UL34 family members using the established PCA. In contrast to the binding site in UL31 family members, which has been shown to be conserved and located within the first conserved

region (chapter 6.3.3.1), published data indicate that the binding site in UL34 family members is not conserved but located in different parts of the proteins. In M50, the binding site was defined in the first third of the protein and narrowed down to nine amino acids (aa51-aa59), but also the insertion of five aa at position 114 of M50 had an effect on the M53 binding (Bubeck et al., 2004 and chapter 6.2.2.1). In HSV-1, a stretch of 44 amino acids (aa137-aa181) was shown to be necessary and sufficient for binding to UL31 (Liang and Baines, 2005). The PCA was applied to confirm the published binding sites and to see if the corresponding stretches in the homologous proteins indeed leaves the binding to the UL31 family member untouched. Therefore the amino acids of the published binding sites in the BlaN-fusions to UL34 of HSV-1 and M50 as well as the corresponding regions in the homologues were deleted (Figure 22B).

**A**



**B**

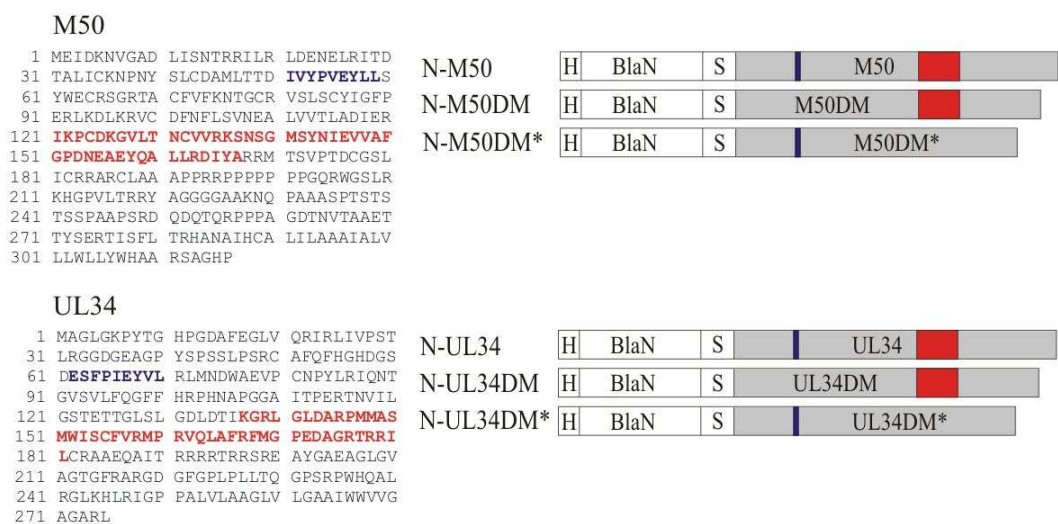


**Figure 22: Bla-fusion constructs to map the UL31 binding site in UL34 family members.**

**A)** Similarity blot obtained by the alignment of the six UL34 proteins of MHV68, EBV, HSV-1 and PrV, MCMV and HCMV. As magnification the aligned amino acids of two predicted binding sites.

**B)** Amino acid sequences of M50 and UL34 of HSV-1. Residues in blue show the predicted binding motif in M50 (M), residues in red show the homologues residues to the predicted binding motif in UL34 (M\*). Right: schematic representation of BlaN-fusions to the mutants of M50 and UL34. The amino acids of the predicted binding sites were deleted. N-M50 mutants were constructed, lacking aa51-aa59 or aa123-aa167, referred to as N-M50DM and N-M50DM\*, respectively. N-UL34 mutants were constructed, lacking aa62-aa71 or aa137-aa181, referred to as N-UL34DM and N-UL34DM\*, respectively.

## Results

---

The M50 and UL34 mutants were co-expressed together with C-UL31 or C-M53 to determine the extent to which the ability to interact remained. Co-expression of C-M53 with N-M50 produced the expected high hydrolysis rate but when C-M53 was co-expressed with N-M50DM, where the deleted stretch corresponded to the published binding motif, the hydrolysis rate diminished to the previously defined background signal. However, co-expression of C-M53 with N-M50DM\* ( $\Delta$ 123-167) also lead to a negative signal in the PCA (Figure 23A). In an HA-probed Western Blot the BlaN-fusions to the M50 mutants were detected at the expected size and expression level (Figure 23C) showing that the lack of signal was not due to an expression problem. Degradation bands were visible as in other HA-probed Western Blots for detection of UL34 proteins.

For both mutants of UL34 of HSV-1, a reduced interaction was observed. When C-UL31 was co-expressed with the mutant lacking the nine amino acids of the predicted binding motif for  $\beta$ -herpesviruses, N-UL34DM ( $\Delta$ 62-71), the signal was reduced by 60% of the wt fusion proteins (Figure 23B). For the mutant in which the predicted binding motif for  $\alpha$ -herpesviruses was deleted, N-UL34DM\* ( $\Delta$ 137-181), binding to UL31 of HSV-1 was nearly abolished. However, a look at the HA-probed Western Blot after isolated expression of the mutant fusion proteins revealed impaired expression of N-UL34DM\* (Figure 23C). The protein was detectable in the Western Blot after several minutes of exposure, indicating either very low expression of N-UL34DM\* or instability of the protein. N-UL34DM, lacking the amino acids of the short binding motif in  $\beta$ -herpesviruses was expressed at the expected size and level.

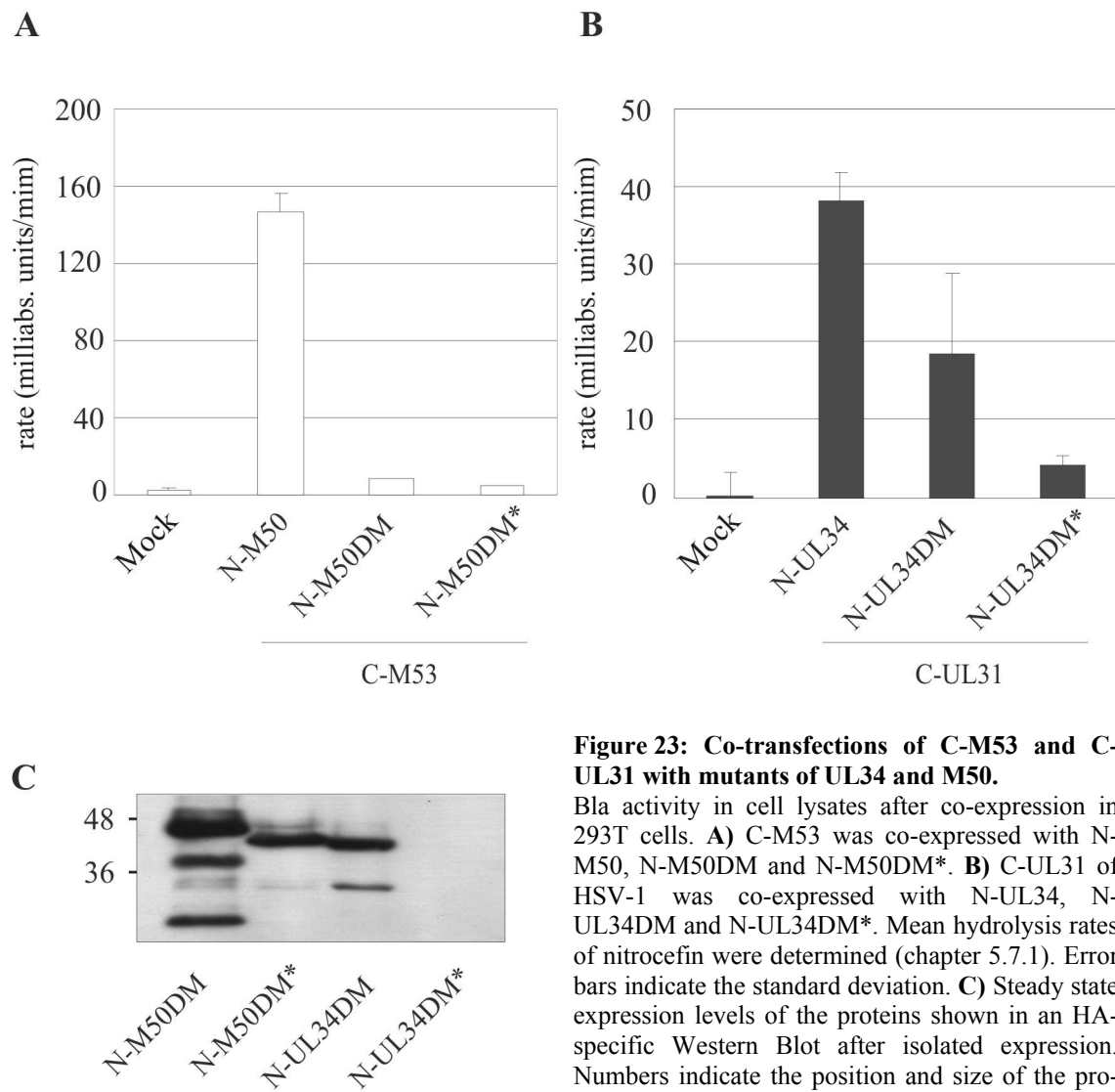


**Figure 23: Co-transfections of C-M53 and C-UL31 with mutants of UL34 and M50.**

Bla activity in cell lysates after co-expression in 293T cells. **A)** C-M53 was co-expressed with N-M50, N-M50DM and N-M50DM\*. **B)** C-UL31 of HSV-1 was co-expressed with N-UL34, N-UL34DM and N-UL34DM\*. Mean hydrolysis rates of nitrocefin were determined (chapter 5.7.1). Error bars indicate the standard deviation. **C)** Steady state expression levels of the proteins shown in an HA-specific Western Blot after isolated expression. Numbers indicate the position and size of the protein marker in kDa.

From these results, it can be concluded that for both, M50 and UL34, the binding site to UL31 family members appears to be built up by a bipartite binding motif incorporating more than the published stretch of amino acids. In order to exclude the structural perturbation by the deletion of, in the first case nine, in the second 44 amino acids, a further study of point mutations needs still to be performed.

---

#### **6.4. Complementation within the MCMV virus context**

The NEC-PCA was established for the two MCMV proteins, M50 and M53 further applied to their homologues, members of the UL34 and UL31 protein family. Data was obtained by transient transfection of the Bla constructs and fusion proteins were either isolated or co-expressed in cell culture. Members of both protein families were shown to complement each other in the PCA within the herpesvirus subfamilies. To determine if the data obtained in the PCA reflects the situation in the virus context, members of both protein families, as well as the chimeric UL31 proteins, were inserted into the MCMV genome for further complementation studies.

##### 6.4.1. UL34 and UL31 family members in MCMV deletion genomes

Since the NEC proteins of viruses belonging to the same subfamily were shown to interact in the PCA (chapter 6.3.2), we subsequently tested them to determine if the observed binding was sufficient for the functional replacement of NEC proteins in the virus context. For this purpose, the representative UL34 and UL31 family members were introduced into the deletion genomes  $\Delta$ M50 and  $\Delta$ M53, respectively. The UL34 family members, UL50, Orf67 and UL34 of HSV-1 and PrV, were introduced into the ectopic position (between the genes m16 and m17, chapter 6.2.2.3) of the  $\Delta$ M50-BAC, which lacks the native M50 gene. In the same way, UL53, Orf69 and UL31 of HSV-1 and PrV, were introduced into the  $\Delta$ M53-BAC, which lacks the native M53 gene. Mutant BACs were analysed by restriction digests, using NotI and BsrDI (Figure 24). Correct insertion of the expression plasmids was confirmed by the appearance of an additional 11,8 kb band in the NotI digests and the absence of an additional 3,5 kb fragment, which would indicate the multiple insertion as tandem repeats. BACs with the  $\Delta$ M50-backbone lack the 5,5 and 13,2 kb DNA fragments. To ensure the deletion of M53 in the  $\Delta$ M53-backbone, respective BACs were digested with BsrDI. The additional band at 8,2 kb confirmed the absence of M53. A shift of the 20 kb DNA fragment in the wt MCMV to 24 kb in the mutants indicated insertion of the pO6T expression plasmids. For viral reconstitution, BAC-DNA was purified from bacteria and transfected into MEF cells.

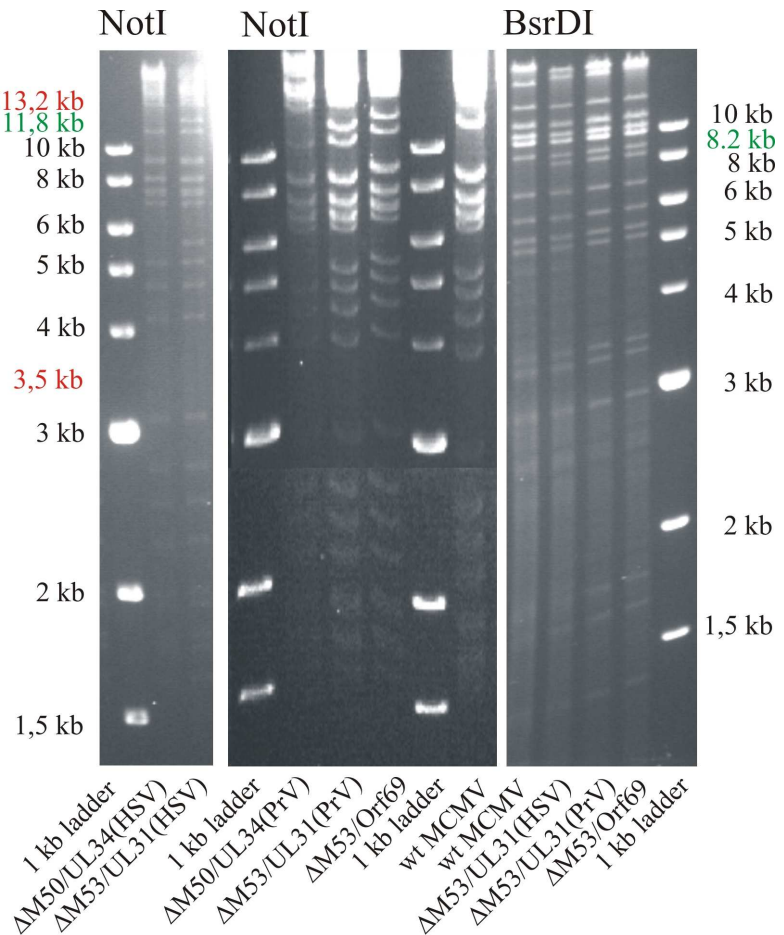
## Results

BAC backbone	Inserted ORF	Mutant	Complementation of M50 or M53	
			in the PCA	in MCMV
$\Delta$ M50-BAC	UL50	$\Delta$ M50/UL50	Yes	Yes
$\Delta$ M53-BAC	UL53	$\Delta$ M53/UL53	Yes	Yes
$\Delta$ M50-BAC	UL34(HSV)	$\Delta$ M50/UL34(HSV)	No	No
$\Delta$ M53-BAC	UL31(HSV)	$\Delta$ M53/UL31(HSV)	No	No
$\Delta$ M50-BAC	UL34(PrV)	$\Delta$ M50/UL34(PrV)	No	No
$\Delta$ M53-BAC	UL31(PrV)	$\Delta$ M53/UL31(PrV)	No	No
$\Delta$ M53-BAC	Orf69	$\Delta$ M53/Orf69	No	No

**Figure 24: Heterologous NEC protein inserted into MCMV deletion genomes.**

Table: Summary of the mutant viruses used to validate the PCA data of the crosscomplementation studies (chapter 6.3.2). The BAC backbone, listed in the first column, indicates the type of deletion genome,  $\Delta$ M50 or  $\Delta$ M53. The second column indicates the ORF inserted in ectopic position of the BAC, followed by the name of the resulting mutant as it is used in the text. The last column summarizes the success of complementation of the inserted ORF in the PCA and in the virus context (reconstitution).

Right: restriction pattern analysis of the mutants by NotI and BsrDI digest. Black numbers on the sides indicate the sizes of the DNA marker bands. Red and green numbers indicate the size of fragments to appear upon insertion or due to the lack of M53 (green) and to be absent in deletion genomes and due to single insertion (red).



UL50 and UL53 were introduced into the MCMV BACs  $\Delta$ M50 or  $\Delta$ M53 and virus was reconstituted in the absence of the respective MCMV gene (experiments done by Anja Bubeck, unpublished). To quantify the ability of mutants to replicate in cell culture, a stock of  $\Delta$ M50/UL50 virus was prepared and viral growth was compared to that of wt MCMV under multi-step growth conditions on NIH3T3 cells. Viral replication of  $\Delta$ M50/UL50 showed no significant attenuation, with the wt MCMV titre of  $1,8 \times 10^5$  PFU/ml at day five being only slightly higher than that of the mutant at  $1,5 \times 10^5$  PFU/ml.

In contrast, UL34 and UL31 homologues of HSV-1, PrV and MHV68 could not functionally replace the NEC proteins in the deletion genomes. Neither of the deletion genomes,  $\Delta$ M50 or  $\Delta$ M53, showing a null-phenotype by themselves, could be complemented by any of the UL34 or UL31 homologues. Viral progeny was not restored by the insertion of heterologous UL34 or UL31 family members (Figure 24) during the six weeks of cultivation of the transfected MEF cells.

These findings confirm the data obtained in the PCA of chapter 6.3.2. The NEC proteins, UL50 and UL53 of HCMV, could not only cross-complement but also functionally replace the MCMV proteins M50 and M53. However, homologues of other herpesvirus subfamilies, shown to be negative for binding in the PCA, failed to functionally complement the respective MCMV proteins.

#### 6.4.2. UL34 and UL31 family members in the wt MCMV genome

The lack of viral progeny observed from the heterologous proteins expressed in the M50 or M53 deletion context might be due to the lack of complementation of proteins, as expected from the PCA data (chapter 6.3.2). However, the heterologous proteins may have other unexpected functions in MCMV that lead to a block of viral progeny. To test the heterologous proteins for a potential negative impact on viral replication by themselves, the ORFs of the heterologous UL34 and UL31 family members tested in chapter 6.4.1 were inserted into ectopic position of the BAC carrying the wt MCMV genome (Figure 25).



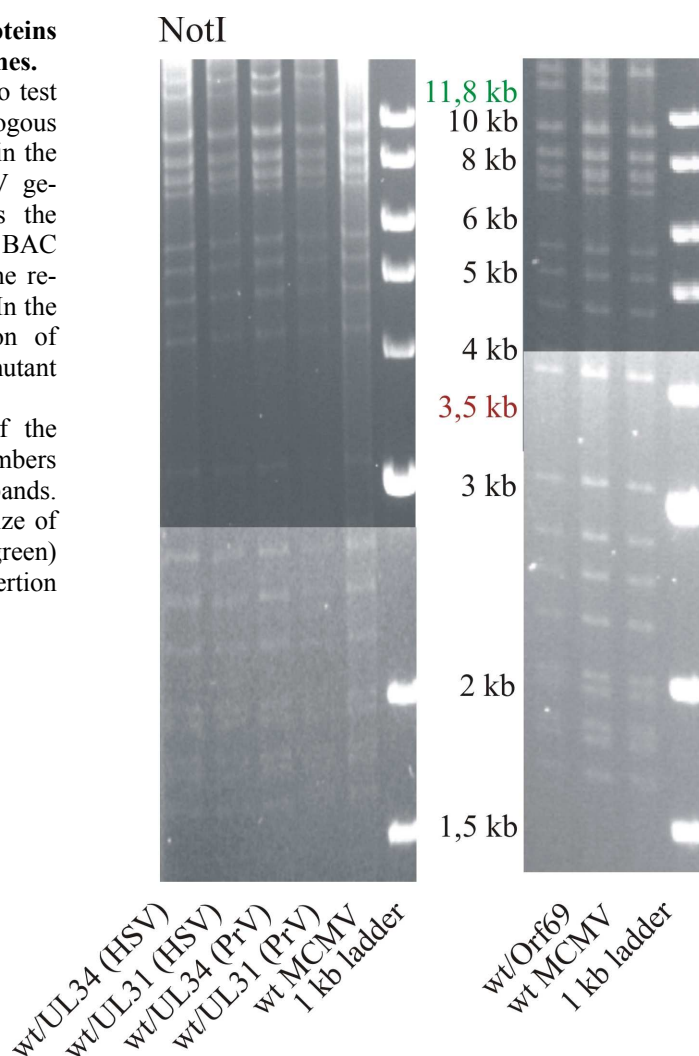
## Results

BAC backbone	Inserted ORF	Mutant	Viral progeny
wt BAC	UL34(HSV)	wt/UL34(HSV)	Yes
wt BAC	UL31(HSV)	wt/UL31(HSV)	Yes
wt BAC	UL34(PrV)	wt/UL34(PrV)	Yes
wt BAC	UL31(PrV)	wt/UL31(PrV)	Yes
wt BAC	Orf69	wt/Orf69	Yes

### Figure 25: Heterologous NEC proteins inserted into MCMV wild type genomes.

Summary of the mutant viruses used to test for a negative influence of the heterologous proteins inserted. The BAC backbone in the first column indicates the wt MCMV genome. The second column indicates the ORF inserted in ectopic position of the BAC backbone, followed by the name of the resulting mutant as it is used in the text. In the last column, success of reconstitution of viral progeny after transfection of the mutant BAC-DNA is depicted.

Right: Restriction pattern analysis of the mutants by NotI digest. Black numbers indicate the sizes of the DNA marker bands. Red and green numbers indicate the size of fragments to appear upon insertion (green) and to be absent due to single insertion (red).



For all tested constructs, virus reconstitution was successful if M50 or M53 was present in the mutant MCMV genome. This shows that the replication deficiency of  $\Delta$ M50 expressing UL34 homologues or  $\Delta$ M53 expressing UL31 homologues was due to the lack of functional replacement rather than toxicity or other inhibitory factors of the ectopically expressed proteins.

### 6.4.3. Chimeric UL31 family members inserted into the MCMV genome

The heterologous UL31 proteins of PrV, HSV-1 and MHV68 were not able to replace M53 in the viral context when inserted into the  $\Delta$ M53 genome (chapter 6.4.2). This was expected as the proteins did not interact with N-M50 in the cross-complementation experiments (chapter 6.3.2.1) and binding of M53 to M50 is essential for viral replication (Bubeck et al., 2004; Lötzerich et al., 2006). As shown in the previous chapter, the binding capacity of heterologous UL31 proteins can be restored if the first conserved region is exchanged by the first conserved region derived from M53, indicating that the CR1 is necessary and sufficient for binding to M50. To test whether the restored binding to M50 is sufficient to allow complementation of the M53 null phenotype, chimeric proteins were analysed in the MCMV context. Chimeras were constructed consisting of the variable region and CR1 of M53 and CR2-CR4 of either UL31 of PrV or Orf69 of MHV68. In contrast to the previously studied chimeras C-MP and C-MG (chapter 6.3.3.1), the hereby resulting constructs, MP and MG, lack the fusion to the BlaC fragment.

MP and MG were inserted into the  $\Delta$ M53, the MCMV genome deficient for the native M53 (Lötzerich et al., 2006), resulting in  $\Delta$ M53/MP and  $\Delta$ M53/MG, respectively. The BAC-DNA was transfected into MEF cells, but neither  $\Delta$ M53/MP nor  $\Delta$ M53/MG lead to infectious progeny despite the cultivation of transfected MEF cells for more than six weeks (Figure 26). This null-phenotype indicated that binding to M50 alone was not sufficient for virus morphogenesis in the M53 deletion context.

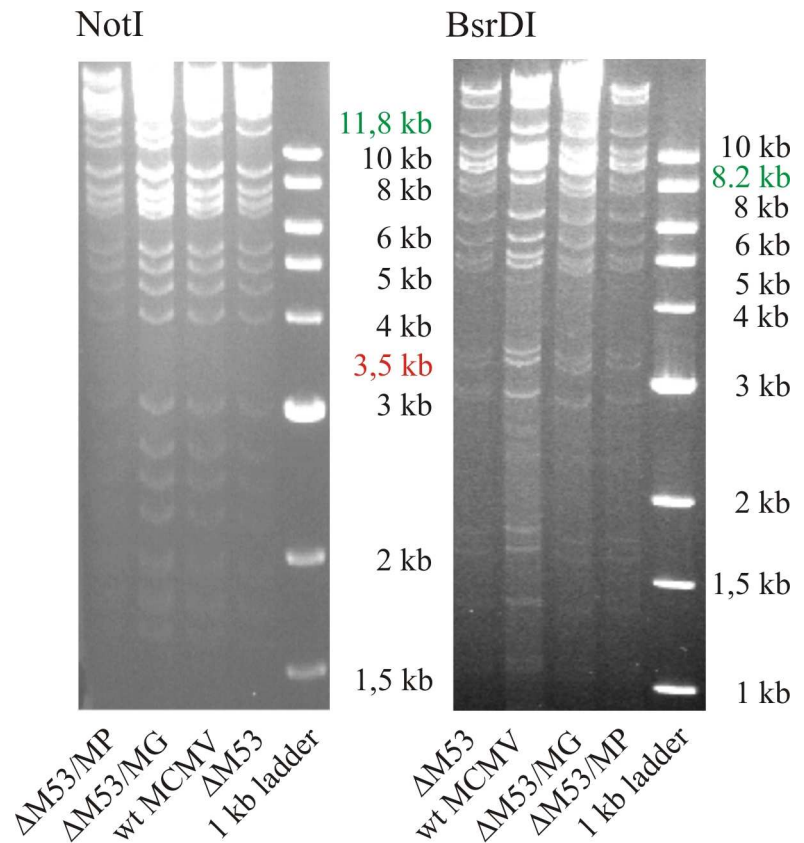
## Results

**Figure 26: Chimeric NEC proteins inserted into the  $\Delta$ M53-BAC.**

Table: Summary of the mutant viruses used to test for the functionality of the chimeric UL31 proteins. The BAC backbone in the first column indicates the MCMV genome lacking the native M53. The second column indicates the ORF inserted in ectopic position of the BAC, followed by the name of the resulting mutant as it is used in the text. The last column summarizes the success of complementation of the inserted ORF in the PCA and in the virus context (reconstitution).

BAC	Inserted ORF	Mutant	Complementation	
			PCA	MCMV
$\Delta$ M53	MP	$\Delta$ M53/MP	Yes	No
$\Delta$ M53	MG	$\Delta$ M53/MG	Yes	No

Right: restriction pattern analysis of the mutants by NotI and BsrDI digest. Black numbers on the sides indicate the sizes of the DNA marker bands. Red and green numbers indicate the size of fragments to appear upon insertion or due to the lack of M53 (green) and to be absent due to single insertion (red).



### 6.4.3.1. An essential function is located in the CR2 to CR4 of M53

As was done for the heterologous UL31 proteins (chapter 6.4.2), the influence of the chimeric UL31 proteins MP and MG on wt MCMV replication was studied. The ORFs coding for the chimeric proteins were therefore introduced into the wt MCMV BAC, resulting in wt/MP and wt/MG. BAC-DNA was extracted and transfected into MEF cells to screen for viral progeny which should occur if the inserted genes leave viral replication untouched.

In MEF cells transfected with wt/MG DNA, first signs of plaque formation and cell lysis were eventually detected after five weeks in contrast to only 7-10 days required for the positive control, transfected wt MCMV BAC-DNA. However, even though the native M53 gene was present in the genome of wt/MP no infectious progeny was detected in transfected MEF cells. This indicates that the presence of the chimeric protein MP

had a negative impact on virus replication and resulted in the inhibition of virus reconstitution from the transfected BAC-DNA. Such an effect is called dominant negative (DN) and indicates the C-terminal part (CR2-CR4) of M53 is crucial for other essential functions of the protein, which cannot be effectively restored by substitution with the C-terminal region of other subgroups. Thus, a protein bearing one essential function like binding via CR1, but lacking another, can interfere negatively with viral processes, such as disturbing complex formation or retrieval of functional binding partners.

To further analyse the DN effect of MP, additional chimeras were constructed that were either expected to abolish or retain the dominant negative effect when inserted into the MCMV genome. The MCMV part in MP was exchanged for the variable region and CR1 of UL53 (C; aa1-aa125) resulting in the chimera CP. UL53 binds to M50 and can replace M53 in the virus (chapter 6.4.1). Furthermore, two chimeras were constructed where the variable region and the CR1 originated from UL31 of PrV or Orf69 and the CR2-CR4 of Orf69 and UL31, respectively. The additional chimeras, namely CP, PG and GP, should prove the dominant negative effect of MP by showing that the binding to M50 alone, either by the CR1 of M53 or UL53, is the reason for the inhibition of viral progeny, and not any influence of the CR2-CR4, if PG and GP appear to be without effect on viral replication.

As expected, the chimeras PG and GP, bearing the variable region and CR1 of UL31 and Orf69 showed no DN effect when introduced in the MCMV context (Figure 27). When the BAC-DNA of wt/PG or wt/GP was transfected into MEF cells, plaque formation was observed after just two weeks. This indeed indicates that in the previously analysed MP and MG the CR1 of M53 and not the heterologous C-terminal CRs are needed for the inhibitory effect of MP and the delay in virus reconstitution of wt/MG.

Contrary to our expectations, the mutant BAC genome wt/CP, carrying the chimera with the variable region and CR1 originating from UL53 did only delay and not completely inhibit virus progeny (Figure 27). This might be explained by a critical amount of M50 that gets retrieved from the native M50/M53 interaction despite of the introduced chimera. As seen in the PCA depicted in Figure 16C, the combination of C-UL53 with N-M50 gave only two thirds of the signal obtained with the NEC proteins of MCMV, C-M53 and N-M50, whereas the Bla signal induced by the combination of N-M50 with the chimera C-CP was even lower (chapter 6.3.3.1). The reduced binding capacity to M50 is likely to abolish the DN effect that was observed in MP and the de-

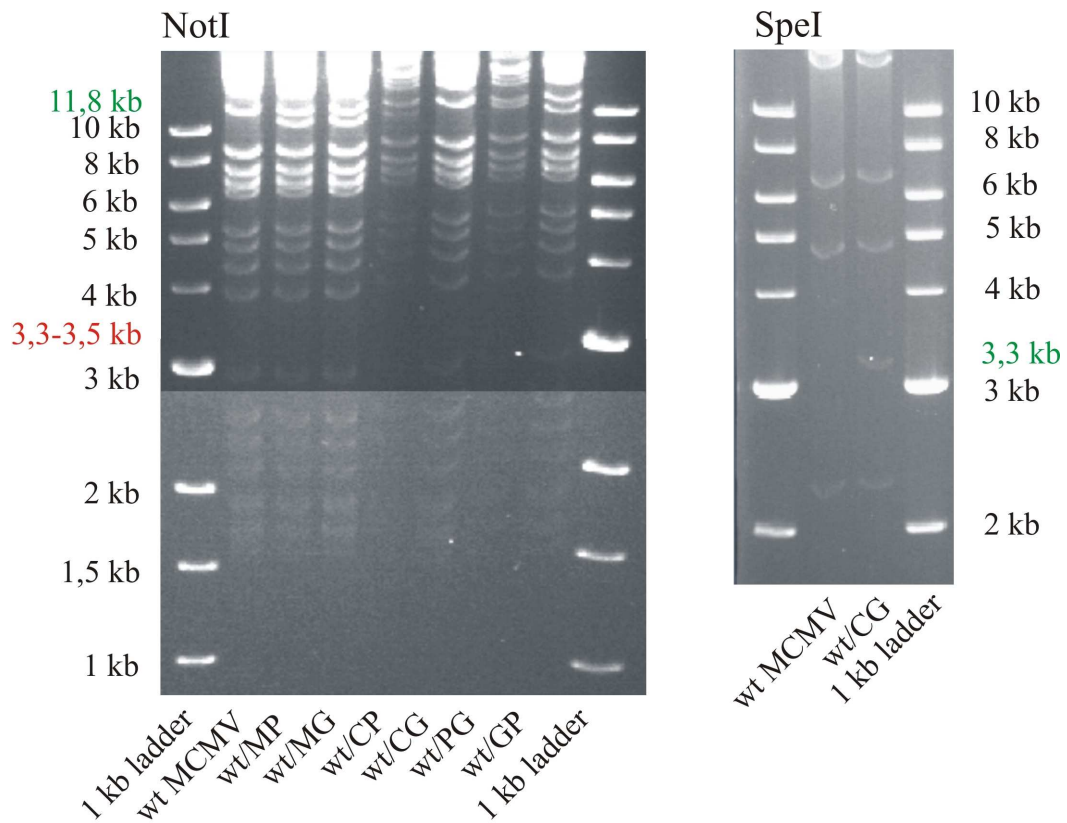
## Results

lay of virus reconstitution of wt/MG, since the influence on the wt NEC interaction was not very strong.

**Figure 27: Chimeric NEC proteins inserted into MCMV wild type genomes.**

Table: Summary of the mutant viruses used to test for the DN effect of chimeric UL31 proteins. The ORFs (second column) were inserted in ectopic position of the wt BAC. Further listed are the names of the resulting mutant and the outcome of reconstitution of viral progeny after transfection. Bottom: Restriction pattern analysis of the mutants by NotI and SpeI digests. Black numbers indicate the size of the DNA marker bands. Red and green numbers indicate the size of fragments to appear (green) upon insertion and to be absent (red) due to single insertion.

BAC	Inserted ORF	Mutant	Progeny
wt BAC	MP	wt/MP	No
wt BAC	MG	wt/MG	Yes
wt BAC	CP	wt/CP	Yes
wt BAC	GP	wt/GP	Yes
wt BAC	PG	wt/PG	Yes



### **6.5. The UL34/UL31 interaction as a potential drug target**

In the previous experiments the PCA was used as a tool to analyse the UL31 and UL34 family members and their interactions necessary for the nuclear egress of herpesvirus capsids. The interacting proteins have been studied in co-expression experiments and in the virus context. The complementation experiments revealed that the binding of the proteins belonging to the two protein families is conserved throughout the herpesviruses.

Even though the binding site in UL31 family members developed in a subfamily specific manner, this essential protein-protein interaction represents a potential target for the interruption of virus replication by antiviral chemotherapy. A prerequisite for an initial inhibitor screen is the study of the protein-protein interaction of interest *in vitro*, free of unknown parameters like cellular uptake or nuclear transport. Such conditions can be met by a bacterial expression system. If indeed neither additional viral or cellular proteins are required for the binding between UL34 and UL31 family members, nor post-translational modifications of the interaction partners, they should interact also after heterologous expression in bacteria, facilitating binding and inhibitor studies on the molecular level.

Under this aspect, two approaches for drug development were followed (chapter 3.2.2). First, the NEC proteins of HCMV were expressed in bacteria and subsequently purified. Isolated proteins can be studied and will allow further conclusions about additional cellular or viral interaction partners, if any, as well as further localization studies of binding sites and motifs. Due to the good protein yield and a sufficient degree of purity, the crystallization of the NEC proteins, isolated and as a complex, was attempted to elucidate the three-dimensional structure of the proteins. The protein structure could allow the rational design of drugs interfering with the NEC formation.

Second, the knowledge gained from the protein purification procedure was used to transfer the NEC-PCA to a cell free system.

#### 6.5.1. Bacterial expression of the NEC proteins

For the analysis of HCMV proteins, first a fragment of UL50 was selected for the optimization of the purification procedure. The amino acid sequence of UL50 was analysed by computer prediction and amino acid stretches were assigned to the secondary structure element that is most likely formed. Predictions about  $\alpha$ -helices,  $\beta$ -sheets and flexi-

## Results

ble loops (coiled-coil regions) in UL50 were obtained by the PHD method (Rost and Sander, 1994) offered by the PBIL Lyon-Gerland. The predicted secondary structure is depicted in Figure 28A and B. For bacterial expression, only the part of UL50 harbouring the predicted binding motif to UL53 (predicted from M50 data; Bubeck et al., 2004); green bar in Figure 28) but lacking additional loops in the extended coiled-coil regions, was selected, making the protein compact.

### A UL50

```
(1) MEMNKVLHQDLVQATRRIKLGPSSELRVTDAGLICKNPNYSVCDAMLKTDTVYCV EYLLSYWESRTDHVP
CCcchHHHHHHHHHHHHHHHHcCCcCEEECCCCcEEcCCCCcchHhhhcCCcEEhhHHHHhhHhCCcC

(71) CFI FKN TGCAVSLCCFVRAPVKLVSPARHVGEFNV LKVNESLIVTLKDI EEIKPSAYGVLTKCVVRKSNS
EEEEcCCcEEEEEEEEEEcEEEEcCCcEEcEEEEcCCcEEcEecchhhcCCcEEcEEEEEEcCC

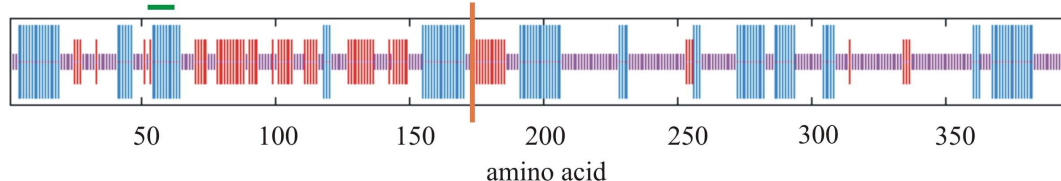
(141) ASVFNI ELIAFGPENEGEYENLLRELYAKKAASTSLAVRNHVTVSSHSGSGPSLWRARMSAALTRTAGKR
CccEEEEEcCCcCHHHHHHHHHHHHHhCcCEEEEEEEcCCcCHHHHHHHHHHHHHHHhCCc

(211) SSRTASPPPPRHPSCSPTMVAAGGAAAGPRPPPPMAAGSWRLCRCEACMGRCGCASEGDADEEEEEELL
CCCcCCCCCCCCCCCCCHHHhCcCCcCCCCCCCCcCCcEEcchhhcCcccccCCCCcHHHHHHHH

(281) ALAGEGKAAAAAAGQDVGG SARRPLEEHVSRRRGVSTHRRHPPSPPCAPSLERTGYR WAPSSWWRARSGP
HHHccHHHHHHHHhCCcCCCCcHHHHhccccEEcCCCCCCCCCccCCcEEcCCccccCCCC

(351) SRPQSGPWLPARFATLGPLVLALLLVLALLWRGHGQSSSPTRSAHRD
CCCCCCCCChhhCcCHHHHHHHHHHHHHHHhCCCCCCCCCCCC
```

### B



### C

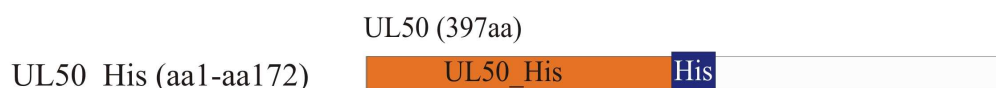


**Figure 28: Secondary structure prediction for UL50 and constructs for bacterial expression.**

**A)** Amino acid sequence of UL50 and the predicted secondary structure: C/c (purple): coiled coil, H/h (blue): alpha helix and e/E (red): beta sheet. Capital letters indicate a reliability index of prediction of 5 and over and are predicted at better than 82%. **B)** Schematic representation of the structural elements of UL50. The red bar indicates the end of the UL50\_His construct. The green line indicates the predicted binding motif to UL53. **C)** Schematic representation of UL50 fragment designed for bacterial expression. UL50\_His contains the first 172 aa of UL50 and is C-terminally His-tagged.

#### 6.5.1.1. Expression and purification of UL50\_His

The truncated UL50 fragment was cloned into a pET-24b expression vector. In pET vectors, target genes are cloned under control of strong bacteriophage T7 promoters and

expression is induced by providing a source of T7 RNA polymerase in the host cell. The *E.coli* strain BL21-CodonPlus (DE3)-RIL (Stratagene), used in this study, carries an integrated genomic T7 RNA polymerase gene under control of a lac promoter, thereby allowing induction by IPTG. The *E.coli* expression strain is optimized for the expression of eukaryotic proteins since the ORFs of three t-RNAs (arginine (R), isoleucine (I), leucine (L)), frequently involved in eukaryotic protein biosynthesis but rare in the bacterial system, are present on a separate plasmid. By introducing the N-terminal part of the UL50 ORF into the pET-24b vector, a C-terminal His-tag was added to the protein, consisting of six histidines for further purification with affinity chromatography using Ni<sup>2+</sup>-NTA.

The pET24UL50\_His, coding for the His-tagged UL50 fragment (UL50\_His (aa1-aa172)) was transferred to the *E.coli* expression strain BL21-CodonPlus (DE3)-RIL one day before the experiment. The next day, a preculture was inoculated. From the preculture, the five litre main culture was started in the afternoon. Cells were grown to an OD<sub>600</sub> of 0,7, cooled on ice and expression of the heterologous proteins induced by the addition of IPTG. For protein expression, culture flasks were incubated overnight at 20 °C in order to slow down bacterial metabolism to enhance efficient and accurate protein synthesis.

After expression of UL50\_His, the bacteria were harvested and cracked by sonication. The proteins in solution were separated from membranes by centrifugation and the His-tagged proteins purified from the supernatant by affinity chromatography using Ni<sup>2+</sup>-NTA. After binding of the His-tagged proteins to the column material, the column was washed with pure binding buffer. Subsequent washing in the presence of a low imidazole concentration competes for positively charged moieties in the column. Finally the bound proteins were eluted from the column in the presence of high imidazole concentrations.

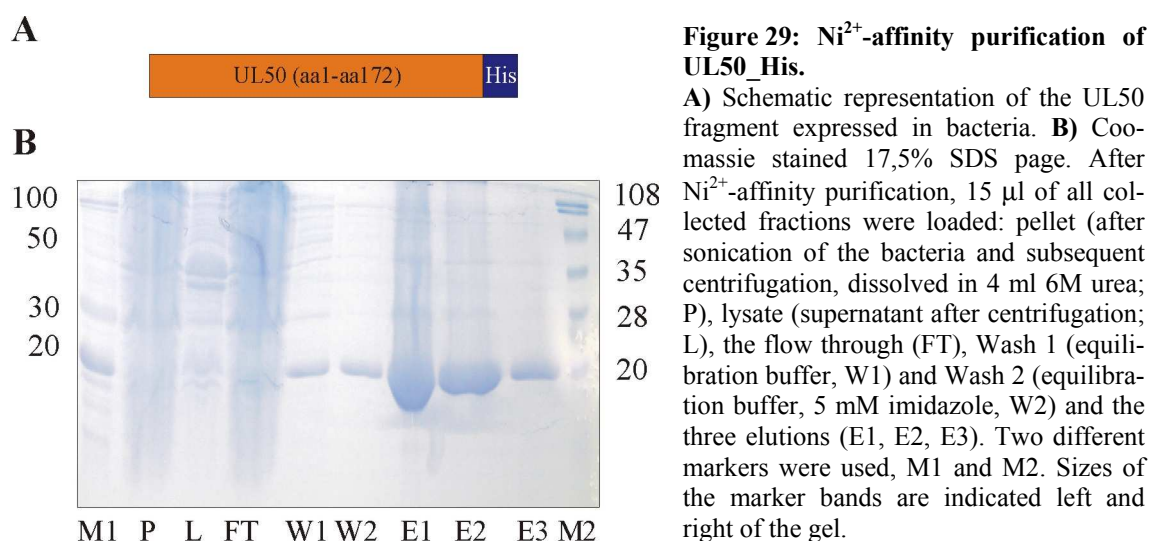
During purification of the expressed UL50\_His, inclusion bodies were observed. Inclusion bodies indicate that a protein is possibly toxic to the bacteria or is expressed to a level not tolerated by the bacterial metabolism, leading to sequestration of the heterologous proteins. Proteins in form of inclusion bodies are usually misfolded but can be recovered by complete defolding in the presence of urea and slow refolding by dialysis. Fortunately, in the case of UL50\_His, sufficient amounts of protein remained in solu-



## Results

tion. To prevent inclusion bodies clogging the  $\text{Ni}^{2+}$ -NTA columns samples were applied after filtration.

Figure 29B shows a Coomassie stained 17,5% SDS-gel with a band corresponding to the UL50\_His at 20 kDa. Protein was already detected in the first two washes prior to elution indicating a huge amount of protein bound to the  $\text{Ni}^{2+}$ -NTA. The 20 kDa band was cut from the gel and protein analysis by Edman sequencing confirmed the protein as UL50\_His.



### 6.5.1.1.1. Anion exchange chromatography of UL50\_His

The protein was eluted from the  $\text{Ni}^{2+}$ -NTA column in a total volume of 5 ml. For further purification of the eluted samples, the total volume was loaded onto an anion exchange column (MonoQ). The principle of ion exchange chromatography is based on the interaction between charged proteins and the contrarily charged groups of the column matrix. Protein binding occurs under low salt conditions (buffer A without NaCl). The continuous increase in anion concentration on a salt gradient (buffer B with 1M NaCl) leads to elution. Different binding properties of the proteins result in a different elution profile and thereby allow the removal of impurities. The protein solution was loaded onto the MonoQ resin using a 50 ml superloop. After loading, elution was mediated by a steady increase of buffer B running through the column and fractions of 0,5 ml were collected. The protein content of the fractions was qualitatively measured at an OD of 280 nm. Fractions containing protein were analysed on an SDS gel.

## Results

The elution profile demonstrated a clear peak of protein at about 14% of buffer B (1M NaCl) indicating a pure protein fraction (Figure 30A). The amount of protein exceeded the upper detection limit as the plateau like part of the blue curve shows. While the red curve showing the course of the absorption at 260 nm peaks as expected at the same fractions as the blue line of 280 nm, it reaches an additional high level earlier in the run. This pattern was observed in all MonoQ runs and most likely represents imidazole, which is present in the loaded samples from the Ni<sup>2+</sup>-NTA column elutions and elutes at low salt concentrations. The 500 µl fractions, collected at the peak of the absorption at 280 nm (C8-B10; ml 85 to 89), were next analysed for their protein content by SDS-page and Coomassie stained (Figure 30B). Only one band corresponding to UL50\_His was visible in the Coomassie stain. The fractions were pooled and used for limited proteolysis (chapter 6.5.1.1.4) or the next purification step, which was gel filtration (chapter 6.5.1.1.2).

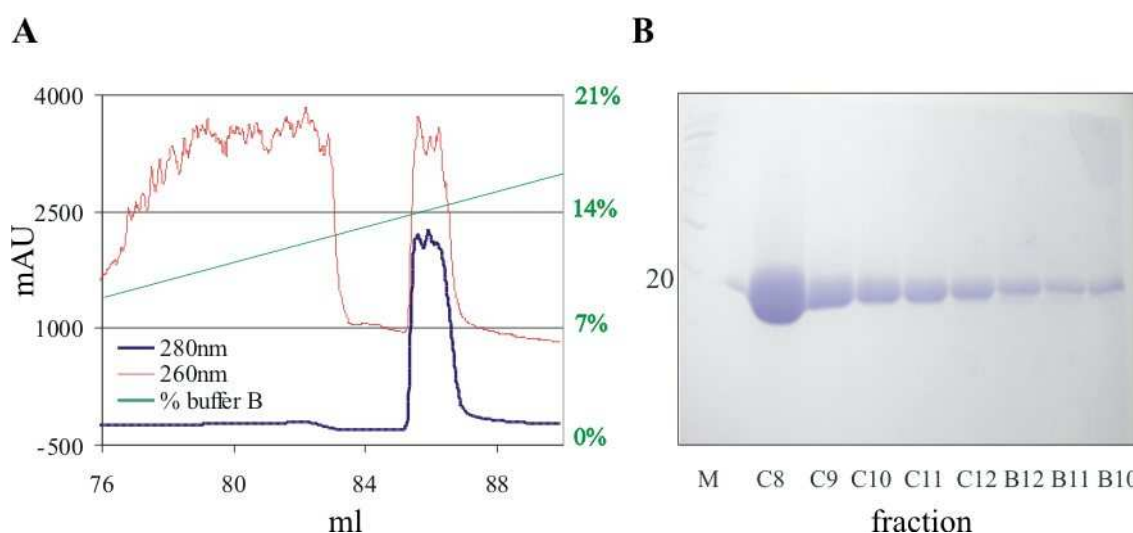


**Figure 30: Purification of UL50\_His by a MonoQ column.**

**A)** Elution profile of the MonoQ purification. Indicated are the measured milliabsorption units at the wavelength of 280 nm (blue) and 260 nm (red) at the volume (in ml) collected from the column. The green line and numbers show the percentage of buffer B (1M NaCl) running through the column. **B)** Coomassie stained 17,5% SDS page. 15 µl of the fractions C8 to B10, corresponding to the ml 85 to 89 were analysed on the gel. Indicated is the size of UL50\_His in kDa.

### 6.5.1.1.2. Gel filtration of UL50\_His

As a third and final purification step, the protein samples were run on a Superose 6 column. This column separates proteins according to their Stokes radius (size exclusion chromatography). The column material consists of a cross linked network of agarose

## Results

molecules, which creates a porous material. Small molecules can easily diffuse in the interspaces, whereas larger molecules move more directly through the column and elute earlier. Large molecules, which have no access to the pores, elute in the void volume. Considering the principle, the applied volume should be small to enable a good elution profile. Therefore, the fractions of the MonoQ column containing the UL50\_His protein were pooled and concentrated to a total volume of 500  $\mu$ l and injected to the equilibrated column.

Since the protein sample loaded onto the Superose 6 column was already rather pure from the two preceding purification steps, the clear peak at 280 nm in the elution profile (Figure 31A) was expected. Fractions collected at the peak absorption of 280 nm were analysed by SDS-page and UL50\_His was detected as a strong band at 20 kDa (Figure 31B).

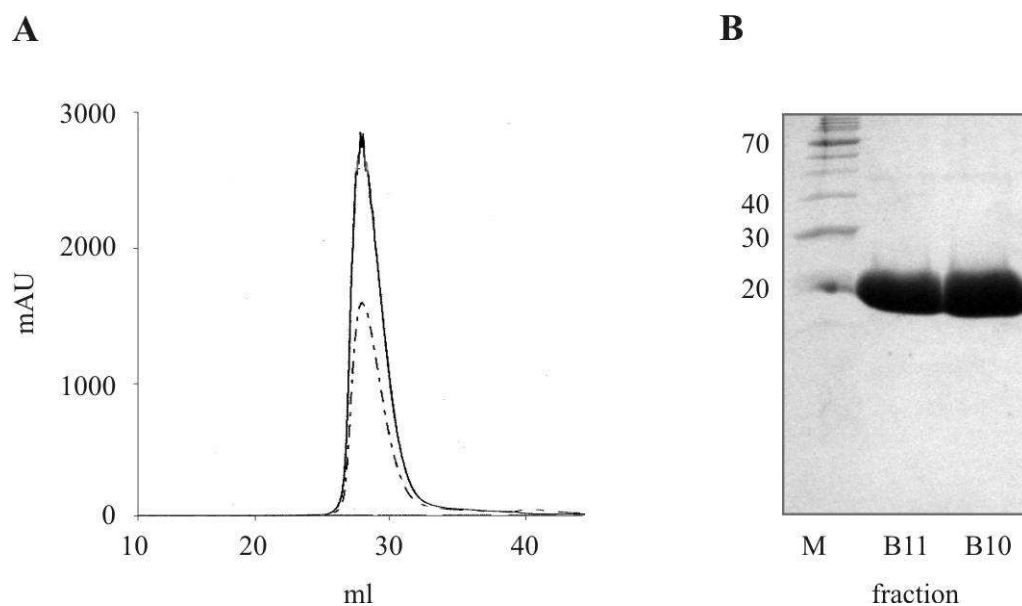


**Figure 31: Purification of UL50\_His by gel filtration.**

**A)** Elution profile of the gel filtration. Indicated are the measured milliabsorption units at the wavelength of 280 nm (continuous line) and 260 nm (dotted line) at the volume (in ml) collected from the column. **B)** Coomassie stained 17,5% SDS page. 15  $\mu$ l of the fractions B11 to B10, corresponding to the 28 and 29 ml elutions were analysed on the gel. Indicated on the right are the sizes of the marker bands in kDa.

### 6.5.1.1.3. Solubility of the purified UL50\_His

The poor solubility of UL50\_His was a major problem during protein purification. When stored in a concentrated form overnight precipitation occurred, making the protein solution inhomogeneous and unsuitable for further purification steps, for analysis of the protein or for crystallization. Protein precipitation was initially noted after the  $\text{Ni}^{2+}$ -

## Results

affinity purification, but was circumvented by immediate dilution of the protein in the MonoQ column buffer used for subsequent purification.

To improve the stability of the UL50\_His protein buffers varying in salt content and pH were tested. Fractions from the MonoQ purification were pooled and the protein was loaded to PD-10 columns (Amersham), equilibrated with the buffer to be tested. In total, 3,5 mg of protein was loaded and subsequently eluted in 3,5 ml of the desired buffer. In table 6 the buffers used are listed. A pH range of 4,5 – 10 was covered using a high and medium salt concentration. The next day, the protein samples were centrifuged and analysed for pellets originating from precipitated protein.

Only protein samples diluted in buffers with the lowest and highest pH, Na-acetate (pH 4,5) and CAPS (pH 10), with a low NaCl concentration of 150 mM, prevented protein precipitation. The proteins could be concentrated to 4,7 µg/µl and 2,5 µg/µl for the Na-acetate and CAPS buffers, respectively. However, after three days protein precipitation was observed in both buffers. Since no adequate buffer was found, purification was further performed in the described buffers (chapter 5.6) but over-night storage of concentrated protein was avoided.

**Table 6 : Buffers tested for better solubility of UL50\_His.**

List of buffers used to screen for optimal stability of the purified UL50\_His. Indicated is the buffer, the pH, the molarity of the respective buffer compounds and the molarity of salt in the buffer.

<b>pH</b>	<b>buffer</b>	<b>Molarity</b>	<b>NaCl</b>
10	CAPS	50 mM	150 mM
10	CAPS	50 mM	400 mM
8	Tris	100 mM	150 mM
8	Tris	100 mM	400 mM
6	Bis-Tris	50 mM	150 mM
6	Bis-Tris	50 mM	400 mM
4,5	Na-acetate	25 mM	150 mM
4,5	Na-acetate	25 mM	400 mM

### 6.5.1.1.4. Limited proteolysis of UL50\_His

Flexible loops and misfolded parts of a protein can cause solubility and stability problems. The fragment of UL50 (UL50\_His) was designed on the basis of computer predictions of the UL50 structure, estimating flexible loops or ordered secondary structure as helices or beta sheets. To identify flexible loops or regions within the UL50 fragment, the purified UL50\_His protein was tested for resistance to proteolysis in the presence of chymotrypsine and trypsin. Trypsin cleaves the polypeptide chain after lysine and arginine residues, whereas chymotrypsine prefers to cut after bulky, non-polar and aromatic amino acids. Loops that might protrude from the globular proteins or proteins consisting of two domains separated by an exposed stretch of amino acids would be cleaved by the proteases. Purified proteins were incubated in the presence of proteases for 1,5 hours and aliquots sampled at different time points to follow the protein degradation over time.

After the anion exchange purification of UL50\_His, the protein was concentrated to 8 µg/µl. 240 µg were treated with either chymotrypsine or trypsin in a total volume of 150 µl at 37 °C. Samples of 20 µl were taken from the digest reaction upon addition of the protease and after 30 s, 1, 3, 10, 30, 60 and 90 minutes. The protein samples were immediately mixed with the denaturing loading buffer and incubated at 95 °C.

Figure 32 shows a Coomassie stained SDS-page with the band corresponding to UL50\_His. Hardly any degradation products were visible either in the form of a decreased size or quantity of the bands. After three minutes, a weak band was visible which appeared slightly smaller than the UL50\_His band. The amount of the smaller protein increased slowly over time but even after 90 min the amount of cleaved protein was estimated to be negligible. Thus the UL50\_His construct appears compact and stable without flexible loops or regions in the protein that might be the cause for the observed solubility problems.

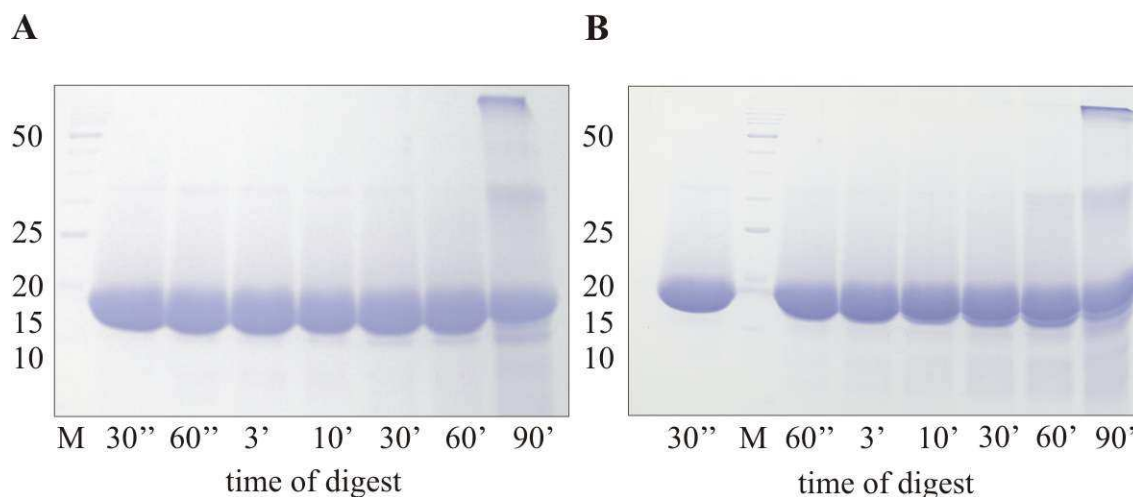


**Figure 32: Trypsin digest of UL50\_His.**

Coomassie stained SDS-page with samples after proteolytic digest with chymotrypsin in **A**) or trypsin in **B**). After the anion exchange purification, UL50\_His (240  $\mu\text{g}$  in 150  $\mu\text{l}$ ) was incubated at 37 °C in the presence of either protease. Samples of 20  $\mu\text{l}$  were taken from the digest reaction after 30 s, 1, 3, 10, 30, 60 and 90 minutes, denatured in SDS-page loading buffer at 95 °C and analysed on a 15% SDS gel. Numbers on the left indicate the size of the marker bands (M) in kDa.

#### 6.5.1.2. Bicistronic expression of UL50\_His and UL53 fragments

UL50 and UL53 form a complex during HCMV morphogenesis. The interaction of proteins often induces a conformational change in the interacting partners, which might influence the three-dimensional structure as well as the stability of the proteins. The UL50 fragment (UL50\_His) and two short versions of UL53 (UL53\_1 and UL53\_2) were co-expressed and co-purified. As for UL50, truncated versions of UL53 were selected that were expected to bind UL50 but lack other protein domains (see also chapter 6.4). Both UL53 fragments lack the variable region, which was localized to the first 56 aa based on the similarity plot of the UL31 protein family (Figure 19A) and M53 studies by our group (Lötzerich et al., 2006). The short 36 aa fragment, UL53\_1, covers the amino acids homologous to the predicted amino acids for M50 binding in M53 (Lötzerich et al., 2006). The long 73 aa UL53 fragment, UL53\_2, covers the entire CR1 of UL53 (Table 5).

UL50\_His (aa1-aa172) and either of the short fragments of UL53 (UL53\_1, aa57-aa92 or UL53\_2, aa57-aa129) were cloned into a modified pET-28b vector (provided by A. Meinhart) and transcribed as bicistronic mRNA. Only UL50\_His was His-tagged. A ribosome binding site was cloned between the two ORFs to allow independent translation initiation for the second part of the transcribed mRNA (Figure 33A). The bicistronic pET-28b vector was transformed into BL21-CodonPlus (DE3)-RIL and protein

## Results

expression as well as bacterial harvesting was performed as described for UL50\_His in chapter 6.5.1.1. After sonication and centrifugation, the bacterial lysates were loaded onto a Ni<sup>2+</sup>-NTA column to purify UL50\_His together with UL53\_1 or UL53\_2 complexed to UL50\_His.

As observed for the purification of UL50\_His after isolated expression, huge amounts of the protein were detected, in the elutions as well as in the preceding washes of the column. In addition, the expected bands of UL53\_1 at 4,5 kDa and UL53\_2 (8,7 kDa) were visible in the elutions collected from the column (Figure 33B). The small bands were cut from the gel and confirmed as the UL53 fragments by Edman sequencing.

The data shows, that both short fragments of UL53, covering 36 or 73 amino acids of UL53, were sufficient for binding to UL50.

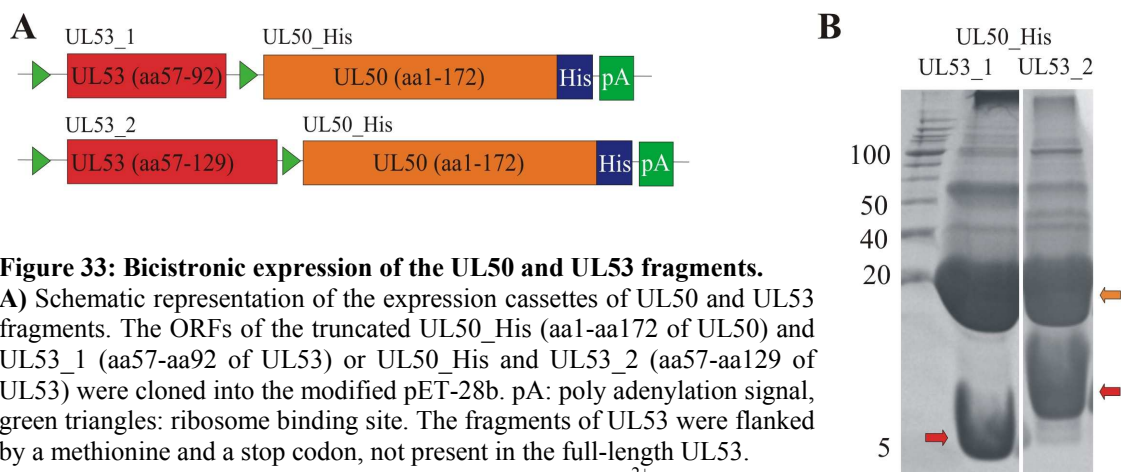


**Figure 33: Bicistronic expression of the UL50 and UL53 fragments.**

**A)** Schematic representation of the expression cassettes of UL50 and UL53 fragments. The ORFs of the truncated UL50\_His (aa1-aa172 of UL50) and UL53\_1 (aa57-aa92 of UL53) or UL50\_His and UL53\_2 (aa57-aa129 of UL53) were cloned into the modified pET-28b. pA: poly adenylation signal, green triangles: ribosome binding site. The fragments of UL53 were flanked by a methionine and a stop codon, not present in the full-length UL53.

**B)** Coomassie stained SDS-page with the elution after Ni<sup>2+</sup>-NTA purification of co-expressed UL50\_His with UL53\_1 or UL53\_2. 15 µl were loaded on a 17,5% SDS gel. Arrows indicate UL50\_His (orange) and the UL53 fragments (red). Numbers indicate the size of the marker bands in kDa.

### 6.5.1.2.1. Anion exchange purification and gel filtration of the complex

Both UL53 fragments were shown to bind to UL50\_His when expressed from bicistronic RNA in bacteria. For a higher degree of purity, the complex of UL50\_His and the small fragment of UL53\_1, harbouring the minimal UL50 binding domain, was further purified. The complex of UL50\_His and the small UL53 fragment is considered more compact, which might pose fewer problems during later attempts for crystallization.

As for UL50\_His alone, the fractions eluted from the Ni<sup>2+</sup>-affinity purification were pooled and used for anion exchange chromatography (MonoQ). In contrast to the clear peak of the absorption at 280 nm for UL50\_His alone (Figure 30A), the peak in the elu-

## Results

tion profile of the complex shows a shoulder following the main peak at the 103 to 106 ml fraction (Figure 34A). SDS-page analysis confirmed this was due to the presence of more than one form of protein, namely UL50\_His alone and the UL50\_His/UL53\_1 complex (Figure 34B). The 4,5 kDa band corresponding to UL53\_1 was only detectable in fractions collected from the main peak (B11 to B9), but not in the following fractions (B8 to B4). Notably, the complex eluted at lower salt concentrations (8% of buffer B, containing 1 M NaCl) than the UL50\_His, when purified after isolated expression (14% buffer B; Figure 30). This might explain the shoulder in the absorption profile at a higher salt concentration (Figure 34A) where only UL50\_His and not the complex is eluted from the column.

This again indicated the interaction between UL50\_His and the small UL53\_1 fragment, however, the interaction of the two protein fragments appears weak and susceptible. Nevertheless, the complex could be further purified and other proteins, which were present in the elutions after the Ni<sup>2+</sup>-affinity purification were removed from the purified protein samples. Fractions B9-B11, containing the UL50\_His/UL53\_1 complex, were pooled and further purified by gel filtration.

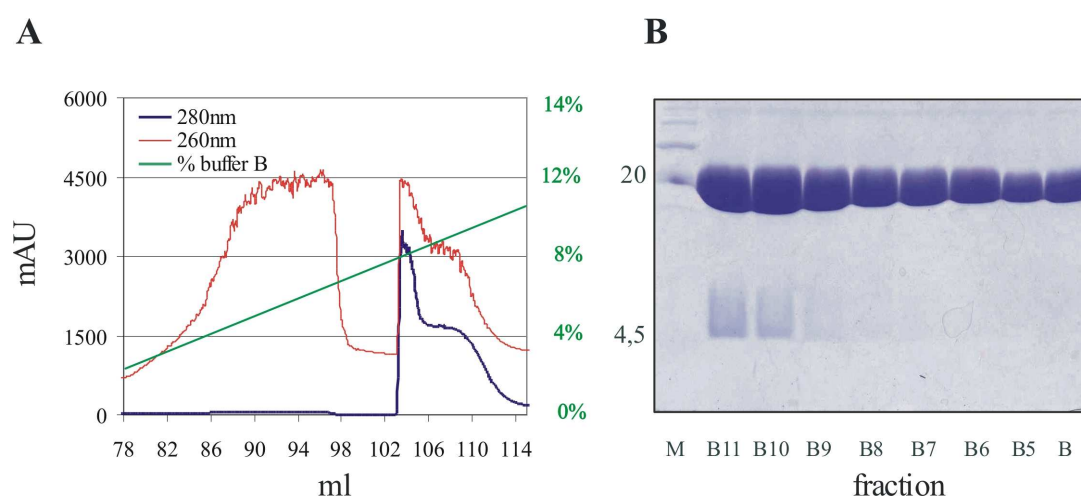


**Figure 34: Anion exchange chromatography for purification of the UL50\_His/UL53\_1 complex.**

**A)** Elution profile of the MonoQ purification. Indicated are the measured milliabsorption units at the wavelength of 280 nm (blue) and 260 nm (red) at the volume (in ml) collected from the column. The green line and numbers show the percentage of buffer B (1M NaCl) running through the column. **B)** Coomassie stained 17,5 % SDS page. 15  $\mu$ l of the fractions B11 to B4, corresponding to the 103 to 111 ml fraction were analysed on the gel. Indicated is the size of UL50\_His and UL53\_1 in kDa.



## Results

Figure 35 shows the elution profile and protein analysis of the collected fraction after gel filtration in a Superose 6 column. The peak absorption at 280 nm was clear and high. However, the Coomassie stained gel again shows a non-equimolar distribution of UL50\_His and UL53\_1.

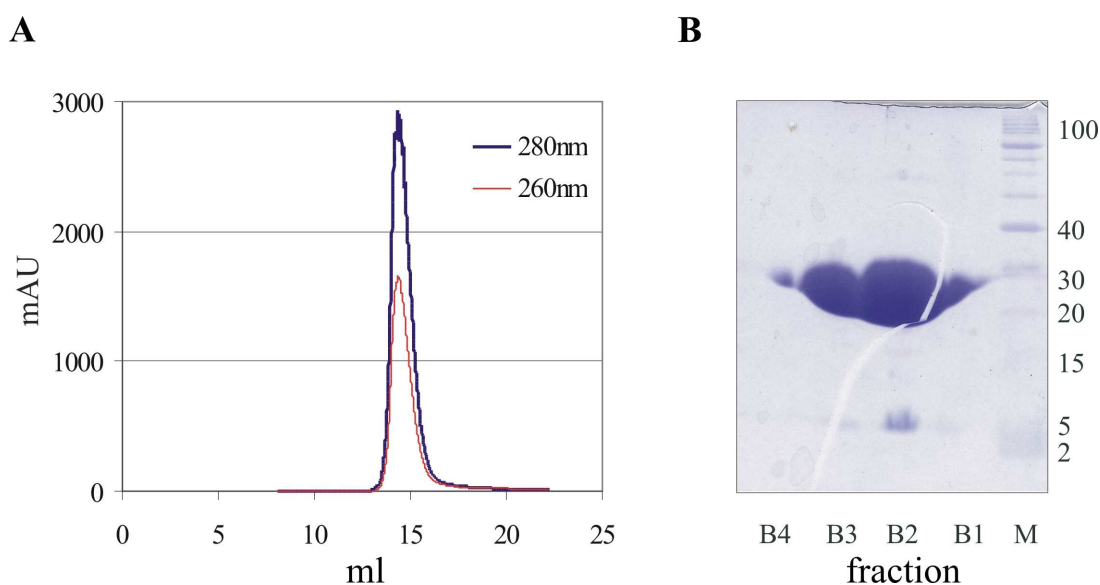


**Figure 35: Gel filtration for purification of the UL50\_His/UL53\_1 complex.**

**A)** Elution profile of the gel filtration. Indicated are the measured milliabsorption units at the wavelength of 280 nm (blue) and 260 nm (red) at the volume (in ml) collected from the column. **B)** Coomassie stained 17,5% SDS page. 15  $\mu$ l of the fractions B4 to B1, corresponding to the 13 to 16 ml fraction were analysed on the gel. Indicated on the right are the sizes of the marker bands in kDa.

### 6.5.1.3. Crystallization attempts of UL50\_His or UL50\_His/UL53\_1

Both, the isolated UL50\_His protein as well as the complex of UL50\_His and UL53\_1 were purified to a sufficiently high degree to initiate crystallization studies. The solubility problems of UL50\_His, not solved when expressed with UL53\_1, were circumvented by a rapid sequence of purifications steps, avoiding over night storage of the purified protein after the anion exchange column or gel filtration. The partial loss of UL53\_1 during co-purification of UL50\_His and UL53\_1 was neglected for the first co-crystallization trials.

Experiments for crystallization and co-crystallization were set up using the vapour diffusion method. For this technique, the purified protein is mixed with a precipitant (crystallization solution) in small drops. Slow evaporation of the precipitant results in up-concentration of the protein and eventual crystal formation. For that purpose, the

UL50\_His or UL50\_His/UL53\_1 containing fractions after gel filtration were pooled and adjusted to a concentration of 7-10  $\mu\text{g}/\mu\text{l}$ . 1  $\mu\text{l}$  of protein was then mixed with 1  $\mu\text{l}$  of crystallization solution from the commercial crystal screen 1 and 2 (Hampton Research). After one day, the protein content of three quarters of the drops precipitated, the other drops stayed clear. The clear drops were checked for crystal several times a week for six weeks. Unfortunately, no crystals were obtained.

### 6.5.2. The *in vitro* NEC-PCA

As the previous experiments showed, fragments of UL50 and UL53 can be expressed in bacteria and purified. For the fragment of UL50 (UL50\_His), a high purity was obtained after just one  $\text{Ni}^{2+}$ -affinity purification step. Roughly estimated from the data obtained by the Coomassie stained gel, UL50\_His represented 80-90% of the eluted protein. This short UL50 version is probably globular as indicated by the long resistance to protease treatment. The short fragment of UL53, UL53\_1, was sufficient for binding to UL50 since UL53\_1 was co-purified by the His-tag fused to the C-terminus of UL50\_His. Co-purification was also successful for the longer UL53 fragment, UL53\_2 (Figure 33). These findings were used to design Bla-tagged fragments for the expression of the NEC-PCA in bacteria as a potential high-throughput screen for inhibitors. The PCA, with herpesviral NEC proteins purified from bacteria, would be the first step towards an inhibitory screen for molecules inhibiting the nuclear egress of viral capsids.

UL50\_His was fused to BlaN and the HA-tag. As a negative control, a UL50 mutant was constructed, lacking the nine homologous amino acids of the binding motif in M50 (chapter 6.3.3.2). Similar to M50DM, this construct was named UL50DM and its Bla- and His-tagged version NUL50DM-His. BlaC was fused to the first 129 amino acids of UL53, thus including the expressed UL53\_2 and the variable region, consisting of the N-terminal first 56 amino acids. The variable region and sequences not involved in binding to UL50 were considered as a natural spacer to retain accessibility and allow proper folding of Bla fragments upon interaction.

## Results



**Figure 36: Constructs for the *in vitro* PCA.**

Schematic representation of the constructs used for bacterial expression of proteins for the *in vitro* NEC-PCA. The HA-tagged BlaN was fused to the UL50\_His fragment (aa1-aa172), separated by the glycine/serine spacer (NUL50-His). As negative control, a BlaN fusion to UL50\_His was constructed, lacking the 9 aa (aa51-aa59) homologous to the binding motif in M50 (NUL50DM-His). The HA-tagged BlaC was fused to a UL53 fragment, containing the first 129 aa of UL53 (CUL53-His).

### 6.5.2.1. Purification of Bla-tagged NEC proteins from bacteria

The Bla-tagged NEC proteins were expressed in BL21-CodonPlus (DE3)-RIL and further processed as described in chapter 6.5.1.1. Batches of 2,5 l of bacterial cultures were used for Ni<sup>2+</sup>-affinity purification of the recombinant proteins. Lysates from bacteria expressing CUL53-His were clear whereas lysates from bacteria expressing NUL50-His and NUL50DM-His were cloudy due to the formation of inclusion bodies. Following the Ni<sup>2+</sup>-NTA column eluted 1,5 ml fractions were analysed by a Coomassie stained SDS-PAGE and equal amounts of protein were tested for Bla-tagged fusions by an HA-specific Western Blot (Figure 37).

Fractions collected from the CUL53-His purification had a far lower protein content than fractions collected from either NUL50-His or NUL50DM-His. The yields of both UL50 derivatives were about 10 times higher than CUL53-His, roughly 5  $\mu$ g/ $\mu$ l total protein.

In Coomassie stained gels, protein bands were detected at the predicted sizes together with numerous impurities (Figure 37A). Judging from the elution patterns of NUL50-His and NUL50DM-His both proteins appear to behave in a similar manner during affinity purification, a prerequisite for the use of NUL50DM-His as a negative control in the PCA. In the HA-specific Western Blot, all Bla-tagged proteins were detected at their predicted size of 28 kDa (CUL53-His), 42 kDa (NUL50-His) and 41,2 kDa (NUL50DM-His) (Figure 37B). Clear signals were obtained when 15  $\mu$ l of the elution of CUL53-His and 10  $\mu$ l of a 1:10 or 1:100 dilution of NUL50-His and NUL50DM-His elutions were loaded on the SDS gel before detection in the Western Blot. The signals obtained for NUL50-His and NUL50DM-His were of comparable strength.

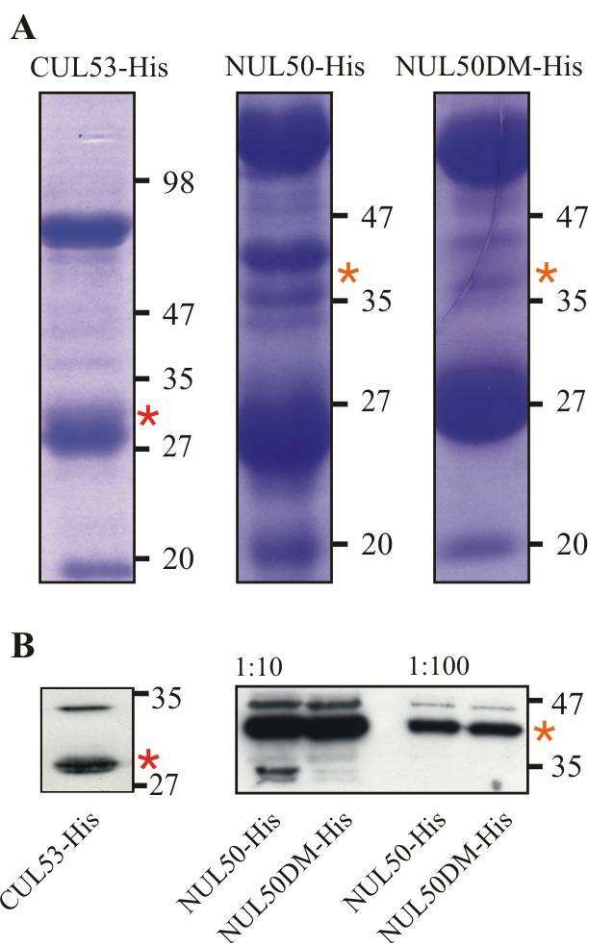


**Figure 37: Bacterial expression Bla-tagged NEC proteins of HCMV.**

**A)** Coomassie stained SDS-pages with samples after  $\text{Ni}^{2+}$ -NTA purification from the expressed CUL53-His, N-UL50-His and N-UL50DM-His. 15  $\mu\text{l}$  of the first elution were loaded on a 12% SDS gel. Sizes of the marker bands in kDa are indicated. Stars show the position of the recombinant proteins.

**B)** HA-specific Western Blots of the eluted proteins. For the Western Blot, 15  $\mu\text{l}$  of the first elution of CUL53-His and 10  $\mu\text{l}$  of a 1:10 or 1:100 dilution of the first elution of NUL50-His and NUL50DM-His were loaded on a 12% SDS gel. Numbers on the right indicate the size of the marker bands in kDa.

#### 6.5.2.1.1. Further purification steps

All His-tagged Bla fusion proteins eluted with significant impurities from the  $\text{Ni}^{2+}$ -NTA columns. Exemplary, two approaches were followed for further purification of NUL50-His, namely anion exchange chromatography (MonoQ; chapter 6.5.1.1.1) and purification by an HA-matrix (chapter 5.6.6) (data not shown). The protein failed to elute as a single peak from the MonoQ column and was detected in elutions throughout the run with a peak at 12% of buffer B (1 M NaCl). The eluted fractions contained contaminating proteins of both higher and lower molecular weight. When the HA-matrix was used, a high protein loss was observed. The majority of the HA-tagged NUL50-His could not be removed from the beads even after extensive washes with the HA-peptide present in the wash buffer. Due to the low yield of the two additional purification methods compared to costs, all Bla fusion proteins were used as eluates from the  $\text{Ni}^{2+}$ -NTA columns.

### 6.5.2.2. Bla complementation by purified NEC proteins

CUL53-His, NUL50-His and the binding negative UL50 mutant NUL50DM-His were tested for the ability to restore  $\beta$ -lactamase activity. 20  $\mu$ l (8  $\mu$ g) of the CUL53-His elution was combined with 20  $\mu$ l (80  $\mu$ g) of either NUL50-His or NUL50DM-His. Since lactamases are enzymes present in bacteria, the background of the assay was determined by measuring the Bla activity in the 20  $\mu$ l of the single elutions (Figure 38A). CUL53-His was complemented by NUL50-His but not by the non-binding mutant NUL50DM-His. The positive Bla signal was about 10 times higher than background for CUL53-His and NUL50-His. The background was defined by the isolated lysates and by the combination of CUL53-His with NUL50DM-His. The lack of Bla complementation for the proteins CUL53-His and NUL50DM-His was not due to low expression of the mutant or altered protein composition of the elutions since signals obtained by the Coomassie stained gel as well as the constructs detected in the HA-specific Western Blot (Figure 37A and B) showed no differences between NUL50-His and the mutant NUL50DM-His.

Purified proteins did not precipitate over night as observed in samples of purified UL50\_His or the complex of UL50\_His and UL53\_1 (chapter 6.5.1.1.3). However, storage reduced the ability of the proteins to restore Bla activity, which indicates alterations of the purified proteins over time.

### 6.5.2.3. Specificity of the Bla signal in the *in vitro* PCA

The signal obtained for NUL50-His and CUL53-His was shown to be specific since the non-binding mutant NUL50DM-His did not complement CUL53-His. The specificity of the NEC-PCA with purified proteins was confirmed by a competition experiment. Purified, non-tagged UL50 (UL50\_His, chapter 6.5.1.1) or BSA was added to the interacting NUL50-His and CUL53-His. BSA was expected to be without influence on the Bla signal whereas UL50\_His was expected to compete with NUL50-His for the binding to CUL53-His, which should then decrease the Bla signal.

Bla activity was measured for CUL53-His and NUL50-His in the presence of different amounts of either BSA or UL50\_His. As more competitive UL50\_His was added to the interacting proteins, the signal obtained by nitrocefin hydrolysis decreased. The signal was not negatively influenced by the presence of BSA. In fact the signal rather increased with the amount of BSA added to the assay. This is due to the background hy-

## Results

drolysis rate of 11 milliabsorption units/min obtained when only 125  $\mu\text{g}$  of BSA was tested for nitrocefin hydrolysis. UL50\_His exhibited no background when tested alone, however, decreased the Bla signal of the CUL53-His/NUL50-His interaction by more than 50%.

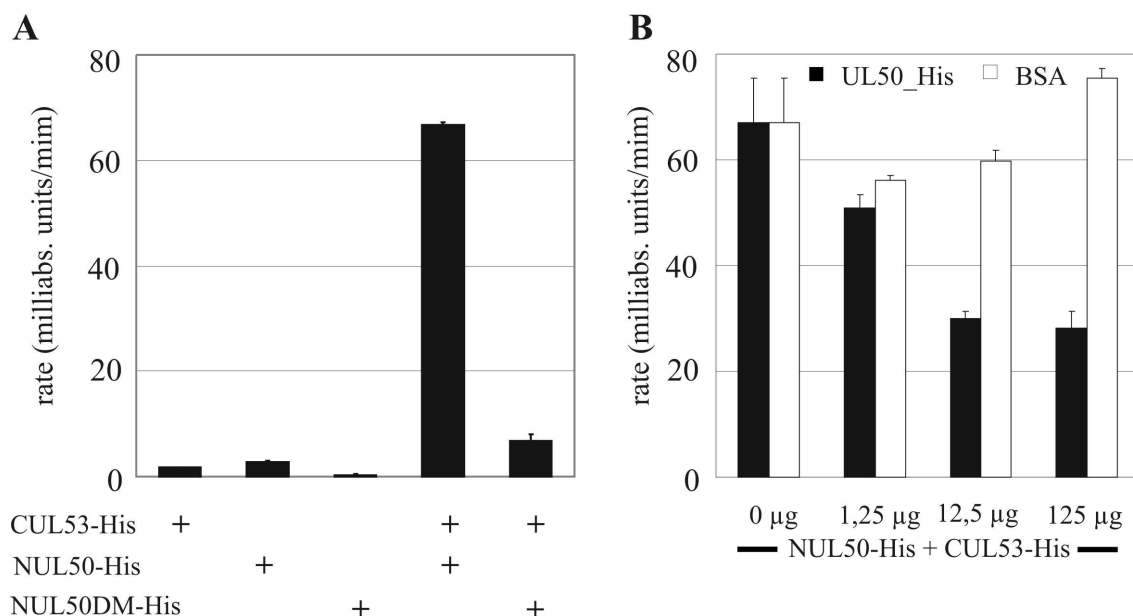


**Figure 38: Specificity of the *in vitro* NEC-PCA.**

Bla activity after combining purified proteins from  $\text{Ni}^{2+}$ -NTA columns. **A)** 20  $\mu\text{l}$  of the indicated elutions, alone or in combination were tested for reconstituted Bla activity by adding nitrocefin (Methods chapter 7.2). **B)** BSA (NEB) or UL50\_His were added to NUL50-His and CUL53-His in the indicated amounts and Bla activity was determined. The indicated detection limit (DL) was defined by the hydrolysis of nitrocefin after combination of CUL53-His and NUL50DM-His. Error bars indicate the standard deviation.

---

## **7. Discussion**

Within the last two decades, the prevention and treatment of herpesvirus related diseases has attracted increasing attention from clinicians and scientists. These viral diseases are primarily self-limiting in the immunocompetent host, however, due to an increase in the human life span together with the number of organ transplantations and the spread of AIDS, the occurrence of symptomatic herpesvirus induced disease has increased and enforced the use of antivirals and vaccines. Most of the currently approved chemotherapeutics target the essential process of viral DNA replication. Unfortunately, the risk of adaptive mutations towards resistant herpesvirus strains is high since they act only on a single target. Moreover most of the existing drugs lead to strong side effects in the treated patient.

### **7.1. Search for new targets of antiherpesviral drugs**

In the past, strategies for the development of antiherpesviral drugs primarily involved anti-metabolite research. For such strategies, a known polymerase substrate is modified to a non-functional analogue to compete for the enzyme's binding site or to become toxic upon enzyme activity. At present, protein-protein contact areas in which interacting surfaces can be blocked by peptides or peptidomimetic compounds (Loregian et al., 2002; Loregian et al., 2003; Loregian and Coen, 2006) are considered to be the most promising drug target sites. Single processes can be blocked with high specificity without further side effects and the involvement of several proteins makes the system less vulnerable to mutations. The main obstacles to the inhibition of protein-protein interactions are large contact areas and multiple contacts involved (reviewed in Archakov et al., 2003). An example of disruption of protein-protein interaction for herpesvirus inhibition that targets a site other than the frequently used nucleoside analogues was recently presented (Loregian and Coen, 2006). Small, peptidomimetic compounds were used to interfere with the assembly of the holoenzyme of HCMV polymerase, thus blocking viral DNA replication. Any viral protein-protein interaction that is essential during the viral life cycle may serve as a potential drug target. Particularly appealing targets would be the highly conserved protein-protein interactions involved in virus morphogenesis (Mettenleiter, 2002).

Having identified a potential drug target, random screens or rational design of interfering compounds can be performed. Any approach for drug discovery and development should be fast, simple and economical. The approach should also be flexible and applicable to numerous settings. This is preferably a high-throughput screen or also a completely virus integrated assay system that enables validation of promising compounds within the viral life cycle. In the present study, a new approach was followed to further characterize a protein-protein interaction, which is not only essential for herpesvirus morphogenesis but is also conserved throughout all herpesvirus subfamilies. Such an interaction could provide a possibility to develop inhibitors of all human herpesviruses.

### **7.2. Exploring protein–protein interactions**

Many methods to monitor protein-protein interactions are designed to screen for unknown interaction partners. The classical yeast two-hybrid system (Y2H) is an easy and efficient method for interaction screens. However, the major drawback of these screens is the high number of false positives and false negatives that occur, requiring careful assessment of the identified interactions by other techniques (Uetz et al., 2006). In contrast to the Y2H screen, techniques to confirm the relevance of an observed interaction and analysis of the detected interactions in the biological context are far more time consuming, expensive and difficult. An assay recently described for protein-protein interactions, the protein complementation assay (PCA), is spatially flexible and technically simple. It may serve as a link between interaction screens and functional studies (Johnsson and Varshavsky, 1994; reviewed in Piehler, 2005). In the PCA, two parts of a reporter enzyme are fused to two putative or known interaction partners. Since the enzyme fragments are non-functional but fold and complement each other upon spatial proximity, reconstituted enzyme activity indicates the interaction of the proteins to which they are fused. The PCA owes its flexibility to the detection mode of the interactions, which in an ideal case is not restricted to particular compartments of the cell or specific cell types. Interactions between membrane proteins as well as between nuclear or cytoplasmatic proteins can be detected (Johnsson and Varshavsky, 1994). The influence of the fused enzyme tags on the folding or function of the proteins under study poses the only limitation. Furthermore, the PCA is not dependant on *de novo* protein synthesis or other cellular functions for the signal to be generated. It allows the detection of the monitored interaction in real time or with a short time shift due to the detec-



tion of the reconstituted enzymatic reaction. In addition to the reported use of a PCA in eukaryotic cells and the few applications which were proposed in bacteria (Mossner et al., 2001; Nord et al., 2005; Pelletier et al., 1999), we here pioneered the application of the PCA in a cell free screening system.

PCAs have been established with a range of reporter proteins, such as the complementation of the murine dihydrofolate reductase (mDHFR), where the fluorescein-conjugated methotrexate binds to the reconstituted mDHFR (Subramaniam et al., 2001). The mDHFR-PCA allows a direct readout and interactions can be monitored in real time. However, due to the lack of signal amplification a considerable amount of interacting protein is required for detection. The  $\beta$ -galactosidase-PCA benefits from an enzymatic amplification of its signal but the active enzyme is a homotetramer with large individual fragments (80 kDa), which increases the possibility that some interactions may be sterically hindered (Blakely et al., 2000; Rossi et al., 1997). Fluorescent reporter proteins such as GFP or YFP were shown to reassemble irreversibly (Magliery et al., 2005; Nyfeler et al., 2005). They can reveal transient interactions but may interfere negatively with the function of a dynamic process like a virus infection. We have chosen the TEM-1  $\beta$ -lactamase of *E. coli* (Bla) as the reporter enzyme (Galarneau et al., 2002) to avoid these disadvantages. The signal of the Bla-PCA is amplified enzymatically, thus, only few interacting proteins are required for detection (Remy et al., 1999; Remy and Michnick, 2004). Furthermore, reversibility of the interaction allows the quantitative assessment of the interaction under study. Finally, Bla was chosen due to the wide variety of substrates available. Fluorescent and colorimetric substrates like CCF2/AM (Zlokarnik et al., 1998) and nitrocefin (O'Callaghan et al., 1972), respectively, are suitable for use in the PCA. In this study nitrocefin was used since it is cost-effective and sensitive enough. The detection procedure does not require expensive instrumentation.

### **7.3. The nuclear egress complex: a potential drug target**

The morphogenesis of herpesviruses involves a large number of specific viral protein-protein interactions. Our group focuses on the elucidation of an early step in morphogenesis, the nuclear egress of nucleocapsids. The DNA-filled capsids, with a diameter of 100 nm, exceed the tolerated size of the nuclear pores. To gain access to the cytoplasm, the nucleocapsids are directed to the nuclear rim and bud at the inner nuclear

membrane whereby capsids acquire their primary envelope (Mettenleiter, 2002 and chapter 3.1.4.). The members of the UL34 and UL31 protein families play a crucial role during this process. As for many steps in morphogenesis, the nuclear egress process is conserved throughout all studied herpesviruses. This is also reflected in the high degree of homology between members of both protein families (Figure 4 and Mettenleiter, 2002). The UL34/UL31 interaction might furthermore meet the requirements for inhibition by peptidomimetic compounds due to the small interaction surface since a single point mutation in M50 and M53 has already been shown to abolish the interaction of the MCMV UL34 and UL31 homologues (Bubeck et al., 2004;Lötzerich et al., 2006).

The Bla-PCA was established to study the UL34 and UL31 protein family members. The assay was used for the localization of the binding site within related proteins as well as for developing an inhibitor screening test. The MCMV homologues, M50 and M53, were used to establish the Bla-PCA. Both proteins have been studied in our group. The mutual binding sites have been identified in both proteins but further structural and functional relationships are not known (Bubeck et al., 2004;Lötzerich et al., 2006). Furthermore, the advanced but simple reverse genetic system, which is available for MCMV, allows mutants to be tested in the virus context.

#### **7.4. The NEC-PCA**

The constructs for the NEC Bla-PCA, involving members of the UL34 and UL31 protein families, were based on the study of Michnick and colleagues (Galarneau et al., 2002). Here, the TEM-1  $\beta$ -lactamase was split between amino acids 194 and 196, producing two fragments that should not exhibit lactamase activity themselves but once within proximity, will complement each other to restore activity. For our study we used the same cleavage point in the reporter protein but further exchanged one amino acid in BlaN to enhance its expression in eukaryotic cells.

In order to confirm that the two Bla fragments can restore enzyme activity, the Bla ORF was not split, but interrupted by a 15 amino acid spacer. After transfection of different amounts of DNA, Bla activity was detected in a dose dependant manner by quantification of nitrocefin hydrolysis. For the second preliminary control experiment, residual affinity of the Bla fragments was excluded and the linear range of Bla activity determined. For that, the Bla fragments were fused to the known interaction partners FRB and FKBP12 (Brown et al., 1994). The interaction of the two proteins was induced by

rapamycin, which allowed not only an on/off control mechanism but also enabled a quantitative measure of the interaction using the same constructs. The low background in the absence of rapamycin and the gradual increase of Bla activity, correlating with increasing rapamycin concentrations, confirmed the lack of basal activity and affinity of the Bla fragments to each other. The semi-quantitative nature of the Bla-PCA also demonstrated the range of signal strength to be expected in subsequent experiments. The Bla fragments were separated from the FRB and FKBP12 proteins by the 15 amino acid spacer used in the previous experiment to interrupt the Bla ORF. The spacer contained serine and glycine residues, small amino acids that lack a defined secondary structure, forming a flexible hinge that separates the protein under study from the Bla fragments. This enabled the Bla fragments to interact freely upon proximity to each other without sterical constraints.

After the set up of the colorimetric Bla assay and approval of the Bla fragmentation, the PCA was established for the well studied NEC proteins of MCMV, M50 and M53.

The N-terminal Bla fragment fused to M50 was complemented by the C-terminal Bla fragment, fused to either the N- or the C-terminus of M53. It was furthermore shown that viral proteins tagged with a Bla fragment are fully functional. The fusion proteins N-M50 and C-M53 were integrated not only in an assay based on isolated expression but were also compatible with virus morphogenesis. This confirmed the flexibility of the assay and the negligible influence of the small Bla-tags on the folding of the proteins. A system where both Bla-tagged proteins are inserted into the same viral context would thus allow the monitoring of the interacting proteins in the complete native system.

### 7.4.1. UL34 and UL31 homologues in the NEC-PCA

The application of the PCA to study the conservation of the interactions within the UL34 and UL31 protein families enabled the identification of binding domains within the interacting proteins. This added another application for PCAs. To date, PCAs were applied for elucidation of signal pathways involved in apoptosis or stress response (Nyfeler et al., 2005; Subramaniam et al., 2001) and as a tool for mapping biological networks (Michnick, 2003). In most studies the PCA is used for an interaction screen or validation of interactions, as it was originally proposed when the technique was estab-

lished. In this study the PCA served for binding studies integrating a whole protein family.

We wanted to apply the knowledge about one interacting protein pair, here M50 and M53 (Bubeck et al., 2004;Lötzerich et al., 2006) to the entire protein family. Most tested members of the UL34 and UL31 protein families reacted as expected in the PCA and confirmed described (Bubeck et al., 2004;Fuchs et al., 2002;Reynolds et al., 2001), or, for HCMV and MHV68, predicted interactions. The signal obtained by the combination of the EBV homologues was not significant, although their interaction was shown by other means (Gonnella et al., 2005;Lake and Hutt-Fletcher, 2004). This might be explained by technical reasons, such as an unfavourable impact of the Bla-tags on the EBV proteins. Although the interaction of MHV68 proteins was significant, it was lower than any other interaction tested positive. Possibly the NEC in  $\gamma$ -herpesviruses needs additional proteins to facilitate or to stabilize the complex.

#### 7.4.2. Evaluation of binding sites in the NEC proteins

The UL34 and UL31 protein families are highly conserved with sequence homology of up to 80% for the UL34 family members and up to 60% for the UL31 protein family. The cross-complementation experiments in our study identified the binding sites and showed that they evolved with the subfamilies. Proteins of the same herpesvirus subfamily successfully replaced each other in the PCA, whereas proteins of different subfamilies failed to bind to one another. HCMV proteins that were found to bind to M50 or M53 were shown to functionally replace the MCMV proteins in the virus context. The lack of replacement in the PCA as observed with proteins of PrV or MHV68 was reflected by the inability to rescue the M50 or M53 null phenotype.

We identified the diverged properties of the binding sites in both protein families. The NEC-PCA was applied to characterize the binding site in UL34 homologues. For M50 of MCMV, the binding site to M53 was mapped to a few amino acids in the N-terminal part of M50, amino acids 51 to 59 (Bubeck et al., 2004), but also an insertion in the middle of the protein, after amino acid 114 affected binding. For UL34 of HSV-1, the binding site to UL31 was located in the middle of the protein between amino acids 137 and 181 (Liang and Baines, 2005). These findings are supported by a Y2H screen including PrV proteins, where only UL34 fragments covering at least the first 162 amino acids were able to bind UL31 (Fuchs et al., 2002). Different binding sites within pro-

teins from different virus subfamilies are not surprising and the cross-complementation experiments showed that only proteins from the same herpesvirus subfamily were able to replace each other in the PCA. This effect was clearly seen for UL34 proteins cross-complemented by the heterologous UL31 proteins to a similar degree. In contrast, UL31 homologues were less effectively cross-complemented when co-expressed with the heterologous UL34 protein of a virus belonging to the same subfamily. This indicated other binding requirements of the UL34 proteins.

The data in the literature can be explained by two structurally diverged binding sites in UL34 proteins or with one bipartite binding motif. To see the influence of the two different binding sites in both subfamilies, mutants were generated lacking either of the two predicted binding sites. We demonstrated that both the N-terminal and the central region of the M50 are important for binding to M53. Deletion of not only the cluster of amino acids in the N-terminus (Bubeck et al., 2004) but also of the residues matching the site which had been shown to be essential for the interaction of UL34 and UL31 in HSV-1 (Liang and Baines, 2005) led to a negative result in the PCA. The deletion of the N-terminal motif in UL34, originally predicted to be important for the M50/M53 interaction, reduced the binding of UL34 to UL31 by half. Conclusions about the UL34 mutant lacking the binding site predicted for UL34 (UL34DM\*) could not be drawn as the protein was unstable and did not allow binding studies in the PCA. Based on these data, we concluded that the binding site in the UL34 family is probably bipartite. In M50, single amino acids within the 9 amino acid motif were exchanged to alanine which abolished binding to M53 (Bubeck et al., 2004). The previous approach was far more subtle than the deletion of 44 amino acids in the middle of UL34. It can't be excluded that the deletion of such a long stretch of amino acids affected protein folding and stability. Confirmation therefore can only be made after a more detailed study of the binding sites and would require shorter deletions or point mutations in the central domain of UL34 and M50.

For the UL31 protein family, alignment of the protein sequences revealed the distribution of conserved amino acids in four regions, which were assigned as the four conserved regions (CR1-CR4) and a variable region (V) in the N-terminus. In M53, the variable region was recently shown to be essential for the nuclear targeting of the protein. Furthermore, the binding site to M50 could be narrowed down to a small stretch of 30 amino acids within the first CR (Lötzerich et al., 2006). The PCA was now used to

confirm this binding domain also in other representative members of the UL31 family. The information gained for the binding site in M53 formed the basis for the construction of the chimeric proteins where the N-terminal variable region and the first CR of the proteins were split from the following three CRs and combined with a protein tail of another UL31 protein. The Bla signal obtained after co-expression of the chimeras with native UL34 proteins revealed that the binding specificity to the different UL34 proteins could be indeed transferred with the CR1. This led to the conclusion that in UL31 proteins the binding sites are generally located in the first conserved region in all three herpesvirus subfamilies. The stability and binding ability of the proteins suggested that the conserved parts of the protein, CR1 and the CR2-CR4, not only harbour certain functions but also form independent folding domains of the proteins.

Studies of the UL31 and UL34 proteins carried out so far evaluated the interaction and co-localization of the homologous proteins using co-immunoprecipitations, immunofluorescence and electron microscopy. M53 and its homologues are expressed with late kinetics, localised within the nucleus of infected cells and are important for the nuclear egress of capsids (Mettenleiter, 2002). The binding site to UL34 homologues, which we assigned to the first CR, suggests that other CRs carry so far unknown functional sites. We further tested whether these functions were conserved within the UL31 family or if they diverged during evolution of the different subfamilies. For that, the UL31 chimeras were analysed in the context of viral replication. The null phenotype of  $\Delta$ M53, the MCMV deficient for M53, could not be rescued by the chimeric proteins MP and MG, which carried the first conserved region of M53 with the C-terminus of UL31 of PrV or Orf69. This experiment showed that binding of the partner protein was not yet sufficient for the functional replacement of M53 in the virus context. At least one further function is required that is also not conserved between the subfamilies. It was shown that the chimeric protein MP acts as a dominant negative inhibitor in MCMV replication (see following chapter). This indicated that the interaction of the chimeric protein MP and M50 was competitive to the wild type M53 due to the sequestration of M50, but could not fulfil other functions of M53 in the virus context, thereby inhibiting the NEC formation.

### 7.4.3. Study of dominant negative NEC proteins

A dominant negative (DN) mutant of a protein is defined by its negative impact on biological processes in the presence of the functional wild type protein. Proteins that can be mutated to DN mutants are often involved in higher ordered protein complexes and have more than one important interaction. While a DN mutant might exhibit one protein function, like binding to a certain partner, it lacks others such as a required signal transduction, an induced change of conformation or the binding of another protein. To act competitively with the wild type the DN mutant has to be stable and needs to be expressed in sufficient quantities to have a strong influence on biological processes. The deficiency of a DN protein helps to assign a function to the wild type counterpart. Indications can be obtained from altered phenotypes of cells or viruses such as the localization of proteins or altered protein binding. The major problem in the study of DN mutants is, as it is the nature of the mutant protein, the block of the virus life cycle. Viral mutants cannot be reconstituted after insertion of the DN mutant in the genome. This problem is circumvented by the regulated expression of the DN protein. Recently such a conditional system to study DN mutants for herpesvirus replication was developed in our lab (Rupp et al., 2005). The virus can be studied in the presence and absence of the protein with the same construct and the same virus preparation.

The chimeric proteins MP and MG, harbouring the three C-terminal conserved regions of either UL31 of PrV or Orf69 of MHV68, were introduced into the wild type MCMV. Mutants carrying the MG showed a delayed reconstitution time, taking five weeks compared to less than a week for the wt MCMV BAC. Mutants carrying the MP protein, however, did not lead to virus progeny even though several independent clones were tested and MEF cultures used for the reconstitution were passaged for more than two months. While the DN effect has not yet been analysed by the conditional expression system (Rupp et al., 2005), the analysis of other chimeric proteins in the MCMV genome clearly supports the DN features of MP. Virus was reconstituted from the MCMV BAC carrying GP, the fusion of CRs of UL31 and Orf69, which shows that the heterologous C-terminal CRs of UL31 *per se* do not exhibit any inhibitory effect on MCMV. Virus was also reconstituted in the presence of CP despite the CR1 of UL53, which can functionally replace M53 when inserted into the M53 deletion genome. Data from the cross-complementation experiments showed a partial replacement of M53 by UL53 in M50 binding. This partial replacement in the PCA was reflected by a lower

affinity of M50 to CP than to MP carrying the first CR of its natural binding partner. CP might still compete for M50 when introduced into the wt MCMV BAC, however, M53 can integrate sufficiently into the functional NEC due to its higher affinity to M50. The fact that wt MCMV was reconstituted in the presence of MG but not in the presence of MP might be explained by the evolutionary distance of the three herpesvirus subfamilies. Genes of  $\beta$ - and  $\gamma$ -herpesviruses show a higher degree of similarity for both UL31 and UL34 protein families than compared to  $\alpha$ -herpesvirus genes. Relevant protein functions might be still conserved between  $\beta$ - and  $\gamma$ -herpesviruses that are already diverged in  $\alpha$ -herpesviruses. Therefore the C-terminal part of Orf69 of the  $\gamma$ -herpesvirus MHV68 may partially complement the function located in the C-terminus of M53. Thus, MG competes for binding to M50 but does not completely fail in the so far unknown processes mediated by the CR2-CR4 of M53.

In conclusion it was shown that the interaction of the NEC components is essential and that interfering solely with their interaction will inhibit viral replication. Furthermore a new essential function of the UL31 protein family was detected. The PCA served as a simple and reliable method to test interacting NEC proteins and the effect of mutations on their binding capacity.

#### 7.4.4. Study of core proteins by functional replacement

UL53 and UL50, the HCMV homologues of M50 and M53, complemented the null phenotype of the respective deletions in MCMV. This is the first example of complete functional replacement of an essential gene in  $\beta$ -herpesviruses. MCMV, a close relative of HCMV, provides a useful model to study various aspects of CMV biology both *in vitro* and *in vivo*. Our data indicate that, at least in some cases, genes from HCMV can be transferred to the MCMV background. This makes it possible to study HCMV functions in the context of the more convenient MCMV system. The viruses carrying UL50 or UL53 instead of M50 or M53, respectively, showed no attenuation in growth when compared to the natural setting. Such recombinants could provide experimental models for inhibitor screening and enable the development and genetics of drug resistance to be studied in a biological context.

In contrast to the full functional replacement of an essential herpesvirus gene as shown in this study, a partial functional replacement of a non-essential herpesviral protein has already been reported for the HCMV core protein UL97. With regard to the study of



drug resistance, UL97 and its homologues were studied in isolation and in the virus context of  $\alpha$ - and  $\beta$ -herpesviruses. UL97, a nucleoside kinase, is not essential for viral replication but UL97 deletion mutants show a strong attenuation in virus growth in cell culture. The UL97 protein was shown to play an important role in DNA replication and encapsidation (Chee et al., 1989; Wolf et al., 2001), which makes it an important drug target (chapter 3.2.1). UL97 and M97, the MCMV homologue, are both expressed late in infection and show a high homology, which peaks at about 41% amino acid identity in protein domains important for substrate recognition and nucleotide binding (Michel et al., 1999; Rawlinson et al., 1997). The growth defect of the M97 deletion mutant of MCMV can be partially restored by the introduction of UL97 in the MCMV genome, thus indicating functional replacement of the two core proteins (Wagner et al., 2000). In the  $\alpha$ -herpesvirus HSV-1, UL97 restored the minor growth disadvantages of UL13 (the UL97 homologue) deletion mutants (Coulter et al., 1993; Ng et al., 1996). The recombinant herpesviruses allow simple *in vitro* testing and, in the case of MCMV, *in vivo* testing for the investigation of novel antiviral drugs targeting UL97 (Wagner et al., 2000). The studies provide evidence for the successful functional replacement of proteins and illustrate the potential of a system to study core proteins of HCMV in a model infection. In contrast to UL97 and its homologues, UL50 and UL53 not only show high similarity at the sequence level but also demonstrate the same biochemical features, as far as they were studied.

The functional replacement of core proteins might have a potential for the study of proteins from viruses lacking a suitable animal model. It is likely that the complementarity seen for UL50, UL53 and UL97 can be found even more frequently within the herpesvirus core genes thereby providing a new and technically not too demanding option to study HCMV functions in MCMV. It is also possible that this cross species complementarity is applicable to more problematic settings. For example, up to now no productive tissue culture system has been available for studies of human  $\gamma$ -herpesvirus replication. In contrast, MHV68, the  $\gamma$ -herpesvirus of mice, grows to high titres *in vitro* echoing the HCMV-MCMV relation. To find appropriate candidate genes for cross-complementation in the virus context, PCA interaction maps could be performed. The combination of the PCA with BAC technology is now available for virtually all herpesviruses.

---

### **7.5. Towards an NEC inhibitor**

Defined and essential viral protein-protein interactions are attractive targets for chemotherapeutics. However, large and multiple contact areas can hamper the disruption of the protein-protein interaction by small molecules. This study examined the interaction of the HCMV proteins UL50 and UL53, members of the UL34 and UL31 protein families, respectively, as potential drug target. The interaction is non-obligatory (De et al., 2005), meaning that both proteins fold independently but meet in the nucleus to form an essential complex. Both gene products are required for virus replication in HCMV and their interaction is needed for their function. The most relevant residues in MCMV have been narrowed down to 9 amino acids of M50 and 30 amino acids of M53 (Bubeck et al., 2004; Lötzerich et al., 2006). The exchange of single amino acids within these binding motifs affected or even abolished the binding to each other. The strong effect of these subtle mutations could indicate that the crucial interface of the M50/M53 interaction is limited, increasing the possibility that a small inhibitor or competing peptides might be able to block the NEC formation.

#### **7.5.1. NEC proteins expressed in bacteria**

For a possible high-throughput inhibitor screen, proteins need to be studied in isolation and the protein-protein interaction has to be reconstituted out of the natural context. Therefore the NEC proteins were expressed in bacteria and purified. The protocol was optimized for the purification of a 20 kDa fragment of UL50, the N-terminal half of the protein, harbouring the predicted UL53 binding site but lacking C-terminal coiled-coil regions that were predicted by computer analysis. Three subsequent purification steps led to a good yield of pure protein. Already after the first purification step, a Ni<sup>2+</sup>-NTA column, the protein made up approximately 95% of the total protein eluted from the column. The protein purity was further improved by anion exchange and size exclusion chromatography.

When the UL50 fragment was co-expressed with one of the two fragments of UL53, the complex of both could be purified by the His-tag, which was attached to the UL50 fragment. The longer UL53 fragment covered with its 73 amino acids the CR1 of UL53, which was shown by PCA to harbour the UL50 binding site. However, even the short, 36 amino acid fragment of UL53 that covers only the minimal binding site predicted for M53 by Koszinowski and colleagues (Lötzerich et al., 2006) was sufficient to form a

complex with UL50 and could be co-purified. The complex of UL50\_His and the small UL53 fragment was selected for further purification since it was assumed to be more compact and thus more suitable for a later co-crystallization. Co-purification was possible during three subsequent purification steps. The complex of HCMV NEC proteins was obtained with a high degree of purity, however, a large part of the UL53 fragment was lost from the complex in the course of purification. This might be explained by harsh purification conditions or the lack of stabilizing parts present in the wt UL53 protein that were deleted in the constructs used for the co-expression. UL53\_2 might form a more stable complex and will be tested in future experiments.

Nevertheless it was shown that the interaction of the two NEC proteins neither requires any other viral or cellular protein nor post-translational modifications by the eukaryotic cell. This is a prerequisite to study the two proteins in isolation and establish any *in vitro* system based on the bacterial expression of the proteins.

Since UL50\_His as well as the complex of UL50\_His and the short UL53 fragment were purified with a high yield and a satisfactory purity degree, crystallization was attempted. A crystal of a protein allows the resolution of its three dimensional structure. Based on that knowledge, the direct design of molecules that fill and thus block binding clefts or contact surfaces is possible. Unfortunately, the two crystal screens, testing crystallization in 200 different buffer conditions, did not lead to crystal formation of the UL50 fragment or the complex. Crystallization of proteins is problematic and reasons for success or failure are often unknown. As future steps, more buffers could be included in the crystallization screen and crystallization methods other than the vapour diffusion method might be tested (DeLucas et al., 2003). However, the protein itself might have to be modified by point mutations, further truncations or deletions (reviewed in Dale et al., 2003). In our case, the longer UL53 fragment (UL53\_2), which was not tested for further co-purification and crystallization, might lead to better results due to conformational changes of the complex. The poor solubility of the isolated UL50\_His or the complex does not necessarily hamper crystal formation, however, further attempts to solve this problem will be considered. The addition of polyethylene glycol (PEG) or a co-crystallization with stabilizing antibodies might enhance stability upon possible crystallization (Kovari et al., 1995; McPherson, Jr., 1976). In many cases, however, the only way to obtain information about the 3D structure of a protein is the crys-

tallization of a homologous protein that might be purified and crystallized with more success.

### 7.5.2. The *in vitro* NEC-PCA

To establish a rapid and easy system for screening small inhibitory compounds, the NEC-PCA for UL50 and UL53 was transferred to the bacterial expression system. Due to the variety of favourable features for eukaryotic application, the PCA is predominantly used in eukaryotic cells. Proteins can be studied in the natural context, ensuring subcellular targeting, post-translational modifications and interactions with other proteins required for correct functioning. Taking these advantages into account, PCAs were proposed as suitable candidates for high-throughput screens for interacting proteins or inhibitors. Remy and Michnick (Remy and Michnick, 2004) reported a GFP-PCA based functional cDNA library screen for interaction partners of the protein kinase PKB/Akt. Within one system, the genome wide screen and functional validation experiments were combined. Similar to the Y2H screen, fusions to the potential interaction partners were constructed. Co-transfections in any cell type can be performed and cells positive for the interaction can be detected by FACS analysis. Functional assays can be based on the PCA by detection of perturbations of protein–protein interactions caused by agents such as hormones or specific inhibitors that are known to modulate the specific biochemical pathway in which the proteins participate. Despite a huge potential, only few applications of the PCA in bacteria were reported. In recent studies, the PCA was proposed as an alternative to phage display (Smith, 1985) or ribosome display (Hanes et al., 1998). Libraries of peptides or antibodies with the respective antigens were screened for optimized protein-protein interactions (Mossner et al., 2001; Nord et al., 2005; Pelletier et al., 1999). The peptides or antibodies were fused to the reporter enzyme fragments and co-transformed in bacteria. Interaction of the studied proteins lead to complementation of the functional reporter enzyme that was either monitored by the ability of the bacteria to grow or in addition by the hydrolysis of CCF2/AM (Nord et al., 2005). This application allows screening of large libraries with little effort and in a reasonable time. One important advantage of the system is that, unlike in phage display, the antigens do not have to be expressed and purified, but successful complementation is monitored *in situ*.

To our knowledge our work represents the first trial to set up a PCA based inhibitor screen for a defined protein-protein interaction using purified proteins. Such a setting

applies the PCA in a cheap, easy and small scale bacterial expression system, however, the constructs can also be used in the more sophisticated, natural, eukaryotic background. Such an integrated approach combines the advantages of both areas of application.

The Bla-tagged UL50 and UL53 of HCMV were expressed in bacteria and purified by the introduced C-terminal His-tag. The N-terminal Bla fragment was fused to the His-tagged UL50 fragment, which was in the previous experiment used for isolated or co-expression. The C-terminal Bla fragment was fused to a fragment of UL53, covering the first 129 amino acids of the wt protein. This fragment included the 73 amino acid fragment (UL53\_2), used for the co-expression experiment, and the variable region of UL53. The thereby larger size of the expressed protein was assumed to stabilize the protein during expression in bacteria, which was in the co-expression experiment mediated by UL50\_His. The additionally included residues should furthermore assure the accessibility of the Bla fragments upon interaction of the HCMV proteins.

The Bla-tagged proteins successfully interacted in the PCA when the purified proteins were mixed. The Bla activity measured for the interaction was more than 30 times higher than the background, which was defined by the Bla activity in the purified samples tested separately. Contrary to expectations, the background was low and comparable to the background seen in mock transfected cells in the cell based PCA. Bacterial lactamases did not co-purify with the Bla-tagged proteins. The interaction of the Bla-tagged proteins was shown to be specific since the signal was gradually reduced by increasing amounts of non-tagged UL50 in the assay. Furthermore, Bla activity was not reconstituted when the tagged UL53 construct was mixed with a Bla-tagged mutant of UL50, constructed on the basis of the well studied HCMV homologue M50DM, deficient in binding to M53 (Bubeck et al., 2004). The lack of signal was not due to inefficient purification of the UL50 mutant, as the protein detection in the Western Blot and Coomassie stained gels revealed. These experiments built the basis of a high-throughput screen for inhibitors of the essential interaction of UL50 and UL53. Purified proteins can be mixed and potential inhibitors added. Subsequent addition of the Bla substrate, nitrocefin, would then allow the inhibition of the interaction of UL50 and UL53 to be measured by detection of a simple colour change. Protein purified from 2,5 l of bacterial culture would enable a minimum of 100 assays to be performed with low expense. The bacterial system allows rapid production of large amounts of proteins and does not de-

pend on the transfection of cells, which is only one of the variables in a cell culture system. For a high-throughput screen, the protein yield and storage conditions of the purified samples have to be further improved, however, already the middle-sized scale of the *in vitro* NEC-PCA might serve as proof of principle for a new platform for drug discovery. Once a promising inhibitor is detected by the cell free high-throughput screen, compounds might be tested in the context of viral replication using the Bla-tagged NEC proteins. For that, a virus mutant could be generated where both N-M50 and C-M53 (or the HCMV homologues) replace the native proteins in the same virus. Thus an MCMV mutant, which is deficient for both the native M50 and M53, but complemented by the Bla fusions would fully integrate the PCA in the virus context. Using the native promoters, a detailed study of the time scale of interaction could be performed. Potential inhibitors can be tested directly for their effect on the essential M50/M53 (or UL50/UL53) interaction, excluding side effects by an unspecific inhibition of cellular or viral processes.

### **7.6. The potential of the NEC-PCA**

The PCA was established for the UL34 and UL31 protein families. As discussed above, future applications might be the evaluation of other viral proteins in regard of analysis and localization of binding sites. Conserved proteins will be of particular interest since they might be functionally replaced in related herpesviruses that infect animals, which serve as models of infection.

The study of chimeric UL31 proteins produced a dominant negative protein, MP. In future, the shuffling of domains in interacting proteins assayed by the PCA would not only allow the localization of the binding domain, but also enable directed construction of DN proteins for the evaluation of other unknown protein functions.

The Bla-PCA can also be applied as a validating tool for hypothetical interactions. As more protein-protein interactions are detected, more comprehensive interaction maps are constructed, the so called interactomes. The PCA could be applied to validate suggested interactions of the interactomes (Uetz et al., 2006).

Here, the cell free PCA was established for the HCMV proteins UL50 and UL53. The set up was shown to be easy and cost effective and proteins successfully interacted when combined after separate expression and purification. It is now possible, with little effort, to rapidly screen small inhibitors for an effect on the HCMV NEC interaction.

---

## 8. References

1. Adler, H., M.Messerle, M.Wagner, and U.H.Koszinowski. 2000. Cloning and mutagenesis of the murine gammaherpesvirus 68 genome as an infectious bacterial artificial chromosome. *J Virol* 74:6964-6974.
2. Akanitapichat, P., C.T.Lowden, and K.F.Bastow. 2000. 1,3-Dihydroxyacridone derivatives as inhibitors of herpes virus replication. *Antiviral Res.* 45:123-134.
3. Anand, K., J.Ziebuhr, P.Wadhvani, J.R.Mesters, and R.Hilgenfeld. 2003. Coronavirus main proteinase (3CLpro) structure: basis for design of anti-SARS drugs. *Science* 300:1763-1767.
4. Appleton, B.A., J.Brooks, A.Loregian, D.J.Filman, D.M.Coen, and J.M.Hogle. 2006. Crystal structure of the cytomegalovirus DNA polymerase subunit UL44 in complex with the C terminus from the catalytic subunit. Differences in structure and function relative to unliganded UL44. *J Biol. Chem.* 281:5224-5232.
5. Archakov, A.I., V.M.Govorun, A.V.Dubanov, Y.D.Ivanov, A.V.Veselovsky, P.Lewi, and P.Janssen. 2003. Protein-protein interactions as a target for drugs in proteomics. *Proteomics.* 3:380-391.
6. Ben Porat, T., R.A.Veach, and S.Ihara. 1983. Localization of the regions of homology between the genomes of herpes simplex virus, type 1, and pseudorabies virus. *Virology* 127:194-204.
7. Benton, M.J. 1997. *In Vertebrate Palaeontology*. Chapman and Hall, London.
8. Bernard, J. and A.Mercier. 1993. Sequence of two Eco RI fragments from Salmonis herpesvirus 2 and comparison with Ictalurid herpesvirus 1. *Arch. Virol* 132:437-442.
9. Betz, U.A., R.Fischer, G.Kleymann, M.Hendrix, and H.Rubsamen-Waigmann. 2002. Potent in vivo antiviral activity of the herpes simplex virus primase-helicase inhibitor BAY 57-1293. *Antimicrob. Agents Chemother.* 46:1766-1772.
10. Biron, K.K., R.J.Harvey, S.C.Chamberlain, S.S.Good, A.A.Smith, III, M.G.Davis, C.L.Talarico, W.H.Miller, R.Ferris, R.E.Dornsife, S.C.Stanat, J.C.Drach, L.B.Townsend, and G.W.Koszalka. 2002. Potent and selective inhibition of human cytomegalovirus replication by 1263W94, a benzimidazole L-riboside with a unique mode of action. *Antimicrob. Agents Chemother.* 46:2365-2372.
11. Blakely, B.T., F.M.Rossi, B.Tillotson, M.Palmer, A.Estelles, and H.M.Blau. 2000. Epidermal growth factor receptor dimerization monitored in live cells. *Nat. Biotechnol.* 18:218-222.
12. Booy, F.P., B.L.Trus, A.J.Davison, and A.C.Steven. 1996. The capsid architecture of channel catfish virus, an evolutionarily distant herpesvirus, is largely conserved in the absence of discernible sequence homology with herpes simplex virus. *Virology* 215:134-141.

## References

---

13. Borst, E.M., G.Hahn, U.H.Koszinowski, and M.Messerle. 1999. Cloning of the human cytomegalovirus (HCMV) genome as an infectious bacterial artificial chromosome in *Escherichia coli*: a new approach for construction of HCMV mutants. *J Virol* 73:8320-8329.
14. Bresnahan, W.A., I.Boldogh, P.Chi, E.A.Thompson, and T.Albrecht. 1997. Inhibition of cellular Cdk2 activity blocks human cytomegalovirus replication. *Virology* 231:239-247.
15. Bresnahan, W.A. and T.Shenk. 2000. A subset of viral transcripts packaged within human cytomegalovirus particles. *Science* 288:2373-2376.
16. Brideau, R.J., M.L.Knechtel, A.Huang, V.A.Vaillancourt, E.E.Vera, N.L.Oien, T.A.Hopkins, J.L.Wieber, K.F.Wilkinson, B.D.Rush, F.J.Schwende, and M.W.Wathen. 2002. Broad-spectrum antiviral activity of PNU-183792, a 4-oxo-dihydroquinoline, against human and animal herpesviruses. *Antiviral Res.* 54:19-28.
17. Brody, A.R. and J.E.Craighead. 1974. Pathogenesis of pulmonary cytomegalovirus infection in immunosuppressed mice. *J Infect. Dis.* 129:677-689.
18. Brown, E.J., M.W.Albers, T.B.Shin, K.Ichikawa, C.T.Keith, W.S.Lane, and S.L.Schreiber. 1994. A mammalian protein targeted by G1-arresting rapamycin-receptor complex. *Nature* 369:756-758.
19. Bubeck, A., M.Wagner, Z.Ruzsics, M.Lotzerich, M.Iglesias, I.R.Singh, and U.H.Koszinowski. 2004. Comprehensive mutational analysis of a herpesvirus gene in the viral genome context reveals a region essential for virus replication. *J Virol* 78:8026-8035.
20. Bubic, I., M.Wagner, A.Krmpotic, T.Saulig, S.Kim, W.M.Yokoyama, S.Jonjic, and U.H.Koszinowski. 2004. Gain of virulence caused by loss of a gene in murine cytomegalovirus. *J Virol* 78:7536-7544.
21. Carfi, A., S.H.Willis, J.C.Whitbeck, C.Krummenacher, G.H.Cohen, R.J.Eisenberg, and D.C.Wiley. 2001. Herpes simplex virus glycoprotein D bound to the human receptor HveA. *Mol. Cell* 8:169-179.
22. Chee, M.S., A.T.Bankier, S.Beck, R.Bohni, C.M.Brown, R.Cerny, T.Horsnell, C.A.Hutchison, III, T.Kouzarides, J.A.Martignetti, and . 1990. Analysis of the protein-coding content of the sequence of human cytomegalovirus strain AD169. *Curr. Top. Microbiol. Immunol.* 154:125-169.
23. Chee, M.S., G.L.Lawrence, and B.G.Barrell. 1989. Alpha-, beta- and gamma-herpesviruses encode a putative phosphotransferase. *J Gen Virol* 70 ( Pt 5):1151-1160.
24. Cherepanov, P.P. and W.Wackernagel. 1995. Gene disruption in *Escherichia coli*: TcR and KmR cassettes with the option of F1p-catalyzed excision of the antibiotic-resistance determinant. *Gene* 158:9-14.



## References

---

25. Chrisp, P. and S.P.Clissold. 1991. Foscarnet. A review of its antiviral activity, pharmacokinetic properties and therapeutic use in immunocompromised patients with cytomegalovirus retinitis. *Drugs* 41:104-129.
26. Coen, D.M. and P.A.Schaffer. 2003. Antiherpesvirus drugs: a promising spectrum of new drugs and drug targets. *Nat. Rev. Drug Discov.* 2:278-288.
27. Cohen, E.A., P.Gaudreau, P.Brazeau, and Y.Langelier. 1986. Specific inhibition of herpesvirus ribonucleotide reductase by a nonapeptide derived from the carboxy terminus of subunit 2. *Nature* 321:441-443.
28. Compton, T., D.M.Nowlin, and N.R.Cooper. 1993. Initiation of human cytomegalovirus infection requires initial interaction with cell surface heparan sulfate. *Virology* 193:834-841.
29. Cooper, L. and R.Longnecker. 2002. Inhibition of host kinase activity altered by the LMP2A signalosome-a therapeutic target for Epstein-Barr virus latency and associated disease. *Antiviral Res.* 56:219-231.
30. Coulter, L.J., H.W.Moss, J.Lang, and D.J.McGeoch. 1993. A mutant of herpes simplex virus type 1 in which the UL13 protein kinase gene is disrupted. *J Gen Virol* 74 ( Pt 3):387-395.
31. Crute, J.J., C.A.Grygon, K.D.Hargrave, B.Simoneau, A.M.Faucher, G.Bolger, P.Kibler, M.Liuzzi, and M.G.Cordingley. 2002. Herpes simplex virus helicase-primase inhibitors are active in animal models of human disease. *Nat. Med.* 8:386-391.
32. Dale, G.E., C.Oefner, and A.D'Arcy. 2003. The protein as a variable in protein crystallization. *J Struct. Biol.* 142:88-97.
33. Dandliker, W.B., M.L.Hsu, J.Levin, and B.R.Rao. 1981. Equilibrium and kinetic inhibition assays based upon fluorescence polarization. *Methods Enzymol.* 74 Pt C:3-28.
34. Davison, A.J. 1992. Channel catfish virus: a new type of herpesvirus. *Virology* 186:9-14.
35. Davison, A.J. 1998. The genome of salmonid herpesvirus 1. *J Virol* 72:1974-1982.
36. Davison, A.J. 2002. Evolution of the herpesviruses. *Vet. Microbiol.* 86:69-88.
37. Davison, A.J., W.Sauerbier, A.Dolan, C.Addison, and R.G.McKinnell. 1999. Genomic studies of the Lucke tumor herpesvirus (RaHV-1). *J Cancer Res. Clin. Oncol.* 125:232-238.
38. Davison, A.J. and N.M.Wilkie. 1983. Either orientation of the L segment of the herpes simplex virus genome may participate in the production of viable intertypic recombinants. *J Gen Virol* 64 (Pt 1):247-250.

## References

---

39. De Clercq, E. and A.Holy. 2005. Acyclic nucleoside phosphonates: a key class of antiviral drugs. *Nat. Rev. Drug Discov.* 4:928-940.
40. De, S., O.Krishnadev, N.Srinivasan, and N.Rekha. 2005. Interaction preferences across protein-protein interfaces of obligatory and non-obligatory components are different. *BMC. Struct. Biol.* 5:15.
41. Delecluse, H.J., T.Hilsendegen, D.Pich, R.Zeidler, and W.Hammerschmidt. 1998. Propagation and recovery of intact, infectious Epstein-Barr virus from prokaryotic to human cells. *Proc Natl Acad Sci U S A* 95:8245-8250.
42. DeLucas, L.J., T.L.Bray, L.Nagy, D.McCombs, N.Chernov, D.Hamrick, L.Cosenza, A.Belgovskiy, B.Stoops, and A.Chait. 2003. Efficient protein crystallization. *J Struct. Biol.* 142:188-206.
43. Dirnberger, D., G.Unsin, S.Schlenker, and C.Reichel. 2006. A small-molecule-protein interaction system with split-ubiquitin as sensor. *Chembiochem.* 7:936-942.
44. Drees, B.L. 1999. Progress and variations in two-hybrid and three-hybrid technologies. *Curr. Opin. Chem. Biol.* 3:64-70.
45. Dutia, B.M., M.C.Frame, J.H.Subak-Sharpe, W.N.Clark, and H.S.Marsden. 1986. Specific inhibition of herpesvirus ribonucleotide reductase by synthetic peptides. *Nature* 321:439-441.
46. Fields, S. and O.Song. 1989. A novel genetic system to detect protein-protein interactions. *Nature* 340:245-246.
47. Fruehling, S. and R.Longnecker. 1997. The immunoreceptor tyrosine-based activation motif of Epstein-Barr virus LMP2A is essential for blocking BCR-mediated signal transduction. *Virology* 235:241-251.
48. Fuchs, W., B.G.Klupp, H.Granzow, N.Osterrieder, and T.C.Mettenleiter. 2002. The interacting UL31 and UL34 gene products of pseudorabies virus are involved in egress from the host-cell nucleus and represent components of primary enveloped but not mature virions. *J Virol* 76:364-378.
49. Galarneau, A., M.Primeau, L.E.Trudeau, and S.W.Michnick. 2002. Beta-lactamase protein fragment complementation assays as in vivo and in vitro sensors of protein protein interactions. *Nat. Biotechnol.* 20:619-622.
50. Geahlen, R.L. and J.L.McLaughlin. 1989. Piceatannol (3,4,3',5'-tetrahydroxy-trans-stilbene) is a naturally occurring protein-tyrosine kinase inhibitor. *Biochem. Biophys. Res. Commun.* 165:241-245.
51. Gershon, A.A., D.L.Sherman, Z.Zhu, C.A.Gabel, R.T.Ambron, and M.D.Gershon. 1994. Intracellular transport of newly synthesized varicella-zoster virus: final envelopment in the trans-Golgi network. *J Virol* 68:6372-6390.

## References

---

52. Ghosh, I., A.D.Hamilton, and L.Regan. 2000. Antiparallel Leucine Zipper-Directed Protein Reassembly: Application to the Green Fluorescent Protein. *J Am. Chem. Soc.* 127.
53. Godowski, P.J. and D.M.Knipe. 1986. Transcriptional control of herpesvirus gene expression: gene functions required for positive and negative regulation. *Proc Natl Acad Sci U S A* 83:256-260.
54. Goldmacher, V.S. 2005. Cell death suppression by cytomegaloviruses. *Apoptosis.* 10:251-265.
55. Goldmacher, V.S., L.M.Bartle, A.Skaletskaya, C.A.Dionne, N.L.Kedersha, C.A.Vater, J.W.Han, R.J.Lutz, S.Watanabe, E.D.Cahir McFarland, E.D.Kieff, E.S.Mocarski, and T.Chittenden. 1999. A cytomegalovirus-encoded mitochondria-localized inhibitor of apoptosis structurally unrelated to Bcl-2. *Proc Natl Acad Sci U S A* 96:12536-12541.
56. Gonnella, R., A.Farina, R.Santarelli, S.Raffa, R.Feederle, R.Bei, M.Granato, A.Modesti, L.Frati, H.J.Delecluse, M.R.Torrise, A.Angeloni, and A.Faggioni. 2005. Characterization and intracellular localization of the Epstein-Barr virus protein BFLF2: interactions with BFRF1 and with the nuclear lamina. *J Virol* 79:3713-3727.
57. Greijer, A.E., C.A.Dekkers, and J.M.Middeldorp. 2000. Human cytomegalovirus virions differentially incorporate viral and host cell RNA during the assembly process. *J Virol* 74:9078-9082.
58. Hahn, G., M.G.Revello, M.Patrone, E.Percivalle, G.Campanini, A.Sarasini, M.Wagner, A.Gallina, G.Milanesi, U.Koszinowski, F.Baldanti, and G.Gerna. 2004. Human cytomegalovirus UL131-128 genes are indispensable for virus growth in endothelial cells and virus transfer to leukocytes. *J Virol* 78:10023-10033.
59. Hanes, J., L.Jermutus, S.Weber-Bornhauser, H.R.Bosshard, and A.Pluckthun. 1998. Ribosome display efficiently selects and evolves high-affinity antibodies in vitro from immune libraries. *Proc Natl Acad Sci U S A* 95:14130-14135.
60. Henderson, S., D.Huen, M.Rowe, C.Dawson, G.Johnson, and A.Rickinson. 1993. Epstein-Barr virus-coded BHRF1 protein, a viral homologue of Bcl-2, protects human B cells from programmed cell death. *Proc Natl Acad Sci U S A* 90:8479-8483.
61. Ho, M. 1982. Cytomegalovirus: biology and infection. Plenum Press.
62. Honess, R.W. and B.Roizman. 1975. Regulation of herpesvirus macromolecular synthesis: sequential transition of polypeptide synthesis requires functional viral polypeptides. *Proc Natl Acad Sci U S A* 72:1276-1280.
63. Hu, C.D., Y.Chinenov, and T.K.Kerppola. 2002. Visualization of interactions among bZIP and Rel family proteins in living cells using bimolecular fluorescence complementation. *Mol. Cell* 9:789-798.

## References

---

64. Hudson, J.B. 1979. The murine cytomegalovirus as a model for the study of viral pathogenesis and persistent infections. *Arch. Virol* 62:1-29.
65. Jault, F.M., J.M.Jault, F.Ruchti, E.A.Fortunato, C.Clark, J.Corbeil, D.D.Richman, and D.H.Spector. 1995. Cytomegalovirus infection induces high levels of cyclins, phosphorylated Rb, and p53, leading to cell cycle arrest. *J Virol* 69:6697-6704.
66. Jelsch, C., L.Mourey, J.M.Masson, and J.P.Samama. 1993. Crystal structure of Escherichia coli TEM1 beta-lactamase at 1.8 Å resolution. *Proteins* 16:364-383.
67. Johnsson, N. and A.Varshavsky. 1994. Split ubiquitin as a sensor of protein interactions in vivo. *Proc Natl Acad Sci U S A* 91:10340-10344.
68. Jordan, M. 1991. Murine models of cytomegalovirus latency. Stevens JG, et al., 805-810.
69. Kadonaga, J.T., A.E.Gautier, D.R.Straus, A.D.Charles, M.D.Edge, and J.R.Knowles. 1984. The role of the beta-lactamase signal sequence in the secretion of proteins by Escherichia coli. *J Biol. Chem.* 259:2149-2154.
70. Karlin, S., E.S.Mocarski, and G.A.Schachtel. 1994. Molecular evolution of herpesviruses: genomic and protein sequence comparisons. *J Virol* 68:1886-1902.
71. Kleymann, G., R.Fischer, U.A.Betz, M.Hendrix, W.Bender, U.Schneider, G.Handke, P.Eckenberg, G.Hewlett, V.Pevzner, J.Baumeister, O.Weber, K.Henninger, J.Keldenich, A.Jensen, J.Kolb, U.Bach, A.Popp, J.Maben, I.Frappa, D.Haebich, O.Lockhoff, and H.Rubsamen-Waigmann. 2002. New helicase-primase inhibitors as drug candidates for the treatment of herpes simplex disease. *Nat. Med.* 8:392-398.
72. Kolter, R., M.Inuzuka, and D.R.Helinski. 1978. Trans-complementation-dependent replication of a low molecular weight origin fragment from plasmid R6K. *Cell* 15:1199-1208.
73. Kovari, L.C., C.Momany, and M.G.Rossmann. 1995. The use of antibody fragments for crystallization and structure determinations. *Structure* 3:1291-1293.
74. Krosky, P.M., M.C.Baek, and D.M.Coen. 2003. The human cytomegalovirus UL97 protein kinase, an antiviral drug target, is required at the stage of nuclear egress. *J Virol* 77:905-914.
75. Krosky, P.M., K.Z.Borysko, M.R.Nassiri, R.V.Devivar, R.G.Ptak, M.G.Davis, K.K.Biron, L.B.Townsend, and J.C.Drach. 2002. Phosphorylation of beta-D-riboseylbenzimidazoles is not required for activity against human cytomegalovirus. *Antimicrob. Agents Chemother.* 46:478-486.
76. Kumar, S. and S.B.Hedges. 1998. A molecular timescale for vertebrate evolution. *Nature* 392:917-920.

## References

---

77. Lake, C.M. and L.M.Hutt-Fletcher. 2004. The Epstein-Barr virus BFRF1 and BFLF2 proteins interact and coexpression alters their cellular localization. *Virology* 320:99-106.
78. Liang, L. and J.D.Baines. 2005. Identification of an essential domain in the herpes simplex virus 1 UL34 protein that is necessary and sufficient to interact with UL31 protein. *J Virol* 79:3797-3806.
79. Licitra, E.J. and J.O.Liu. 1996. A three-hybrid system for detecting small ligand-protein receptor interactions. *Proc Natl Acad Sci U S A* 93:12817-12821.
80. Loregian, A. and D.M.Coen. 2006. Selective anti-cytomegalovirus compounds discovered by screening for inhibitors of subunit interactions of the viral polymerase. *Chem. Biol.* 13:191-200.
81. Loregian, A., H.S.Marsden, and G.Palu. 2002. Protein-protein interactions as targets for antiviral chemotherapy. *Rev. Med. Virol* 12:239-262.
82. Loregian, A. and G.Palu. 2005. Disruption of the interactions between the subunits of herpesvirus DNA polymerases as a novel antiviral strategy. *Clin. Microbiol. Infect.* 11:437-446.
83. Loregian, A., R.Rigatti, M.Murphy, E.Schievano, G.Palu, and H.S.Marsden. 2003. Inhibition of human cytomegalovirus DNA polymerase by C-terminal peptides from the UL54 subunit. *J Virol* 77:8336-8344.
84. Lötzerich, M., Z.Ruzsics, and U.H.Koszinowski. 2006. Functional Domains of Murine Cytomegalovirus Nuclear Egress Protein M53/p38. *J Virol* 80:73-84.
85. Luker, K.E., M.C.Smith, G.D.Luker, S.T.Gammon, H.Piwnicka-Worms, and D.Piwnicka-Worms. 2004. Kinetics of regulated protein-protein interactions revealed with firefly luciferase complementation imaging in cells and living animals. *Proc Natl Acad Sci U S A* 101:12288-12293.
86. Magliery, T.J., C.G.Wilson, W.Pan, D.Mishler, I.Ghosh, A.D.Hamilton, and L.Regan. 2005. Detecting protein-protein interactions with a green fluorescent protein fragment reassembly trap: scope and mechanism. *J Am. Chem. Soc.* 127:146-157.
87. Marshall, W.L., C.Yim, E.Gustafson, T.Graf, D.R.Sage, K.Hanify, L.Williams, J.Fingerroth, and R.W.Finberg. 1999. Epstein-Barr virus encodes a novel homolog of the bcl-2 oncogene that inhibits apoptosis and associates with Bax and Bak. *J Virol* 73:5181-5185.
88. Mayo, D.R., J.A.Armstrong, and M.Ho. 1977. Reactivation of murine cytomegalovirus by cyclophosphamide. *Nature* 267:721-723.
89. McGeoch, D.J., S.Cook, A.Dolan, F.E.Jamieson, and E.A.Telford. 1995. Molecular phylogeny and evolutionary timescale for the family of mammalian herpesviruses. *J Mol. Biol.* 247:443-458.

## References

---

90. McGeoch, D.J., D.Gatherer, and A.Dolan. 2005. On phylogenetic relationships among major lineages of the Gammaherpesvirinae. *J Gen Virol* 86:307-316.
91. McGeoch, D.J., F.J.Rixon, and A.J.Davison. 2006. Topics in herpesvirus genomics and evolution. *Virus Res.* 117:90-104.
92. McGeoch, D.J.D.A.J. 1999. The molecular evolutionary history of the herpesviruses. In *Origin and Evolution of Viruses*. Domingo E. and R.H.J.Webster, editors. Academic Press, London. 441-465.
93. McLeod, M., S.Craft, and J.R.Broach. 1986. Identification of the crossover site during FLP-mediated recombination in the *Saccharomyces cerevisiae* plasmid 2 microns circle. *Mol. Cell Biol.* 6:3357-3367.
94. McPherson, A., Jr. 1976. Crystallization of proteins from polyethylene glycol. *J Biol. Chem.* 251:6300-6303.
95. Meijer, L., A.Borgne, O.Mulner, J.P.Chong, J.J.Blow, N.Inagaki, M.Inagaki, J.G.Delcros, and J.P.Moulinoux. 1997. Biochemical and cellular effects of roscovitine, a potent and selective inhibitor of the cyclin-dependent kinases cdc2, cdk2 and cdk5. *Eur. J Biochem.* 243:527-536.
96. Merchant, M., R.G.Caldwell, and R.Longnecker. 2000. The LMP2A ITAM is essential for providing B cells with development and survival signals in vivo. *J Virol* 74:9115-9124.
97. Messerle, M., I.Crnkovic, W.Hammerschmidt, H.Ziegler, and U.H.Koszinowski. 1997. Cloning and mutagenesis of a herpesvirus genome as an infectious bacterial artificial chromosome. *Proc Natl Acad Sci U S A* 94:14759-14763.
98. Mettenleiter, T.C. 2002. Herpesvirus assembly and egress. *J Virol* 76:1537-1547.
99. Michel, D., S.Kramer, S.Hohn, P.Schaarschmidt, K.Wunderlich, and T.Mertens. 1999. Amino acids of conserved kinase motifs of cytomegalovirus protein UL97 are essential for autophosphorylation. *J Virol* 73:8898-8901.
100. Michnick, S.W. 2003. Protein fragment complementation strategies for biochemical network mapping. *Curr. Opin. Biotechnol.* 14:610-617.
101. Miller, C.L., A.L.Burkhardt, J.H.Lee, B.Stealey, R.Longnecker, J.B.Bolen, and E.Kieff. 1995. Integral membrane protein 2 of Epstein-Barr virus regulates reactivation from latency through dominant negative effects on protein-tyrosine kinases. *Immunity* 2:155-166.
102. Miller, V.L. and J.J.Mekalanos. 1988. A novel suicide vector and its use in construction of insertion mutations: osmoregulation of outer membrane proteins and virulence determinants in *Vibrio cholerae* requires toxR. *J Bacteriol.* 170:2575-2583.

## References

---

103. Mocarski, E.S., Tan Courcelle J., and Tan Courcelle C. 2001. Cytomegaloviruses and their replication. *In* Fields Virology. D.M.Knipe and P.M.Howley, editors. Lippincott Williams & Wilkins, 2301-2326.
104. Moore, J.T., S.T.Davis, and I.K.Dev. 1997. The development of beta-lactamase as a highly versatile genetic reporter for eukaryotic cells. *Anal. Biochem.* 247:203-209.
105. Mossner, E., H.Koch, and A.Pluckthun. 2001. Fast selection of antibodies without antigen purification: adaptation of the protein fragment complementation assay to select antigen-antibody pairs. *J Mol. Biol.* 308:115-122.
106. Muranyi, W., J.Haas, M.Wagner, G.Krohne, and U.H.Koszinowski. 2002. Cytomegalovirus recruitment of cellular kinases to dissolve the nuclear lamina. *Science* 297:854-857.
107. Neubauer, A., J.Rudolph, C.Brandmuller, F.T.Just, and N.Osterrieder. 2002. The equine herpesvirus 1 UL34 gene product is involved in an early step in virus egress and can be efficiently replaced by a UL34-GFP fusion protein. *Virology* 300:189-204.
108. Newcomb, W.W. and J.C.Brown. 2002. Inhibition of herpes simplex virus replication by WAY-150138: assembly of capsids depleted of the portal and terminase proteins involved in DNA encapsidation. *J Virol* 76:10084-10088.
109. Ng, T.I., C.Talarico, T.C.Burnette, K.Biron, and B.Roizman. 1996. Partial substitution of the functions of the herpes simplex virus 1 U(L)13 gene by the human cytomegalovirus U(L)97 gene. *Virology* 225:347-358.
110. Nord, O., A.Gustrin, and P.A.Nygren. 2005. Fluorescent detection of beta-lactamase activity in living Escherichia coli cells via esterase supplementation. *FEMS Microbiol. Lett.* 242:73-79.
111. Nyfeler, B., S.W.Michnick, and H.P.Hauri. 2005. Capturing protein interactions in the secretory pathway of living cells. *Proc Natl Acad Sci U S A* 102:6350-6355.
112. O'Callaghan, C.H., A.Morris, S.M.Kirby, and A.H.Shingler. 1972. Novel method for detection of beta-lactamases by using a chromogenic cephalosporin substrate. *Antimicrob. Agents Chemother.* 1:283-288.
113. Oien, N.L., R.J.Brideau, T.A.Hopkins, J.L.Wieber, M.L.Knechtel, J.A.Shelly, R.A.Anstadt, P.A.Wells, R.A.Poorman, A.Huang, V.A.Vaillancourt, T.L.Clayton, J.A.Tucker, and M.W.Wathen. 2002. Broad-spectrum antiherpes activities of 4-hydroxyquinoline carboxamides, a novel class of herpesvirus polymerase inhibitors. *Antimicrob. Agents Chemother.* 46:724-730.

## References

---

114. Orozco-Topete, R., J.Sierra-Madero, C.Cano-Dominguez, J.Kershenovich, G.Ortiz-Pedroza, E.Vazquez-Valls, C.Garcia-Cosio, A.Soria-Cordoba, A.M.Armendariz, X.Teran-Toledo, J.Romo-Garcia, H.Fernandez, and E.J.Rozhon. 1997. Safety and efficacy of Virend for topical treatment of genital and anal herpes simplex lesions in patients with AIDS. *Antiviral Res.* 35:91-103.
115. Paulmurugan, R., Y.Umezawa, and S.S.Gambhir. 2002. Noninvasive imaging of protein-protein interactions in living subjects by using reporter protein complementation and reconstitution strategies. *Proc Natl Acad Sci U S A* 99:15608-15613.
116. Pelletier, J.N., K.M.Arndt, A.Pluckthun, and S.W.Michnick. 1999. An in vivo library-versus-library selection of optimized protein-protein interactions. *Nat. Biotechnol.* 17:683-690.
117. Pertel, P.E. and P.G.Spear. 1996. Modified entry and syncytium formation by herpes simplex virus type 1 mutants selected for resistance to heparin inhibition. *Virology* 226:22-33.
118. Philippon, A., J.Dusart, B.Joris, and J.M.Frere. 1998. The diversity, structure and regulation of beta-lactamases. *Cell Mol. Life Sci* 54:341-346.
119. Piehler, J. 2005. New methodologies for measuring protein interactions in vivo and in vitro. *Curr. Opin. Struct. Biol.* 15:4-14.
120. Poole, L.J., J.C.Zong, D.M.Ciufo, D.J.Alcendor, J.S.Cannon, R.Ambinder, J.M.Orenstein, M.S.Reitz, and G.S.Hayward. 1999. Comparison of genetic variability at multiple loci across the genomes of the major subtypes of Kaposi's sarcoma-associated herpesvirus reveals evidence for recombination and for two distinct types of open reading frame K15 alleles at the right-hand end. *J Virol* 73:6646-6660.
121. Prichard, M.N., M.E.Penfold, G.M.Duke, R.R.Spaete, and G.W.Kemble. 2001. A review of genetic differences between limited and extensively passaged human cytomegalovirus strains. *Rev. Med. Virol* 11:191-200.
122. Prusoff, W.H. 1959. Synthesis and biological activities of iododeoxyuridine, an analog of thymidine. *Biochim. Biophys. Acta* 32:295-296.
123. Puig, O., F.Caspary, G.Rigaut, B.Rutz, E.Bouveret, E.Bragado-Nilsson, M.Wilm, and B.Seraphin. 2001. The tandem affinity purification (TAP) method: a general procedure of protein complex purification. *Methods* 24:218-229.
124. Radsak, K., M.Eickmann, T.Mockenhaupt, E.Bogner, H.Kern, A.Eis-Hubinger, and M.Reschke. 1996. Retrieval of human cytomegalovirus glycoprotein B from the infected cell surface for virus envelopment. *Arch. Virol* 141:557-572.
125. Rawlinson, W.D., H.E.Farrell, and B.G.Barrell. 1996. Analysis of the complete DNA sequence of murine cytomegalovirus. *J Virol* 70:8833-8849.



## References

---

126. Rawlinson, W.D., F.Zeng, H.E.Farrell, A.L.Cunningham, A.A.Scalzo, T.W.Booth, and G.M.Scott. 1997. The murine cytomegalovirus (MCMV) homolog of the HCMV phosphotransferase (UL97(pk)) gene. *Virology* 233:358-363.
127. Reddehase, M.J., F.Weiland, K.Munch, S.Jonjic, A.Luske, and U.H.Koszinowski. 1985. Interstitial murine cytomegalovirus pneumonia after irradiation: characterization of cells that limit viral replication during established infection of the lungs. *J Virol* 55:264-273.
128. Remy, I. and S.W.Michnick. 2004. A cDNA library functional screening strategy based on fluorescent protein complementation assays to identify novel components of signaling pathways. *Methods* 32:381-388.
129. Remy, I., I.A.Wilson, and S.W.Michnick. 1999. Erythropoietin receptor activation by a ligand-induced conformation change. *Science* 283:990-993.
130. Reschke, M. Detailed 2d model of HCMV. 1994. Institute of Virology, University of Marburg, Germany.
131. Reynolds, A.E., B.J.Ryckman, J.D.Baines, Y.Zhou, L.Liang, and R.J.Roller. 2001. U(L)31 and U(L)34 proteins of herpes simplex virus type 1 form a complex that accumulates at the nuclear rim and is required for envelopment of nucleocapsids. *J Virol* 75:8803-8817.
132. Rickinson, A.B. and E.Kieff. 2001. Epstein-Barr Virus. *In* Fields Virology. D.M.Knipe and P.M.Howley, editors. Lippincott Williams & Wilkins, 2575-2627.
133. Rigaut, G., A.Shevchenko, B.Rutz, M.Wilm, M.Mann, and B.Seraphin. 1999. A generic protein purification method for protein complex characterization and proteome exploration. *Nat. Biotechnol.* 17:1030-1032.
134. Roizman, B. and P.E.Pellett. 2001. The family of herpesviridae: a brief introduction. *In* Fields Virology. D.M.Knipe and P.M.Howley, editors. Lippincott Williams & Wilkins, 2301-2326.
135. Rossi, F., C.A.Charlton, and H.M.Blau. 1997. Monitoring protein-protein interactions in intact eukaryotic cells by beta-galactosidase complementation. *Proc Natl Acad Sci U S A* 94:8405-8410.
136. Rost, B. and C.Sander. 1994. Combining evolutionary information and neural networks to predict protein secondary structure. *Proteins* 19:55-72.
137. Rupp, B., Z.Ruzsics, T.Sacher, and U.H.Koszinowski. 2005. Conditional cytomegalovirus replication in vitro and in vivo. *J Virol* 79:486-494.

## References

---

138. Saeki, Y., T.Ichikawa, A.Saeki, E.A.Chiocca, K.Tobler, M.Ackermann, X.O.Breakefield, and C.Fraefel. 1998. Herpes simplex virus type 1 DNA amplified as bacterial artificial chromosome in *Escherichia coli*: rescue of replication-competent virus progeny and packaging of amplicon vectors. *Hum. Gene Ther.* 9:2787-2794.
139. Sambrook, J. and D.W.Russel. 2001. Molecular cloning - a laboratory manual. Cold Spring Harbor laboratory press, Cold Spring Harbor, New York.
140. Sanchez, V., K.D.Greis, E.Sztul, and W.J.Britt. 2000. Accumulation of virion tegument and envelope proteins in a stable cytoplasmic compartment during human cytomegalovirus replication: characterization of a potential site of virus assembly. *J Virol* 74:975-986.
141. Sarid, R., T.Sato, R.A.Bohenzky, J.J.Russo, and Y.Chang. 1997. Kaposi's sarcoma-associated herpesvirus encodes a functional bcl-2 homologue. *Nat. Med.* 3:293-298.
142. Schang, L.M., A.Bantly, M.Knockaert, F.Shaheen, L.Meijer, M.H.Malim, N.S.Gray, and P.A.Schaffer. 2002. Pharmacological cyclin-dependent kinase inhibitors inhibit replication of wild-type and drug-resistant strains of herpes simplex virus and human immunodeficiency virus type 1 by targeting cellular, not viral, proteins. *J Virol* 76:7874-7882.
143. Schang, L.M., J.Phillips, and P.A.Schaffer. 1998. Requirement for cellular cyclin-dependent kinases in herpes simplex virus replication and transcription. *J Virol* 72:5626-5637.
144. Serrano, M., A.W.Lin, M.E.McCurrach, D.Beach, and S.W.Lowe. 1997. Oncogenic ras provokes premature cell senescence associated with accumulation of p53 and p16INK4a. *Cell* 88:593-602.
145. Siminoff, P. and M.G.Menefee. 1966. Normal and 5-bromodeoxyuridine-inhibited development of herpes simplex virus. An electron microscope study. *Exp. Cell Res.* 44:241-255.
146. Smith, G.A. and L.W.Enquist. 1999. Construction and transposon mutagenesis in *Escherichia coli* of a full-length infectious clone of pseudorabies virus, an alphaherpesvirus. *J Virol* 73:6405-6414.
147. Smith, G.P. 1985. Filamentous fusion phage: novel expression vectors that display cloned antigens on the virion surface. *Science* 228:1315-1317.
148. Spector, F.C., L.Liang, H.Giordano, M.Sivaraja, and M.G.Peterson. 1998. Inhibition of herpes simplex virus replication by a 2-amino thiazole via interactions with the helicase component of the UL5-UL8-UL52 complex. *J Virol* 72:6979-6987.
149. Subramaniam, R., D.Desveaux, C.Spickler, S.W.Michnick, and N.Brisson. 2001. Direct visualization of protein interactions in plant cells. *Nat. Biotechnol.* 19:769-772.

## References

---

150. Sutcliffe, J.G. 1978. Nucleotide sequence of the ampicillin resistance gene of *Escherichia coli* plasmid pBR322. *Proc Natl Acad Sci U S A* 75:3737-3741.
151. Taylor, S.L., P.R.Kinchington, A.Brooks, and J.F.Moffat. 2004. Roscovitine, a cyclin-dependent kinase inhibitor, prevents replication of varicella-zoster virus. *J Virol* 78:2853-2862.
152. Timbury, M.C. and J.H.Subak-Sharpe. 1973. Genetic interactions between temperature-sensitive mutants of types 1 and 2 herpes simplex viruses. *J Gen Virol* 18:347-357.
153. Tomicic, M.T., E.Bey, P.Wutzler, R.Thust, and B.Kaina. 2002. Comparative analysis of DNA breakage, chromosomal aberrations and apoptosis induced by the anti-herpes purine nucleoside analogues aciclovir, ganciclovir and penciclovir. *Mutat. Res.* 505:1-11.
154. Uetz, P., Y.A.Dong, C.Zeretzke, C.Atzler, A.Baiker, B.Berger, S.V.Rajagopala, M.Roupelieva, D.Rose, E.Fossum, and J.Haas. 2006. Herpesviral protein networks and their interaction with the human proteome. *Science* 311:239-242.
155. van Zeijl, M., J.Fairhurst, T.R.Jones, S.K.Vernon, J.Morin, J.LaRocque, B.Feld, B.O'Hara, J.D.Bloom, and S.V.Johann. 2000. Novel class of thiourea compounds that inhibit herpes simplex virus type 1 DNA cleavage and encapsidation: resistance maps to the UL6 gene. *J Virol* 74:9054-9061.
156. Wagner, M., A.Gutermann, J.Podlech, M.J.Reddehase, and U.H.Koszinowski. 2002. Major histocompatibility complex class I allele-specific cooperative and competitive interactions between immune evasion proteins of cytomegalovirus. *J Exp. Med.* 196:805-816.
157. Wagner, M., S.Jonjic, U.H.Koszinowski, and M.Messerle. 1999. Systematic excision of vector sequences from the BAC-cloned herpesvirus genome during virus reconstitution. *J Virol* 73:7056-7060.
158. Wagner, M., D.Michel, P.Schaarschmidt, B.Vaida, S.Jonjic, M.Messerle, T.Mertens, and U.Koszinowski. 2000. Comparison between human cytomegalovirus pUL97 and murine cytomegalovirus (MCMV) pM97 expressed by MCMV and vaccinia virus: pM97 does not confer ganciclovir sensitivity. *J Virol* 74:10729-10736.
159. Wathen, M.W. and M.F.Stinski. 1982. Temporal patterns of human cytomegalovirus transcription: mapping the viral RNAs synthesized at immediate early, early, and late times after infection. *J Virol* 41:462-477.
160. Weber, O., W.Bender, P.Eckenberg, S.Goldmann, M.Haerter, S.Hallenberger, K.Henninger, J.Reefschlager, J.Trappe, A.Witt-Laido, and H.Ruebsamen-Waigmann. 2001. Inhibition of murine cytomegalovirus and human cytomegalovirus by a novel non-nucleosidic compound in vivo. *Antiviral Res.* 49:179-189.

## References

---

161. Wehrman, T., B.Kleaveland, J.H.Her, R.F.Balint, and H.M.Blau. 2002. Protein-protein interactions monitored in mammalian cells via complementation of beta-lactamase enzyme fragments. *Proc Natl Acad Sci U S A* 99:3469-3474.
162. Whitley, R.J. 2001. Herpes simplex viruses. *In* Fields Virology. D.M.Knipe and P.M.Howley, editors. Lippincott Williams & Wilkins, 2301-2326.
163. Wolf, D.G., C.T.Courcelle, M.N.Prichard, and E.S.Mocarski. 2001. Distinct and separate roles for herpesvirus-conserved UL97 kinase in cytomegalovirus DNA synthesis and encapsidation. *Proc Natl Acad Sci U S A* 98:1895-1900.
164. Wray, G.A.L.J.S.S.L.H. 1996. Molecular Evidence for Deep Precambrian Divergences Among Metazoan Phyla. *n* 274:568-573.
165. WuDunn, D. and P.G.Spear. 1989. Initial interaction of herpes simplex virus with cells is binding to heparan sulfate. *J Virol* 63:52-58.
166. Yamauchi, Y., C.Shiba, F.Goshima, A.Nawa, T.Murata, and Y.Nishiyama. 2001. Herpes simplex virus type 2 UL34 protein requires UL31 protein for its relocation to the internal nuclear membrane in transfected cells. *J Gen Virol* 82:1423-1428.
167. Yang, H., W.Xie, X.Xue, K.Yang, J.Ma, W.Liang, Q.Zhao, Z.Zhou, D.Pei, J.Ziebuhr, R.Hilgenfeld, K.Y.Yuen, L.Wong, G.Gao, S.Chen, Z.Chen, D.Ma, M.Bartlam, and Z.Rao. 2005. Design of wide-spectrum inhibitors targeting coronavirus main proteases. *PLoS. Biol.* 3:e324.
168. Zlokarnik, G., P.A.Negulescu, T.E.Knapp, L.Mere, N.Burres, L.Feng, M.Whitney, K.Roemer, and R.Y.Tsien. 1998. Quantitation of transcription and clonal selection of single living cells with beta-lactamase as reporter. *Science* 279:84-88.

## 9. Abbreviations

A	absorption
A	adenine
aa	amino acid
Ab	antibody
amp	ampicillin
ANOVA	analysis of variance
APS	ammonium persulfate
ATCC	American Type Culture Collection
$\beta$ -ME	$\beta$ -Mercaptoethanol
BAC	Bacterial artificial chromosome
Bla	$\beta$ -lactamase
BlaC	C-terminal part of Bla
BlaN	N-terminal part of Bla
bp	base pair
BSA	bovine serum albumin
C-	C-terminal part of the b-lactamase
C	cytosine
$^{\circ}$ C	degree Celsius
C	HCMV
cam	chloramphenicol
cm	centimeter
Co-IP	co-immuno precipitation
CR	conserved region
CV	column volumes
dd	deionized distilled
DL	detection limit
DMEM	Dulbecco's modified Eagle medium
DMSO	dimethylsulfoxid
DN	dominant negative
DNA	desoxyribonucleid Acid
DTT	1,4 dithiotreitol
E	EBV
E. coli	Escherichia coli
e.g.	exempli gratia (Lat. = for instance)
EBV	Epstein-Barr virus
EDTA	ethylenediamine tetraacetic acid
EGF	epidermal growth factor
ER	endoplasmic reticulum
et al.	et alii (Lat. = and others)
EtOH	ethanol
FCS	fetal calf serum
FLP	flippase
FRT	Flp recognition target
G	MHV68
GFP	green fluorescent protein
GST	glutathione S-transferase

## Abbreviations

---

H	HSV-1
HA	hemagglutinin –tag
HCMV	human cytomegalovirus
HSV	herpes simplex virus
IPTG	isopropyl $\beta$ -D-1-thiogalactopyranoside
kan	kanamycine
kb	kilo bases
kDa	kilodaltons
KSHV	Kaposi-sarcoma associated herpesvirus
LB	Luria-Bertani
M	MCMV
m	milli ( $10^{-3}$ )
M	mol/liter, molar
MCMV	mouse cytomegalovirus
MEF	mouse embryonic fibroblasts
MHV	murine herpes virus
min	minute(s)
ml	millilitre
mm	millimetre
mM	millimolar
MOI	multiplicity of infection
MWCO	Molecular weight cut-off
N-	N-terminal part of the $\beta$ -lactamase
NEC	nuclear egress complex
NLS	nuclear localization signal
nm	nanometer
NM	nuclear membrane
NMR	nuclear magnetic resonance
o.n.	over night
OD	optical density
ORF	open reading frame
P	PrV
p.i.	post infection
PAGE	polyacrylamide gel electrophoresis
PBS	phosphate buffered saline
PCA	protein complementation assay
PCR	polymerase chain reaction
Pen/Strep	penicillin/streptomycin
PFU	plaque forming unit
RNA	ribonucleid acid
rpm	rounds per minute
RPMI	Roswell Park Memorial Institute
RT	room temperature
S	glycine/serine spacer
s	second(s)
SDS	sodium dodecylsulfate
ST	strep-tag
Strep	streptomycin
T	thymine
Tab.	table

## Abbreviations

---

TAE	Tris-acetate-EDTA
TBST	Tris buffered saline with Tween 20
TEMED	N, N, N', N'-tetramethylenediamine
Tet	tetracyclin
TP	tegument protein
Tris	Tris(hydroxymethyl)aminomethan
U	unit(s), enzyme activity
V	Volt
V	variable region
v/v	volume/volume
VZV	Varicella-Zoster virus
w/v	weight/volume
WB	Western Blot
wt	wild type
Y2H	Yeast two-hybrid
μ	micro (10 <sup>-6</sup> )
μg	microgram
μl	microlitre
μm	micrometer
zeo	zeozin

### Amino acids

A, Ala	alanine	M, Met	methionine
C, Cys	cysteine	N, Asn	asparagine
D, Asp	aspartic acid	P, Pro	proline
E, Glu	glutamic acid	Q, Gln	glutamine
F, Phe	phenylalanine	R, Arg	arginine
G, Gly	glycine	S, Ser	serine
H, His	histidine	T, Thr	threonine
I, Ile	isoleucine	V, Val	valine
K, Lys	lysine	W, Trp	tryptophan
L, Leu	leucine	Y, Tyr	tyrosine

## **10. Acknowledgements**

First of all I want to thank Prof. Ulrich Koszinowski for the opportunity to carry out this work in his laboratory. Dr. Bettina Kempkes I want to thank for her supervision, her interest and fruitful discussions all over the time.

I want to thank my supervisor Dr. Zsolt Ruzsics for his many ideas and enthusiasm for my work, the productive discussions, his patience and his never ending list of possible solutions for problems that aroused. I further want to thank all my colleagues of the AG Koszinowski and AG Conzelmann, Heike Sperling, Mrs Stüfer and Mrs Petrovic for the good working atmosphere we had on the second floor. Simone Boos and Natalie Röder I want furthermore thank for their excellent technical assistance and Jennie Swan, Lars Dölken and Zsolt Ruzsics for reading the manuscript.

Anton Meinhart, Stephanie Bayerlein, Prof. Patrick Cramer and all other members of the AG Cramer I want to thank for the help and material for the bacterial expression and protein purification. This part of my work would not have been feasible without their ideas, patience and technical assistance.

During the thesis I was financially supported by the DFG Graduiertenkolleg “Infektion und Immunität”, thus I thank the DFG, Prof. Jürgen Heesemann and his committee for offering me this opportunity.

Furthermore I want to thank Paul Sondermeier and Jürgen Haas for providing me with plasmids and viral DNA.

I am grateful for all the occasions of scientific exchange offered to me for example by the SFB 455 “Virale Infektion und Immunmodulation”, here especially the Junior Faculty, seminars of the graduate college and the national and international congresses I was able to attend.

Finally I want to thank my family and all my friends for their support and friendship all over the time.



## 11. Supplementary information

### 11.1. List of figures

Figure 1 : Phylogenetic tree for mammalian herpesviruses.	5
Figure 2 : The herpesvirus virion.	7
Figure 3 : Herpesvirus replication.	9
Figure 4 : Similarity blots of the UL34 and UL31 protein families.	11
Figure 5 : Working model of the NEC in MCMV.	12
Figure 6 : BAC mutagenesis.	14
Figure 7 : Principle of the PCA.	24
Figure 8 : Establishment of the PCA.	60
Figure 9 : FRB and FKBP12 in the PCA.	62
Figure 10 : The MCMV proteins M50 and M53 in the PCA.	64
Figure 11 : Background of the NEC-PCA.	66
Figure 12 : Specificity of the NEC-PCA.	67
Figure 13 : Restriction pattern analysis of MCMV BAC-DNA	69
Figure 14 : Bla-fusion proteins are functional.	71
Figure 15 : Bla-fusions to members of the UL34 and UL31 family.	74
Figure 16 : The NEC-PCA with members of the UL34 and UL31 family of different viruses.	75
Figure 17 : Cross-complementation by UL31 family members.	76
Figure 18 : Cross-complementation of UL34 family members.	77
Figure 19 : BlaC-fusions to chimeric UL31 proteins.	79
Figure 20 : Mapping the binding site in M53.	81
Figure 21 : Mapping of the binding site in UL31 family members of $\alpha$ - and $\gamma$ -herpesviruses.	82
Figure 22 : Bla-fusion constructs to map the UL31 binding site in UL34 family members.	84
Figure 23 : Co-transfections of C-M53 and C-UL31 with mutants of UL34 and M50.	86
Figure 24 : Heterologous NEC protein inserted into MCMV deletion genomes.	88
Figure 25 : Heterologous NEC proteins inserted into MCMV wild type genomes.	90
Figure 26 : Chimeric NEC proteins inserted into the $\Delta$ M53-BAC.	92
Figure 27 : Chimeric NEC proteins inserted into MCMV wild type genomes.	94
Figure 28 : Secondary structure prediction for UL50 and constructs for bacterial expression.	96
Figure 29 : Ni <sup>2+</sup> -affinity purification of UL50_His.	98
Figure 30 : Purification of UL50_His by a MonoQ column.	99
Figure 31 : Purification of UL50_His by gel filtration.	100
Figure 32 : Tryptic digest of UL50_His.	103
Figure 33 : Bicistronic expression of the UL50 and UL53 fragments.	104
Figure 34 : Anion exchange chromatography for purification of the UL50_His/UL53_1 complex.	105
Figure 35 : Gel filtration for purification of the UL50_His/UL53_1 complex.	106
Figure 36 : Constructs for the <i>in vitro</i> PCA.	108
Figure 37 : Bacterial expression Bla-tagged NEC proteins of HCMV.	109
Figure 38 : Specificity of the <i>in vitro</i> NEC-PCA.	111

**11.2. List of tables**

Table 1: Proteins and their corresponding expression plasmids.	31
Table 2: BACs constructed during this study.	38
Table 3: Cell lines used during this work.	49
Table 4: Members of the UL31 and UL34 protein families of representative herpesviruses.	73
Table 5: Chimeric UL31 proteins.	80
Table 6: Buffers tested for better solubility of UL50_His.	101

**11.3. Oligonucleotides****11.3.1. Oligonucleotides for the establishment of the NEC-PCA**

<b>Name</b>	<b>Oligonucleotide sequence (5'-3')</b>	<b>Note</b>
S1	TTAAGGGTACCCGTACGGATATCGCTAGCGGCTCTTCCG GAGGCGGCGGCTCCGGCGGCGGCTCGAGCGG	Spacer
S2	CCGCTCGAGCCGCGCCGCGGAGCCGCGCTCCGGAA GAGCCGCTAGCGATATCCGTACGGGTACCC	Spacer
S3	CGGCTCGAGCGGCGGCGGCGGATCCATGCGAAGAGCCCC TAGGGTTAACACCGGTGCGGCGGCGGGCCCA	Spacer
S4	GATCTGGGCCCCGCGCCGACCGGTGTTAACCCCTAGGGG CTCTTCGCATGGATCCGCCCGCCGCTCGAGCCG	Spacer
HA1	CCGGAAGAGCCGATATCGGTACCGCTAGCGTAGTCGGG- CACGTCGTAGGGGTACATGGTC	HA-tag
HA2	TTAAGACCATGTACCCCTACGACGTGCCCCACTACGC- TAGCGGTACCGATATCGGCTCTT	HA-tag
ST1	GGCCGCCTACTTCTCGAACTGGGGGTGGGACCAACCGGT GTTAACCCCTAGGGGCATCTTCTAGAG	Strep-tag
ST2	GATCCTCTAGAAGATGCCCTAGGGTTAACACCGGTTGG TCCCACCCCAAGTTCGAGAAGTAGGC	Strep-tag
BlaNfor	GTGTGCTAGCGACCCAGAAACGCTGGTGAAAGT	Amplification of the N-terminal Bla fragment
BlaNrev	TGTGTCCGGAGCCAGTTAATAGTTTGCGCAACGTTGTTG CCATTGCTACAGGCGTCGTGGTGTACGCTCGTCGT	Amplification of the N-terminal Bla fragment
BlaCfor	GTGTGCTAGCCTACTTACTCTAGCTTCC	Amplification of the C-terminal Bla fragment
BlaCrev	TGTGTCCGGACCAATGCTTAATCAGTGAG	Amplification of the C-terminal Bla fragment
M50for	GTGTGGCTCTTCCATGGAGATCGACAAGAATGTGGGC	Amplification of the M50 ORF
M50rev	AAAACCGGTCACGGATGACCCGCC	Amplification of the M50 ORF
M53for	GTGTGGATCCATGTTTAGGAGCCCGGAGGGAGAGGAAC	Amplification of the M53 ORF
M53rev	CTCTGGGCCCTCACAACGAGTAACTCTCGAACTTC- TCGTT	Amplification of the M53 ORF
M53Aflfor	GTGTCTTAAGATGTTTAGGAGCCCGGAG	Amplification of the M53 ORF
M53Saprev	GTGTGGCTCTTCATCCCAACGAGTAACTCTCGAAC	Amplification of the M53 ORF
delmo-Nhe-for	GATGCTAGCAGCTATTGGGAGTGTAGGAGC	Amplification of the M50 ORF for deletion of the binding motif
delmo-Nhe-rev	GCTGCTAGCATCGGTGGTCAACATCGCGTCGC	Amplification of the M50 ORF for deletion of the binding motif

Supplementary information

11.3.2. Oligonucleotides for the UL34 and UL31 family in the NEC-PCA

Name	Oligonucleotide sequence (5'-3')	Note
HSVUL34for	GTGTCTCGAGCGGCGGCGGCGGATCCATGGCGG- GACTGGGCAAGCCCTACACC	Amplification of the HSV UL34 ORF
HSVUL34rev	GTGTGTACCGGTTTATAGGCGCGGCCAGC	Amplification of the HSV UL34 ORF
HSVUL31for	ACACACCGGATCCATGTATGACAC- CGACCCCATCGC	Amplification of the HSV UL31 ORF
HSVUL31rev	CTCTGCGGCCGCCTACGGCGGAGGAACTC	Amplification of the HSV UL31 ORF
UL34PrVfor	ACACACCGGATCCATGAGCGGCACCCTGGTC	Amplification of the PrV UL34 ORF
UL34PrVrev	GTGTGTACCGGTTTAAACGCATGTTTCAGGATGATGAC	Amplification of the PrV UL34 ORF
UL31PrVfor	ACACACCGGATCCATGTTTGAGCGACGGCGGCTCC- TGC	Amplification of the PrVUL31 ORF
UL31PrVrev	GTGTGTGGGCCCTCACGGGCGAGGGGGCGAAAG	Amplification of the PrV UL31 ORF
UL50for	GTGTGTACCGGTTTCAGTCGCGGTGTGCGGAGCGTG- TCGGAGACGACGAC	Amplification of the UL50 ORF
UL50rev	ACACACCGGATCCATGGAGATGAACAAGGTTCTC- CATCAGGATCTGGT	Amplification of the UL50 ORF
UL53for	ACACACCGGATCCATGTCTAGCGTGAGCGGCGT	Amplification of the UL53 ORF
UL53rev	GTGTGTGGGCCCTCAAGGCGCACGAATGCT	Amplification of the UL53 ORF
ORF67for	GTGTGTACCGGTTACCATACTAGTTTACTGGCC	Amplification of the ORF 67
ORF67rev	ACACACCGGATCCATGGCTAACCAGAAGAAGCT	Amplification of the ORF 67
ORF69for	ACACACCGGATCCATGCGCTCAACAGGCT	Amplification of the ORF 69
ORF69rev	GTGTGTGGGCCCTTATTGCTGAGAAAGACGAGATAC	Amplification of the ORF 69
BFRF1for	ACACACCGGATCCATGGTGAGCCCGGAAGAGAGGC- TCCT	Amplification of the BFRF1 ORF
BFRF1rev	GTGTGTACCGGTTTCAGGCCACCTCAGAAA	Amplification of the BFRF1 ORF
BFLF2for	ACACACCGGATCCATGGCCCCGGTCACCCAGAT	Amplification of the BFLF2 ORF
BFLF2rev	GTGTGTGGGCCCTACTGTTTATTTTCCAAAAT- GAGCTGGG	Amplification of the BFLF2 ORF

Supplementary information

11.3.3. Oligonucleotides for the chimeric UL31 proteins

Name	Oligonucleotide sequence (5'-3')	Note
GM-Gfor	TGGGTCTCGCGGTATCATTGCAGCA	Amplification of the CR1 of ORF69
GM-Grev	GTCTCCTTGCAGGTTTTCACATTGGA	Amplification of the CR1 of ORF69
MG-Gfor	TGCGCGTGCACCACCTGCAC- CGACCCAAACCTCAACAA	Amplification of the CR2-4 of ORF69
MG-Grev	GCTCGAGCGGCCCGCCAGTGTGATGGATGTAATACGA CT	Amplification of the CR2-4 of ORF69
MP-Mfor	GTATCATTGCAGCACTGGGGCCAGATGGTAAGCC	Amplification of the CR1 of M53
MP-Mrev	CACAGCAATGGGTGGTGCACGCGCTCCG	Amplification of the CR1 of M53
MP-Pfor	AGCCGCAATGCCTGCGCCGCCGCCGAGCCG	Amplification of the CR2-4 of UL31 (PrV)
MP-Prev	CTCTGCGGCCGCTCACGGGCGAGGGGGGCG	Amplification of the CR2-4 of UL31 (PrV)
PM-Pfor	GGTATCATTGCAGCACTGGGGCCAGA	Amplification of the CR1 of UL31 (PrV)
PM-Prev	GTCGTCTCCTTGCAGGTGGGGCAGCAGCCGCCGAGG	Amplification of the CR1 of UL31 (PrV)
PG-Prev	GCTCTGCTCTTCAGCAGGTGGGGCAGCAGC	Amplification of the CR1 of UL31 (PrV)
PG-Gfor	AGAGGCTCTTCTTGCACCGACCCAAACCTCAAC	Amplification of the CR2-4 of ORF69
GP-Grev	GTCTGCAATGGCGCAGGTTTTCACATTGGAAA	Amplification of the CR1 of ORF69
GP-Pfor	AGAGGCAATGGCCGCCGCCGAGCCGCGG	Amplification of the CR2-4 of UL31 (PrV)
CP-Cfor	GTATCATTGCAGCACTGGGGCC	Amplification of the CR1 of UL53
CP-Crev	GGTCTGCAATGGCGCACGAGGTGCAGGCGAT	Amplification of the CR1 of UL53
CG-for	ACTGCACCTCGTGCACCGACCCAAACCTCAACAA	Amplification of the CR1 of UL53

Supplementary information

11.3.4. Oligonucleotides for the UL34 and UL31 family in MCMV

Name	Oligonucleotide sequence (5'-3')	Note
5'KpnIUL50	CGCGGTACCATGGAGATGAAC	Amplification of the UL50 ORF
3'XhoIUL50	CGCCTCGAGTCAGTCGCGGTGTGCGGAG	Amplification of the UL50 ORF
5'KpnIUL53	CGCGGTACCATGTCTAGCGTGA	Amplification of the UL53 ORF
3'XhoIUL53	CGCCTCGAGTCAAGGCGCACGAA	Amplification of the UL53 ORF
HSVUL31(pOri)for	AGAGGATATCACCATGTATGACAC- CGACCCCATCGC	Amplification of the HSV UL31 ORF
HSVUL34(pOri)for	AGAGGGTACCGGGAATGGCGGGACTGGGCAAGC- CCTACA	Amplification of the HSV UL34 ORF
HSVUL34(pOri)rev	TGTGTGATATCCTCTTATAGGCGCGCCAG	Amplification of the HSV UL34 ORF
PrVUL34(pOri)for	AGAGGGTACCGGGAAGAGCGGCACCCTGGTCCAAC	Amplification of the PrV UL34 ORF
PrVUL34(pOri)rev	TGTGTGATATCCTCTTAACGCATGTTCAGGA	Amplification of the PrV UL34 ORF
PrVUL31(pOri)for	AGAGGGTACCGGGAATGTTTGAGCGACGGCG	Amplification of the PrV UL31 ORF
PrVUL31(pOri)rev	GTGTGATATCCTCTTCACGGGCGAGGGGGC	Amplification of the PrV UL31 ORF
Orf69(pOri)for	AGAGGGTACCGGGAATGCGCTCAACAGGCTCTG	Amplification of the ORF69

Supplementary information

11.3.5. Oligonucleotides for the bacterial expression of NEC proteins

Name	Oligonucleotide sequence (5'-3')	Note
UL50-Hisfor	GTGTCATATGGAGATGAACAAGGTTCTCCATCAGG	Amplification of UL50_His
UL50-Hisrev	ACACGCGGCCGCTTTTCTTGCGTACAGCTCGCGCAG	Amplification of UL50_His
UL53_1for	GTGTGAAGACAGCATGCCGCGCCTCACGCTG	Amplification of UL53_1 and UL53_2
UL53_1rev	CCACAAGCTTATTAGATCGATTCTTTGCCCGTG	Amplification of a UL53_1
UL53_2rev	CCACAAGCTTATTACGGTTGTCCTCGCACG	Amplification UL53_2
UL50_PCАfor	AGAGGGATCCGCTAGCATGGAGATGAACAAGGTTCTCCATCAGG	Amplification of a NUL50 fragment
UL50DMfor	GTGTGGCTCTTCCTCGAGCTACTGGGAGAGCCGCA-CAGA	Amplification of UL50 for deletion of the binding motif
UL50DMrev	ACACACGCTCTTCACGAGGCGTCTGTCTTGAGCAT-GGCGTCGCA	Amplification of UL50 for deletion of the binding motif
UL53_PCАrev	TCTCTGCGGCCGCCCGGTTGTCCTCGCACGA	Amplification of a CUL53 fragment
HAfor	GTGTCATATGTACCCCTACGACGTGCCC	Amplification of a CUL53/NUL50 fragment
BlaNbactfor	TCTCCATATGGGAGACCCAGAAACGCTGGTGAAAG	Amplification BlaN
BlaNbactrev	GAACCTTGTTTCATCTCCATGGA	Amplification of BlaN

## **12. Publications**

Parts of this work were presented on conferences or submitted for publication.

### Publications:

**Margit Schnee, Zsolt Ruzsics, Anja Bubeck and Ulrich H. Koszinowski.**

Common and specific properties of herpesvirus UL34/UL31 protein family members revealed by Protein Complementation Assay. *J.Virol.* 80: 11658-11666.

**Tina Schmidt, Yvonne Schmitt, Ginette Guay, Margit Schnee, Friedrich Grässer, Roger Lippé and Susanne M. Bailer.**

A conserved interaction between the Heterogeneous Nuclear Ribonucleoprotein K and the HSV-1 nuclear egress proteins UL34 and UL31 (submitted).

### Posters and oral presentations:

**Annual Meeting of the “Gesellschaft für Virologie”, 2004, Tübingen, Germany**

*Poster presentation:* Protein fragment complementation assay for studying viral protein-protein interactions.

**Annual Meeting of the “Gesellschaft für Virologie”, 2005, Hannover, Germany**

*Poster presentation:* Protein fragment complementation assay for studying conserved protein interactions within the herpesvirus nuclear egress complex.

**30th International Herpesvirus Workshop 2005, Turku, Finland**

*Oral presentation:* Protein fragment complementation assay for studying protein interactions within the herpesvirus nuclear egress complex.

**Annual Meeting of the “Gesellschaft für Virologie”, 2006, München, Germany**

*Poster presentation:* Exploring the Nuclear Egress Complex (NEC) of Herpesviruses by Protein Complementation Assay.



### **13. Curriculum vitae**

#### Personal data:

Name: Margit Schnee  
Date of Birth: 21.02.1977  
Place of Birth: Berlin, Germany  
Nationality: German

#### Education

01/2003- 02/2007: **Max von Pettenkofer-Institut, LMU, München, Germany.**

Doctoral thesis, “Protein fragment complementation assay for studying viral protein-protein interactions“.

Supervisors: Prof. U. H. Koszinowski and Dr. B. Kempkes.

01/2002-08/2002: **Australian Institute of Marine Science, Townsville, Australia.**

Diploma thesis, “Sinus gland peptides in *Penaeus monodon*. A study of the physiological role, regulation and target organs”. Supervisor: Dr. K. Wilson.

09/1999-09/2002: **Ecole Supérieure de biotechnologie de Strasbourg, Strasbourg, France.**

Study of biotechnology. Degree: Ingénieur de biotechnologie / Diplombiotechnologin.

10/1997-07/1999: **University of Konstanz, Konstanz, Germany.**

Pre-graduate studies (Vordiplom) in biology.

10/1983-07/1996: **Ellentalgymnasium, Bietigheim-Bissingen, Germany.**

Abitur (equivalent to A-levels) with the main subjects mathematics and biology.

Practical trainings and work experience

10/2003-present: **Deutsches Museum, München, Germany.**

Teaching courses in the visitor's laboratory.

08/2000-09/2000: **University of Konstanz, Konstanz, Germany.**

Practical work experience in phytopathology in the group of Prof. Mendgen. Supervisor: Dr. R. Vögele.

10/1999 –12/2001: **Ecole Supérieure de biotechnologie de Strasbourg, Strasbourg France.**

Practical courses of several weeks in microbiology, plant physiology, genetics and process engineering.

08/2001-09/2001: **University of Würzburg, Würzburg, Germany.**

Practical work experience at the institute for molecular infection biology in the group of Prof. Leippe. Supervisor: Dr. H. Bruhn.

01/1998-07/1999: **University of Konstanz, Konstanz, Germany.**

Student research assistant in phytopathology in the group of Prof. Mendgen.